Estuary & Coastal Engineering Laboratory
Graduate School of Urban Innovation
Yokohama National University

Assessing the Beach Vulnerability to Storm-induced Erosion using an Index-based Approach

「沿岸環境を指標に用いた高波浪に伴う海浜侵食に対する脆弱性評価」

September 2023

Salika THILAKARATHNE

ティラカランナ・サリカ

Assessing the Beach Vulnerability to Storm-induced Erosion using an Index-based Approach

「沿岸環境を指標に用いた高波浪に伴う海浜侵食に対する脆弱性評価」

September 2023

A Dissertation in the Field of Coastal Engineering for the Degree of
DOCTOR OF PHILOSOPHY IN ENGINEERING

Supervised by
Professor Takayuki SUZUKI

Salika THILAKARATHNE

ティラカランナ・サリカ

Abstract

Coastal areas are highly vulnerable to frequent hazards, which can disrupt community life and have significant social and economic impacts. While vulnerability assessments using index-based approaches are common for coastal areas, studies focusing specifically on beach vulnerability are limited. This study addresses this gap by examining exposure, susceptibility, and recovery potential as key components of beach vulnerability. To assess beach vulnerability, a temporal and spatial beach vulnerability assessment tool called the Beach Vulnerability Index (BVI) is developed using Multiple Linear Regression (MLR) and Artificial Neural Networks (ANN). Additionally, a comprehensive analysis investigates beach susceptibility and resilience by considering beach morphology.

Data from the Hasaki Oceanographic Research Station (HORS) in Ibaraki prefecture, Japan, including hourly wave and water level observations, tidal predictions, and daily beach profile data from 1987 to 2010, were collected. The MLR model was initially used to predict storm-induced erosion, and the BVI was formulated based on MLR predictions, incorporating variables of wave energy flux, initial shoreline position, and maximum surge. Subsequently, an ANN model was introduced and compared to MLR in terms of predicting shoreline change during storms. The BVI is refined for both models, resulting in BVI_{ANN} for the ANN model and BVI_{MRL} for the MLR model.

The comprehensive analysis categorizes beach profiles into four groups: unbarred, inner zone sandbar, outer zone sandbar, and double sandbar. Statistical analyses and metric development were conducted to assess beach susceptibility using the Beach Erosion Susceptibility Number (BESN) and beach resilience using the Beach Resilience Number (BRN). The study successfully identified key morphometric factors that influence beach erosion and quantified the BESN accordingly. Additionally, 10-day post-storm beach recovery calculations were employed to quantify the BRN as a ratio relative to the erosion that occurred during the storm. Both the BESN and BRN are valuable tools for chronological analysis of beach characteristics

and for identifying abrupt changes in the beach system resulting from unexpected events in coastal zones. To select the morphometric indicators, XGBoost regression models were fitted for both susceptibility and resilience quantification. The SHAP explanation method was then applied to globally and locally quantify the importance of each morphometric feature in influencing the outcomes of the models.

During the preliminary study period using data from 1993 to 2000, 48 storms were identified, and the first 38 storms were used to create two MLR models. These models achieved R^2 values of 0.58 and 0.52 for predicting shoreline change (dSL) and volume change (dV) during the training period, respectively. During testing, the corresponding R^2 values were 0.48 for shoreline change (dSL) and 0.52 for volume change (dV). The comparison of the BVI calculated from the MLR predictions with observed erosion values showed satisfactory model performance. However, when the complete storm data set from 1987 to 2010 was used, the MLR model proved less effective in capturing the dynamic behaviour of beach profiles under different storm conditions. In this expanded period, a total of 347 storm cases were identified, and 5% of the data (18 storms) were used to test each regression model. In contrast, the ANN model demonstrated superior performance, resulting in more accurate predictions of beach vulnerability. Specifically, when comparing the BVI predictions from each model, the Mean Absolute Errors (MAE) for MLR were 1.33, 0.83, 0.78, 0.90, and 1.07, while for BVI_{ANN} they were 1.00, 0.20, 0.69, 1.05, and 0.57 for indexes 1-5, respectively. The BVI_{ANN} model also achieved higher R^2 scores for both training (0.65) and testing (0.62) data in predicting dSL compared to the MLR model (0.26 for training and 0.35 for testing).

The comprehensive analysis revealed that the contributing morphometrics for beach susceptibility varied depending on the beach profile types. The initial shoreline position was found to have an impact only in the unbarred and double sandbar profiles. When comparing the predictions of the BESN with observed beach changes, a Pearson correlation coefficient (r) of 0.75 was obtained for unbarred profiles for average storm conditions, indicating satisfactory performance. However, the accuracy of the BESN was found to be lower under certain conditions, likely due to variations caused by storm characteristics. In terms of beach resilience analysis, 104 cases were were identified with no sequencing storms and initial shoreline erosion cases during the storm events. Among these cases, 79 incidents exhibited partial or full shoreline recovery, while 25 cases experienced further erosion.

The results indicate that the MLR models provide moderate predictions of beach erosion and adequate predictions of beach vulnerability when tested with a small

sample of storms during the preliminary study period. However, when the larger and more diverse storm data set from 1987 to 2010 was utilized, the MLR model showed limitations in capturing the dynamic behavior of beach profiles under different storm conditions. In contrast, the ANN model demonstrated superior performance, delivering more accurate predictions of beach vulnerability. The Mean Absolute Errors for the BVI predictions were lower for BVI_{ANN} compared to BVI_{MLR}, indicating the improved accuracy of the BVI_{ANN} model. Additionally, the BVI_{ANN} model achieved higher R^2 scores for both training and testing data in predicting shoreline change compared to the MLR model.

The comprehensive analysis revealed that beach susceptibility varies depending on the beach profile types, with the initial shoreline position playing a significant role in unbarred and double sandbar profiles. The BESN demonstrated satisfactory performance, particularly for inner zone sandbar profiles, indicating its potential as a tool for assessing beach susceptibility. However, it also highlighted the need for further improvements to account for variations in storm conditions that can affect the accuracy of the predictions. The beach resilience analysis identified cases of partial or full shoreline recovery, as well as instances of further erosion, providing insights into the post-storm behavior of beach profiles.

These findings further underscore the potential of employing machine learning-based algorithms such as ANN and XGBoost to enhance the accuracy of beach vulnerability studies, particularly in capturing the dynamic nature of beach morphology changes under diverse storm conditions. The study also highlights the importance of considering sandbar formations and sediment volume as crucial factors in determining the processes of erosion and recovery associated with beach vulnerability.

Future work should focus on testing the BESN and BRN under various beach conditions and conducting numerical simulations to explore beach morphology changes in similar wave climates. Furthermore, the direct applicability of the BVI, trained using the ANN model, represents a key advantage that can be leveraged for assessing beach vulnerability in other coastal areas. This study contributes to the growing body of research on beach vulnerability by utilizing Machine Learning algorithms to predict coastal morphology changes and assess beach vulnerability, highlighting their potential for future applications in coastal engineering.

Acknowledgments

I would like to begin by expressing my deepest appreciation to my supervisor, Professor Takayuki Suzuki, for his exceptional mentorship throughout this research endeavor. His profound expertise, scholarly guidance, and unwavering encouragement have been invaluable in shaping the direction and quality of this dissertation. I am immensely grateful for his patience, availability, and continuous support, which have greatly enriched both my academic and personal growth.

I would also like to extend my sincere gratitude to the members of my dissertation committee: Professors Matsuyuki Mihoko, Kikumoto Mamoru, Hirato Higa, and Komatsu Satoshi. Their valuable insights, constructive feedback, and critical evaluation of my research have significantly contributed to refining and strengthening the scientific rigor of this work.

Furthermore, I would like to acknowledge the faculty and staff of Yokohama National University for fostering an enriching academic environment conducive to learning and research. Their dedication, knowledge, and willingness to assist have played a crucial role in my academic development. I am also deeply appreciative of the financial support provided by the Monbukagakusho (MEXT), which has enabled the necessary resources and opportunities to pursue this PhD study.

I extend my gratitude to the past and present students in the Coastal Engineering lab for creating a friendly and supportive atmosphere during my time at YNU. Special thanks go to Dr Kullarchart, Dr Martin, and CJ, who have become more like family than friends to me. I also fondly remember my Sri Lankan supervisors, Dr Lalith and Dr Nimal, who have guided me since my bachelor's degree.

To my friends and family, I owe a debt of gratitude for their unwavering support and encouragement throughout this academic journey. I am particularly grateful to *Amma*, *Thatta*, *Ayya*, *Nangi*, *Akka*, and my close Sri Lankan friends for their constant motivation during the challenging phases of this endeavour. Finally, I want to express my deepest appreciation to my loving wife, Kalpana, for her unwavering love, encouragement, and steadfast support.

Contents

List of Figures

List of Tables

Notation

ANN	Artificial Neural Network
BESN	Beach Erosion Susceptibility Number
BRN	Beach Resilience Number
BVI	Beach Vulnerability Index
BVI_{ANN}	Beach Vulnerability Index from Artificial Neural Networks
BVI_{MLR}	Beach Vulnerability Index from Multiple Linear Regression
BVI_{obs}	Beach Vulnerability Index from observed data
CVI	Coastal Vulnerability Index
dSL	Shoreline erosion during a storm
dV	Volumetric erosion during a storm
E_f	Energy flux
GIS	Geographic Information System
GBR	Gradient Boosting Regression
H_S	Significant wave height
HWL	High water level
MLR	Multiple Linear Regression
ML	Machine Learning
RF	Random Forrest
S_{max}	Maximum surge
SE_{TS-n}	n^{th} storm in the testing data set
SHAP	SHapley Additive exPlanations
SI	Scatter Index
SL_i	Initial shoreline position
VI_{dSL}	Vulnerability Index: shoreline erosion
VI_{dV}	Vulnerability Index: volumetric erosion
$XGBoost$	eXtreme Gradient Boosting
η	Water level

Chapter 1

Introduction

1.1 Background

A natural beach zone is considered a valuable asset that provides economic and environmental benefits to the local community. The beach and its natural beauty must be protected from destructive human activities, climate change-related hazards, and extreme weather conditions. Frequent natural hazards to beach zones often cause instabilities to their long-term profile migrations both landward and seaward (Turner et al., 2016). The seasonal beach profile setting involves many complex coastal processes, and holistic approaches are commonly used to understand the vulnerability of coastal regions, especially focusing on climate change-driven factors (Kantamaneni et al., 2017). Although discussions on coastal vulnerability have been ongoing since 1991, only a few vulnerability studies have focused on risk-related concepts specific to the beach zone.

Alexandrakis and Poulos (2014) first tried to quantify the beach vulnerability using key morphological and metocean data elements. They focused on sediment transport mechanisms, sea level rising effect, and land-form characteristics to numerically approximate the beach vulnerability. Several studies investigated the characteristics of coastal processes to assess beach zone vulnerability to hazards such as erosion, sea level rise, and flooding (de Andrade et al., 2019; Kim et al., 2021). Kim et al. (2021) proposed the beach recovery factor and beach response factors, which emphasize beach resilience and susceptibility, respectively. However, studies addressing both susceptibility and resilience, two key aspects of vulnerability, are limited. Although significant research in coastal engineering has examined the influence of hydrodynamic and wave climate on beach erosion (Callaghan et al., 2008; Mendoza et al., 2022), there is a dearth of information regarding the morpho-

metric characteristics of beach profiles. The discussions on specific relationships between coastal morphometrics such as sandbar formation and beach erosion exist (Janušaitė et al., 2021) and the risk-related vulnerability aspects are absent.

There have been a number of studies focusing on coastal vulnerability to various hazards such as sea level rise, flooding, and erosion (Gornitz et al., 1991, 1994; Alexandrakis and Poulos, 2014; Koroglu et al., 2019). The term of vulnerability can be defined as a component of risk, while hazard and exposure being the remaining components in risk analyses. IPCC defines the vulnerability as the degree of fragility of a system including their capacity to cope (Response capacity) under a hazardous condition (Field et al., 2011). Therefore, susceptibility and recovery potential both are key elements in beach vulnerability discussions. With the ongoing development of vulnerability assessment approaches, there is an increasing need for comprehensive studies that separately quantify the susceptibility and resilience components of beach vulnerability.

While previous studies on coastal vulnerability have predominantly focused on climate-related hazards, it is important to note that frequent coastal storms also inflict significant damage upon sandy beaches worldwide. Coastal storms are capable of exerting significant influence on both short-term and long-term changes in beach morphology. These storms are typically characterized by strong winds, high waves, and heavy rainfall, and they can cause significant damage to the coastal landscape (Harley, 2017). During a storm, waves can reach high elevations and cause significant erosion of the shoreline (Ciavola and Coco, 2017). This erosion can be particularly severe in areas where it is already vulnerable due to factors such as high tides, steep gradients, and weak soils. Coastal storms can also lead to the loss of beach sand and vegetation, which can have a significant impact on local ecosystems. To mitigate the impact of coastal storms on beach erosion, coastal managers often implement measures such as beach nourishment, dune restoration, and the construction of seawalls and other protective structures.

Beach morphometrics encompasses the physical characteristics of the coastal environment, including the shoreline, beach width and slope, sediment properties, and profile shape (Hillyer, 1996). These morphometric indicators play a pivotal role in comprehending coastal processes and the behavior of coastal systems. Coastal engineers rely on morphometric data to develop models and simulations that can predict the response of coastal environments to various stimuli like waves, tides, and storms (Hieu et al., 2020). Moreover, morphometric data inform decisions about coastal management and engineering projects, such as beach nourishment,

dune restoration, and the construction of seawalls and groins. The availability of accurate and up-to-date morphometric data is crucial for the success of coastal engineering endeavors, enabling engineers to design structures that suit the specific characteristics of the local coastal environment.

1.2 Motivation and guide to the dissertation work

1.2.1 Definitions of key terminologies

Exposure: signifies the frequency of occurrence of storm events and their associated hydrodynamic characteristics.

Vulnerability: examines how the internal attributes of a sandy beach respond to external influences, particularly storm events. Within this context, the primary focus lies on two essential internal attributes of the sandy beach system: susceptibility and resilience.

Susceptibility: represents the fragility of beach profile to storm-induced beach erosion. A beach profile with high susceptibility will undergo more pronounced erosion, revealing heightened vulnerability to external hazards. On the contrary, a less susceptible beach profile boasts robust internal morphometric properties that can effectively withstand erosion caused by storms

Resilience: refers to a system's ability to recover from adverse impacts, particularly concerning its potential to restore the initial condition after substantial erosion events.

1.2.2 Significance of the study

This dissertation introduces innovative approaches to quantifying beach vulnerability. Firstly, it outlines novel regression-based methods for predicting beach vulnerability. Subsequently, a comprehensive analysis is presented, focusing on quantifying the susceptibility and resilience characteristics of beach profiles.

By utilizing a substantial and valuable dataset encompassing hydrodynamic features of storms, alongside morphodynamic characteristics of subsequent beach profiles, an application of the Beach Vulnerability Index (BVI) is developed. The regression models, trained with a significant number of storm cases, are expected to make a significant contribution to quantifying beach vulnerability within comparable beach profile settings, thereby enabling both spatial and temporal analyses.

The comprehensive analysis of the susceptibility and resilience characteristics of beach profiles provides unprecedented insights into beach morphology and erosion processes concerning vulnerability. The present dissertation offers substantial support in formulating effective strategies to mitigate erosion risks and enhance the resilience of coastal systems.

This research initiative holds the potential to offer valuable guidance for coastal management and engineering practices, thereby contributing to the sustainable management of coastal regions.

1.2.3 Applicability and beneficiaries

Sandy beaches hold both ecological and economic value, rendering them vulnerable to adverse effects when structures are placed in close proximity to the shoreline. The extraction of sand, inadequate construction practices, and disruption of sediment supply sources can result in significant damage to these beaches. Consequently, a thorough quantification of beach vulnerability is imperative to comprehend the implications of human activities and natural processes on beach morphology. This dissertation's contributions concerning beach vulnerability provide invaluable insights for stakeholders engaged in coastal management.

The identification of areas grappling with severe erosion, coupled with an examination of temporal variations in short-term erosion processes, yields substantial advantages for a diverse range of entities. These encompass coastal managers, engineers, local government authorities, the tourism sector, communities, and various industrial and economic activities along the coastline.

A fundamental approach to effective beach management involves safeguarding both the natural processes that supply sand to the beach and the sand-storage capacity of the beach elements themselves (Clark, 2018). In this light, a numerical quantification of beach vulnerability would facilitate the understanding of long-term beach evolution, centering on its inherent traits as a resilient and minimally susceptible system for sand retention. The proposed methodology for assessing beach vulnerability emerges as a valuable tool for systematically scrutinizing chronological and spatial transformations in beach morphology. Consequently, coastal managers can apply the proposed quantification methods as preliminary studies to accurately pinpoint key locations along the coastline.

Beaches inherently shift over seasons, temporarily yielding sand to storm erosion, gradually moving landward with rising sea levels, or growing seaward due to shifts in ocean currents (Clark, 2018). Hence, an extended analysis of beach sus-

ceptibility and resilience plays a pivotal role in studying persistent changes. These transformations are intrinsically tied to the economic and environmental values associated with beaches. Furthermore, quantifying susceptibility can help to evaluate the impact of diverse gray structures on seasonal shifts in sandy beaches. As discussions advocating for beaches as green structures gain momentum, this dissertation's work furnishes quantitative insights into alterations in beach profiles prompted by external influences.

1.3 Objectives

The main objective of this study was to advance the comprehension of beach vulnerability while refining the precision of assessment techniques. This enhancement was pursued through innovative regression-based prediction models. In the initial section of the dissertation, a predictive beach vulnerability assessment tool was developed and tested. This was accomplished by utilizing a concise set of hydrodynamic and morphometric indicators. Subsequently, the research work endeavored to develop and evaluate matrices related to susceptibility and resilience characteristics of beach. These quantification were developed using novel deep learning methodologies.

Centered around these focal areas, the study aims to propel our understanding of beach vulnerability forward. Moreover, it aspires to provide valuable insights that can effectively inform the development of strategies in coastal management and adaptation. In pursuit of the main objective, three specific objectives were formulated and are presented below.

(1) To refine the accuracy of beach vulnerability prediction by enhancing the multiple linear regression model. The focus was on utilizing an extensive 8-year storm data set to identify and rectify any limitations present within the model.

(2) To investigate the utility of artificial neural networks in predicting beach vulnerability. The analysis utilized a 24-year storm data set to assess the effectiveness and potential advantages of employing this approach.

(3) To examine the key morphometric indicators that impact beach susceptibility and resilience. The goal was to devise matrices that offer quantification of these factors, while also accounting for diverse beach morphology shapes.

1.4 Presentation of the dissertation work

The dissertation is organized as follows: Chapter 2 offers a concise overview of relevant literature, focusing on key discoveries and identified limitations. It aims to provide a foundation for the subsequent research by examining existing knowledge and gaps in the field. Chapter 3 presents a comprehensive exploration of the research methodology and materials employed. It begins by describing the study location and the collection of pertinent data. Special emphasis is placed on the distinct characteristics of the data and their importance to the research. The chapter then proceeds to detail the methods employed for the application of beach vulnerability assessment and the subsequent comprehensive analysis.

Chapter 4 is dedicated to presenting and discussing the application of the Beach Vulnerability Index (BVI). It highlights the practical implementation of the BVI in evaluating beach vulnerability, providing insights into its efficacy as a predictive tool. The chapter includes thorough examinations of two regression models, illustrating the applicability and utility of each BVI approach. Chapter 5 sheds light on the intricate dynamics of beach vulnerability focusing on the susceptibility and resilience. The findings are critically dissected, drawing connections between diverse beach morphometrics and their roles in erosion processes. This chapter offers a deeper understanding of the intricate interactions between coastal elements and beach morphology.

Finally, in Chapter 6, the key findings of the research are synthesized, encapsulating the primary contributions and insights stemming from the study. Following the conclusion, the bibliography and appendix sections provide valuable additional resources and supporting materials for further exploration.

Chapter 2

Literature Review

A comprehensive overview of crucial subjects related to beach vulnerability and coastal engineering and management literature is presented here. The content is structured into sub-chapters, each dedicated to delving into specific key aspects of the current study.

2.1 Vulnerability Studies

An index-based approach established on set criteria is common to quantify and analyze the vulnerability whereas the definition of vulnerability highly depends on the study objectives and location. Coastal vulnerability studies focus on various diverse aspects of the coastal region such as land-use patterns, coastal morphology, social and economic factors, and wave climate (Gornitz et al., 1994). However, studies on beach vulnerability assist various stakeholders in better managing and planning measures against erosion by identifying, and quantifying ranking the vulnerability of beaches (Alexandrakis and Poulos, 2014). Indeed, beach vulnerability studies specifically focus on the changes to the beach zone whereas coastal vulnerability research involves a more comprehensive view of the coastal zone.

2.1.1 Coastal Vulnerability Studies

Coastal vulnerability to storm-induced erosion is a critical aspect of coastal management, particularly considering the potential impacts of global climate change. A large and growing body of literature has explored coastal vulnerability in various parts of the world, though with varying degrees of emphasis on beach sections. The Development of a Coastal Risk Assessment Database by Gornitz et al. (1991)

presented a comprehensive approach to identifying coastal areas at risk of erosion, inundation, and episodic flooding. While it offers valuable insights into coastal vulnerability, it does not specifically focus on beach sections and their unique characteristics. Similarly, the study by Small and Naumann (2001) examined the global distribution of the human population with respect to community exposure to coastal hazards. In contrast, the study by Koroglu et al. (2019) compared different methodologies for assessing coastal vulnerability using the Coastal Vulnerability Index (CVI) along the Barcelona coastline. Their analysis revealed that Shaw et al. (1998)'s method provided a more realistic assessment of vulnerability. However, this study also fell short in explicitly addressing beach sections and their significance for ecology and tourism. They further suggested the need for site-specific databases and region-specific ranking categories within the CVI framework to improve overall vulnerability assessments. Additionally, the study by Shaw et al. (1998) investigated the potential impacts of global sea-level rise on Canadian coasts. While they acknowledged the importance of societal response strategies, they did not specifically address beach sections or their relevance for coastal protection. The reviews emphasized the necessity for specific characteristics and dynamics of beach sections, encompassing erosion rates, sediment transport, and the influence of natural and anthropogenic factors.

To advance the present understanding of coastal vulnerability, future studies should build upon the existing research by incorporating a comprehensive analysis of beach sections and their unique vulnerability factors. This would involve conducting detailed assessments using site-specific databases, considering region-specific ranking categories within vulnerability assessment frameworks like the CVI, and examining erosion rates, sediment transport, and the influence of natural and anthropogenic factors.

2.1.2 Beach Vulnerability Studies

This sub-chapter discusses the research work with the broader focus on beach vulnerability and points out the lack of focus on this aspect in the selected literature. Several studies have addressed beach vulnerability, some focusing on vulnerability to erosion as well, each using different methods and approaches depending on the characteristics of study site. Alexandrakis and Poulos (2014) proposed the Beach Vulnerability Index (BVI), which combines simplicity, easily obtainable data, and low processing capacity. Their index considered indicators related to sediment availability, wave climate, beach morphodynamics, and sea level change. While

the BVI offers a comprehensive approach, it lacked a specific emphasis on the ecological and tourism aspects of beaches.

Ruggiero et al. (2005) have discussed a beach monitoring program aimed at collecting coastal change data to enhance decision-making. Although the program has quantified beach trends and fluctuations, they have not explicitly addressed beach vulnerability. The lack of a comprehensive examination of vulnerabilities in beaches can be identified as a common weakness observed in these literature. de Andrade et al. (2019) assessed beach vulnerability based on environmental indicators such as terrain elevation, wave exposure, wave incidence angle, and wave run-up. Their study evaluated the vulnerability of specific beaches in Guarujá, Brazil. While providing valuable insights, the paper does not extensively discuss the ecological and tourism significance of beaches or offer a comparative analysis of different assessment methods.

Alexandrakis and Kampanis (2013) adopted an economic perspective by estimating the value of eroded beaches in terms of tourism revenue, though the sediment related discussions were limited. Their approach composed of environmental and economic factors, especially, incorporating the beach width (Table 2.1 summarizes their methods to collect each variable). However, the paper has not delved into the specific methodologies used to assess beach vulnerability, limiting their comprehensive analysis. Whereas Perch-Nielsen (2010) have analyzed the beach vulnerability with the broader focus on climate change impacts. They have developed a vulnerability framework considering exposure, sensitivity, and adaptive capacity indicators which provides in-depth discussion on vulnerability assessments. While recognizing the importance of weather and climate for beach, it lacked ecological vulnerabilities.

In comparing the methods used, BVI offered a comprehensive and easily applicable approach to assessing beach vulnerability. However, some of the available literature lacked a much-needed discussions on the impact of morphological and hydrodynamic variables on beach vulnerability. In contrast, de Andrade et al. (2019) considered environmental indicators, providing valuable insights into vulnerability assessment, but have not offered a comparative analysis. Table 2.2 highlights the use of beach characteristics of existing literature.

Table 2.1: Variables, methods, and scales used in the study of Alexandrakis and Kampanis (2013)

Variable	Method	Scale
Coastal geomorphology	Field measurements / Satellite images	Large
Shoreline erosion /accretion rate [m]	Field measurements / Satellite images	Large
Coastal slope [%]	Field measurements / Satellite images	Large
Relative sea-level change [mm]	Tide gauges / Bibliographical	Large
Mean significant wave height [m]	Field measurements / Bibliographical	Large
Tidal range [m]	Tide gauges / Bibliographical	Large
Profile length [m]	Field measurements	Small
Beach slope (degrees)	Field measurements	Small
Profile length subaerial [m]	Field measurements	Small
Maximum profile elevation [m]	Field measurements	Small
Wave breaking height [m]	Numerical modeling	Small
Wave breaking angle (degrees)	Numerical modeling	Small
Significant wave height [m]	Numerical modeling	Small
Wave length [m]	Numerical modeling	Small
Wave period	Numerical modeling	Small
Wave run up [m]	Estimate by equation	Small
Sea level rise [m]	Bibliographical	Small
Closure depth [m]	Estimate by equation	Small
Wind speed [$m\,s^{-1}$]	Bibliographical	Small
River sediment flux [m^3/year]	Estimate by equation	Small
Fall velocity [$m\,s^{-1}$]	Estimate by equation	Small
Grain size (subaqueous) [mm]	Field measurements	Small
Grain size (subaerial) [mm]	Field measurements	Small

Table 2.2: Use of beach morphological indicators in past coastal vulnerability studies.

Study	Number of indicators focused on	
	In total	Beach
Gornitz et al. (1994)	7	1
Shaw et al. (1998)	7	1
Abuodha and Woodroffe (2006)	8	3
Hegde and Reju (2007)	4	1
Balica et al. (2012)	22	2
Alexandrakis and Poulos (2014)	7	7
Sambah and Miura (2014)	3	1
Barnard et al. (2015)	9	1
Kantamaneni et al. (2017)	4	1
Kantamaneni et al. (2018)	7	2
Kim et al. (2021)	NA	NA

2.2 Coastal storms

Coastal storms are one of the most frequent coastal hazards and cause catastrophic damages such as erosion and inundation (Martzikos et al., 2021). Definitions to identify coastal storms are, in general, site-specific. Significant wave height is largely employed to identify storm events. However, Basco and Mahmoudpour (2012) proposed a generalized approach to identify extreme storm events using long-term significant wave height characteristics and a minimum storm duration threshold. In some cases, water surface level is also used to separate storm events though this approach is not popularly compared to the two-threshold approach discussed antecedently. After Gornitz et al. (1994) proposed the concept of CVI which can be applicable for various coastal hazards including coastal storms, index-based approaches are widespread in storm impact assessments.

Coastal storms are extreme hydrometeorological events that have significant impacts on coastal areas and communities. Understanding the characteristics and risks associated with these storms is crucial for effective coastal zone management and the design of resilient coastal structures. Harley (2017); Martzikos et al. (2021) thoroughly investigated different aspects of coastal storms and analysis methods, providing a much-needed comprehensive overview of storms for the researchers. Harley (2017) have further addressed the challenges in defining coastal storms by emphasizing the diverse coastal environments and their responses to maritime forc-

ing, storm timing, and the effects of climate change. They have further highlighted the importance of assessing coastal storminess through various measures, including storm frequency, timing, tele-connections with climate patterns, directional shifts, extreme storm events, and the impacts of storm surge. They have raised awareness of the dangers associated with climate change and the need for accurate storm definitions to mitigate risks to low-lying coastlines. Martzikos et al. (2021)'s findings focus on the statistical analysis of Mediterranean coastal storms to understand the risk associated with extreme events by analyzing parameters such as wave height, wave period, storm duration, calm periods, and storm energy. The authors have utilized buoy data sets from 30 locations in the Mediterranean Sea to identify and characterize coastal storms. Their analysis provides insights into the frequency of occurrence, seasonal distribution, and site-dependent variations of coastal storms, which are valuable for coastal zone management and the design of coastal structures.

2.3 Nearshore morphodynamics

Numerous experiments have been conducted both in laboratory settings and in the field to study beach transformation. The outcomes have indicated that beach shape and its evolutionary process are significantly influenced by the energy level of incident waves, as well as the geological and geomorphological characteristics of the coastal zone (Horikawa, 1988). Defeo et al. (2009) provided an overview of the physical and ecological attributes of sandy beach ecosystems and discuss the various anthropogenic pressures threatening these ecosystems. While they have primarily focused on the broader threats to beach ecosystems, the need for long-term field experiments and monitoring programs to quantify the dynamics of key ecological attributes on sandy beaches has been emphasized. However, they have not specifically addressed the direct connection between nearshore morphology and beach vulnerability to erosion. Understanding the causes of beach erosion is essential for implementing effective mitigation strategies. Bird and Lewis (2015) explored the factors contributing to beach erosion, including alterations in processes, sediment supply, and anthropogenic influences. Their analysis have highlighted the importance of identifying the underlying causes of beach erosion before implementing mitigation measures. However, they do not suffice extensively discussions on the specific role of nearshore morphology related to beach vulnerability.

To address the prediction of coastal erosion, the paper "Combining Artificial

Neural Networks and GIS Fundamentals for Coastal Erosion Prediction Modeling" by Peponi et al. (2019) introduced a model that integrates geographic information systems (GIS) and Artificial Neural Networks (ANN). This approach enabled a comprehensive analysis of the factors influencing coastal erosion changes. While they provides valuable insights into erosion prediction modelling, it does not explicitly focus on nearshore morphology as a primary factor. However, Suzuki and Kuriyama (2012) highlighted the correlations between shoreline change rates and frequency-sectioned wave energy fluxes, taking into account the influence of foreshore shape. They demonstrated the importance of considering both wave energy and shoreline position in accurately estimating shoreline change rates. Their findings further highlight the significance of nearshore morphology, particularly foreshore shape, in understanding beach vulnerability. However, they have not extensively explore other hydrodynamic and morphometric indicators beyond wave energy flux and foreshore shape.

On steep beaches, cross-shore movement of sand can lead to temporal changes between the barred winter profile and unbarred summer profile with a pronounced berm in the upper swash zone Ruessink et al. (2016). Severe wave conditions during winter often lead to the erosion of beaches, causing the shoreline to shift landward. Furthermore, eroded profiles are often accompanied by the formation of sandbars, which serve as underwater seawalls and assist in dissipating wave energy (Ciavola and Coco, 2017). Whereas, accreted beaches have a more seaward shoreline during the summer, with fewer sandbars. Despite scientific discussions on the impact of sandbar formations and coastal erosion, a thorough investigation of the role of sandbar morphometrics is lacking.

By synthesizing the insights from these literature, it demonstrates that characteristics of nearshore morphology are vital in assessing beach vulnerability. While the reviewed articles offer valuable contributions to different aspects of nearshore processes and beach erosion, there is a need for more comprehensive research that explicitly focuses on the role of nearshore morphology in beach vulnerability. Such research would enhance the present understanding of the complex dynamics and interactions between nearshore processes, morphology, and storm-induced erosion, ultimately leading to more effective strategies for mitigating the impacts of erosion on vulnerable coastlines.

2.4 Machine Learning models

In recent years, the application of machine learning models engineering sciences has gained significant attention. Therefore, not-surprisingly, discussions regarding their applicability in coastal engineering are also substantial. Among them, neural networks and decision trees have emerged as powerful tools for predicting wave characteristics, tides, storm surges, and shoreline fluctuations, offering advantages over traditional approaches. Incorporating the Shapley Additive Explanations (SHAP) framework enhances interpretability at both local and global levels. This sub-chapter aims to delve into the applications of novel machine learning models, emphasizing their advancements, challenges, and comparative strengths in the context of coastal engineering.

2.4.1 Artifical Neural Nets

Discussion on the application of Articial Neural Networks (ANN) in civil engineering goes back to Adeli (2001). The majority of applications utilize the backpropagation algorithms, with some recent works integrating more powerful and efficient neural network models with other computing paradigms like genetic algorithms, fuzzy logic, and wavelet. Portillo Juan and Negro Valdecantos (2022) investigated the applicability of ANN specifically in ocean and maritime engineering. They have highlighted the advantages of ANNs over traditional approaches and summarized the progress made since the 1990s. The review identifies general rules for applying ANNs in ocean engineering and emphasizes the importance of selecting the correct network and algorithm for successful implementation. Wei (2021) proposed an ANN model for forecasting wind waves along the US Atlantic Coast. The model utilized the Long Short-Term Memory (LSTM) technique and has been trained using historical wind, wave, temperature, and atmospheric pressure data. The study demonstrated accurate short-term predictions, particularly for storm events, and suggests the potential of ANN models as an alternative tool for wave prediction and storm forecasting in coastal areas.

Comparing these works, it shows that neural networks, particularly the backpropagation algorithm, have been successfully applied in various areas of civil and coastal engineering. They have shown superiority over traditional approaches and have been successfully integrated with other computational techniques to enhance their performance. The use of ANNs in coastal engineering has proven advantageous due to their ability to model random patterns, which are common in ocean

and maritime problems.

2.4.2 Ensemble models for regression

In the review of Kim and Lee (2022), most of the available applications of machine learning in coastal engineering have been highlighted with a focus on its effectiveness in predicting various parameters such as wave parameters, tides, storm surges, design parameters, and shoreline fluctuations. One notable aspect discussed in this literature is the use of ensemble methods to improve the performance of machine learning models. Ensemble methods, such as bagging and boosting, are described as techniques for combining multiple weak classifier models to create a strong prediction model. Bagging reduces variance by averaging or voting on predictions from various models while boosting focuses on creating strong classifiers by iteratively adjusting weights on the data (Chen and Guestrin, 2016).

Random Forest (RF) is presented as a specific ensemble method that improves upon the decision tree algorithm. RF also incorporates the concept of bagging and randomization to address the shortcomings of traditional decision trees. By generating bootstrap samples and creating decision trees based on random subsets of predictors, RF introduces randomness and creates multiple low-importance learners. The important hyperparameters in RF include $max_{features}$, bootstrap, and $n_{estimator}$, which control the number of features used in each node, data sampling conditions, and the number of trees in the model, respectively. Boosting is another ensemble method, particularly AdaBoost and Gradient Boosting Regression (GBR) (Kim and Lee, 2022). AdaBoost adjusts the distribution of training data based on the performance of weak classifiers, iteratively increasing the weight of samples with low prediction accuracy. This adaptive weighting improves training accuracy and leads to the creation of a strong classifier with better performance. GBR, on the other hand, employs a loss function to classify errors and sequentially adds multiple models, similar to AdaBoost. The distinction lies in the method of recognizing weak classifiers, with AdaBoost emphasizing weight adjustments and GBR using a loss function for evaluation.

2.4.3 SHAP explanation method

Various statistical tools are commonly used in coastal engineering to assess the relationship between two or more variables. One big advantage of these tools is their ability to explain the mathematical reason behind any correlation. However, these tools are not always effective in dealing with complex and holistic environmental

phenomena such as beach erosion. Identifying key parameters for beach erosion is common. However, the research work of Lundberg and Lee (2017) as one of the recently bloomed machine learning approaches has developed feature importance algorithms such as entropy, feature importance, and SHAP (SHapley Additive exPlanations) values, which are explanatory tools to understand the impact of different variables. SHAP explanation method can be identified as a statistical tool to quantify how much influence each of the input variables has on output variable/s. Such analysis can help to make more informed decisions in coastal engineering management.

2.5 Literature summary and research gap

The presented literature review has narrowed down the research work from coastal vulnerability to beach vulnerability, examining the factors that influence beach erosion and the methods employed to evaluate and alleviate vulnerability. Additionally, the review explores coastal storms and nearshore sediment dynamics, shedding light on their impacts on coastal environments. Moreover, it delves into the application of machine learning models, specifically neural networks, XGBoost, and the SHAP explanation method, to predict and interpret the dynamics of the nearshore morphology. The review further underscores the necessity for comprehensive assessments of beach vulnerability that integrate site-specific databases and account for the unique dynamics and factors influencing different beach sections. It also emphasizes the significance of nearshore morphology in comprehending beach vulnerability and highlights the potential of machine learning models in coastal engineering research.

Based on the literature review, it was determined that further investigation and analysis in specific areas related to beach vulnerability are needed. The comprehension of nearshore morphology and its link to beach vulnerability remains inadequate, underscoring the need for additional research to reveal the underlying mechanisms driving coastal erosion. Furthermore, limited research exists regarding the application and interpretability of machine learning models in coastal engineering, suggesting the necessity for additional studies to explore the effectiveness and practicality of these advanced models in predicting beach vulnerability. The objectives of this dissertation work were formulated to address these research gaps and contribute to the development of more accurate and comprehensive strategies for managing and mitigating erosion risks in coastal areas.

Chapter 3

Methodology

This chapter provides an in-depth account of the methods utilized to address the study objectives. It also outlines the specific approaches applied in the beach vulnerability assessment, encompassing the selection and implementation of regression models. Furthermore, the chapter underscores the comprehensive analysis undertaken to scrutinize beach susceptibility and resilience. The overall research methodology is presented in Figure 3.1.

3.1 Study area

The data set used in this study was collected at Hasaki Oceanographic Research Station (HORS), Japan facing the Pacific Ocean as shown in Figure 3.2. Located in Kamisu city of Ibaraki prefecture, HORS is situated at the center of a 16 km stretch of straight beach that runs from Choshi port in the South to Kashima port in the North. HORS features a 392.0 m long pier that was constructed perpendicular to the Hasaki coastline, allowing for chronological measurements of morphological and hydrodynamic data since 1987 (Thilakarathne et al., 2022). The Port and Airport Research Institute (PARI) manages the survey and research facilities at HORS. This micro-tidal beach has a tidal range of 1.45 m and is angled at 59°counterclockwise from the North.

Beach erosion was quantified using daily measurements of a 500.0 m cross-section obtained at 5.0 m intervals along the HORS pier (Suzuki and Kuriyama, 2012). The positive distances represents the seaward distance perpendicular to the shore from the HORS coordinate system origin. Hourly measurements of significant wave heights were recorded at 380.0 m along the HORS pier, with an average water depth of 6.0 m. At Hasaki, the water levels relative to the datum level (Tokyo

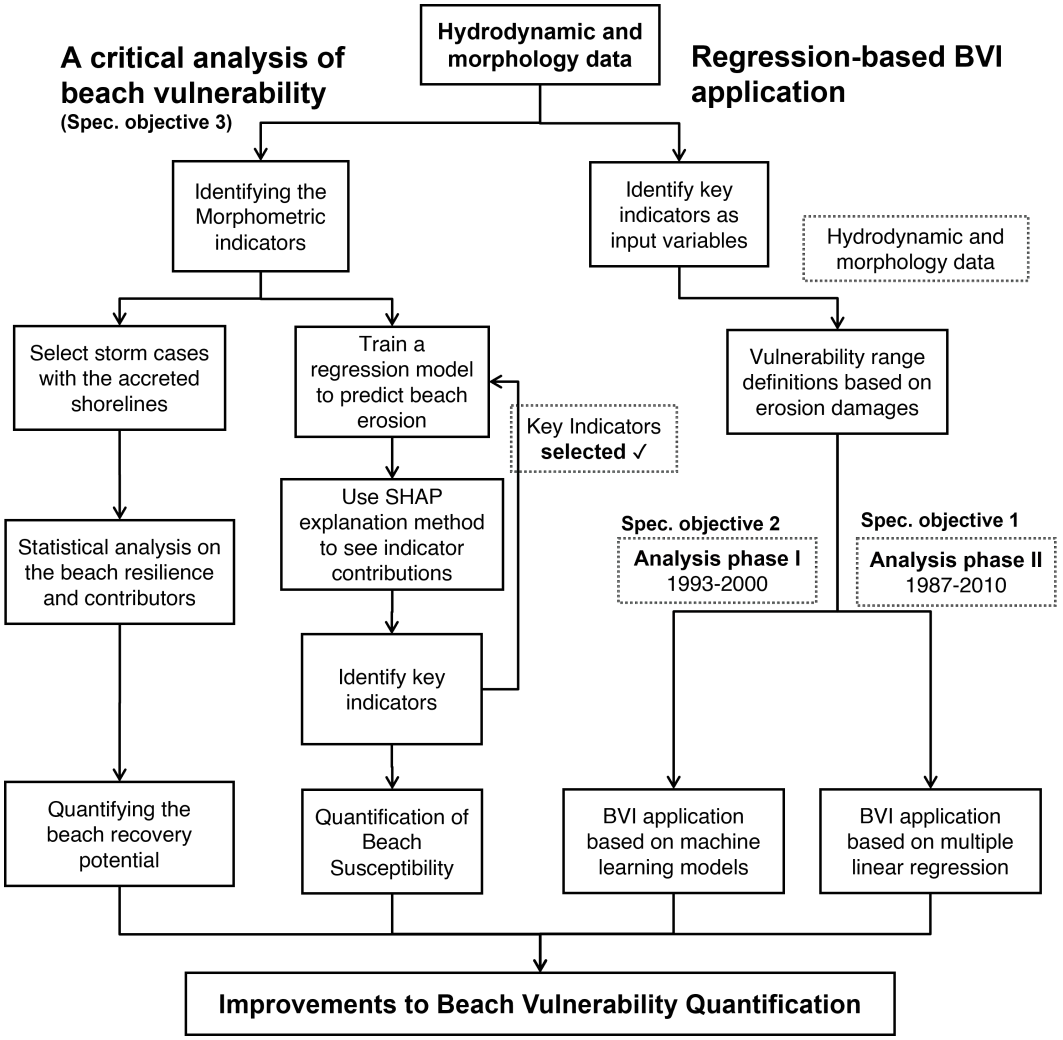

Figure 3.1: Flow chart of research methodology. The flowchart depicts the two-stage analysis of the critical analysis as well as regression based BVI application.

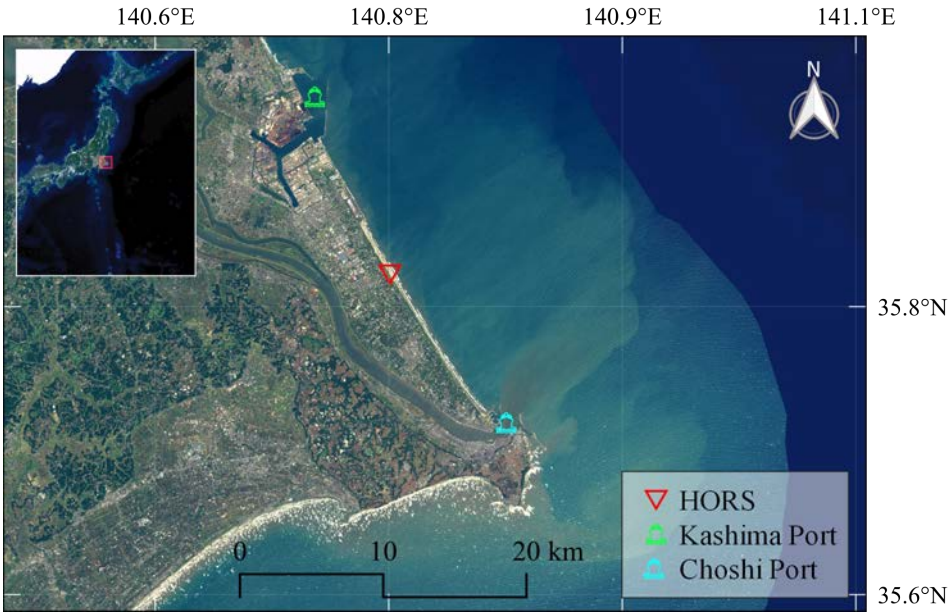

Figure 3.2: Location of Hasaki Oceanographic Research Station (HORS). Morphological and metocean data are collected at the 500 m long pier located at the HORS (Base map source: Geographical Survey Institute, Japan).

Peil +0.687 m) were as follows: the high water level was 1.25 m, the mean water level was 0.65 m, and the low water level was −0.20 m. The median sediment diameter (d_{50}) is 0.18 mm, although storm events could alter it to 1.0 mm (Karunarathna et al., 2016). Notably, significant beach erosion is observed during the typhoon season, which spans from late August to October. In contrast, natural nourishment occurs throughout the rest of the year (Banno et al., 2020).

3.2 Data collection

The data collection for this study spanned from 1987 to 2010 and involved the acquisition of hydrodynamic data at an hourly resolution. The measuring point, located 380.0 m along the pier, was selected as the primary location for data collection. This specific location is depicted in Figure 3.5. In addition to the hydrodynamic measurements, daily cross-sectional measurements were conducted at 5-meter intervals. These data collection efforts aimed to capture a comprehensive understanding of the coastal dynamics and provide valuable insights into the beach vulnerability and morphological changes over the specified time period. Table 3.1 shows a statistical summary of data during the 24-year period and during high-

wave storm conditions.

Table 3.1: Statistical summary of the complete data set and filtered data set in storm conditions.

Variable	Mean (± St. d)	
	24-year data	During Storms
Mean sig. wave height [m]	1.20 (±0.61)	2.20 (±0.36)
Mean sig. wave period [s]	7.84 (±1.91)	9.15 (±1.68)
Mean shoreline [m]	4.19 (±13.93)	2.67 (±12.97)
Maximum surge [m]	–	0.39 (±0.25)
Storm power [$m^2 \cdot h$]	–	549.6 (±448.9)
Beach slope (Tangent)	0.0309 (±0.0095)	0.0336 (±0.0106)

3.2.1 Wave data

Significant wave height (H_S) is a fundamental wave parameter extensively employed in coastal engineering to characterize the wave climate of a specific location. It represents the average height of the highest one-third of waves observed within a given time period, typically measured over a period of 20 min. H_S is a key descriptor of wave conditions as it provides a reliable estimate of the wave energy present in a particular sea state.

The calculation of significant wave height involves statistical analysis of wave data collected by wave buoys, coastal gauges, or numerical wave models. Initially, raw wave measurements, typically in the form of time series data, are processed to remove outliers, noise, and non-wind-generated waves. The remaining wave heights are then sorted in descending order, and the average of the highest one-third is determined to obtain the significant wave height value. Figure 3.3 highlights the significant wave height (m) variation during the study period.

3.2.2 Tidal and water levels

Water level (η) observations were conducted at 380.0 m point along the Hasaki pier (Figure 3.5). The water level observations and tidal predictions for each hour were used to calculate the storm surge during storm conditions. Though the tidal predictions are periodical, the water levels vary depending on many factors, Figure 3.4 highlights the mean water levels (m) variation during 24-year study period.

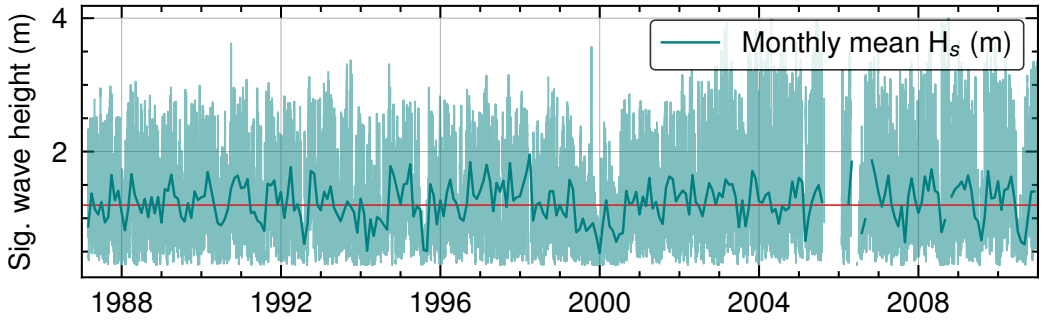

Figure 3.3: Distribution of the Significant Wave Height observations [H_s] during the study period (1987-2010). Monthly mean H_S values are shown in the thick line. Daily H_S values are shown in light teal color and red line shows the mean H_S at Hasaki.

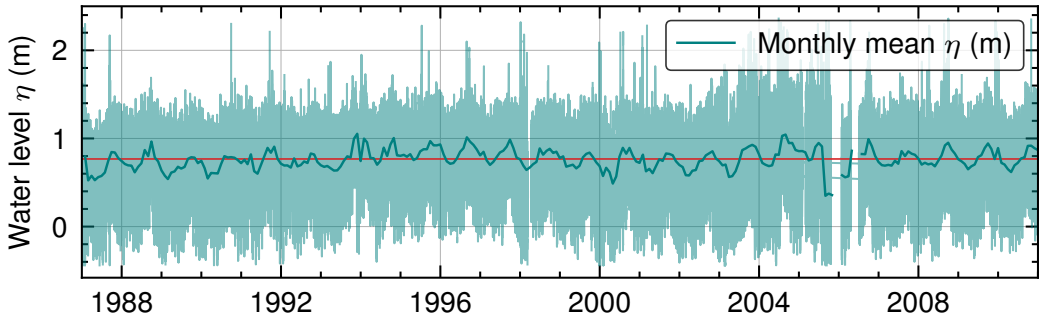

Figure 3.4: Distribution of the water level observations [η] during the study period (1987-2010). Monthly mean water level (η) values are shown in the thick line. Daily η values are shown in light teal color and red line shows the mean water level at Hasaki.

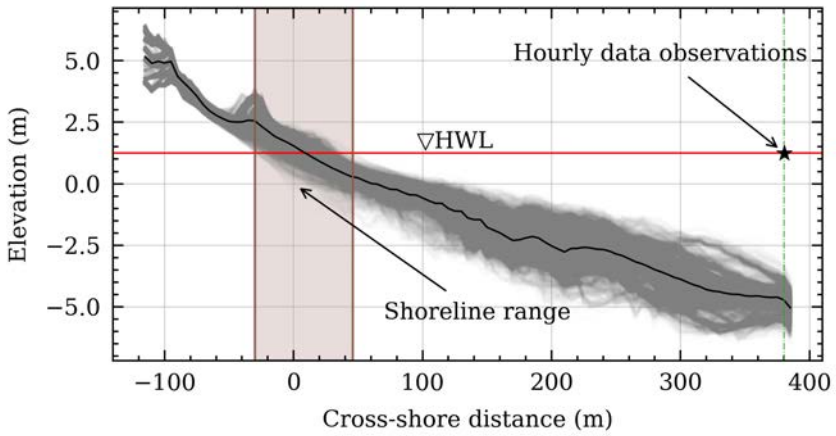

Figure 3.5: Bed profile variation from 1987 to 2010. Shoreline range during the 24-year period is shown in brown color. Hourly wave and water level (η) observation point was at the star point.

3.2.3 Cross sectional data measurements

To accurately assess the sediment exchange along the beach, cross-sectional measurements were taken along an x-coordinate system ranging from -115.0 m to +385.0 m, corresponding to shoreline positions from -36.9 m to +45.7 m over the 24-year period. However, recognizing the critical role of shoreline position in cross-shore sediment balance and long-term morphology changes, a new cross-shore coordinate system was introduced. This system centers on the shoreline, ensuring the shoreline position remains fixed at x=0. This novel approach allows us to focus on beach erosion and better understand the vulnerability of the beach. Surprisingly, previous studies examining beach vulnerability have not considered the impact of shoreline variation on the results (Thilakarathne et al., 2022).

It was found through previous research that the initial shoreline position strongly influences the impact of storms on the beach, further emphasizing the importance of using a shoreline-based approach in beach profiling (Thilakarathne et al., 2022). Figure 3.6 highlights the impact of closure depth on the nearshore sediment movement specially during storm conditions. Considering this, the beach zone was set as defined in the Figure 3.7. In the comprehensive analysis, lesser discussed morphometrics on the beach zone as well as sandbar formations are thoroughly examined. Moreover, sandbar height, depth and distance is defined as shown in the Figure 3.8

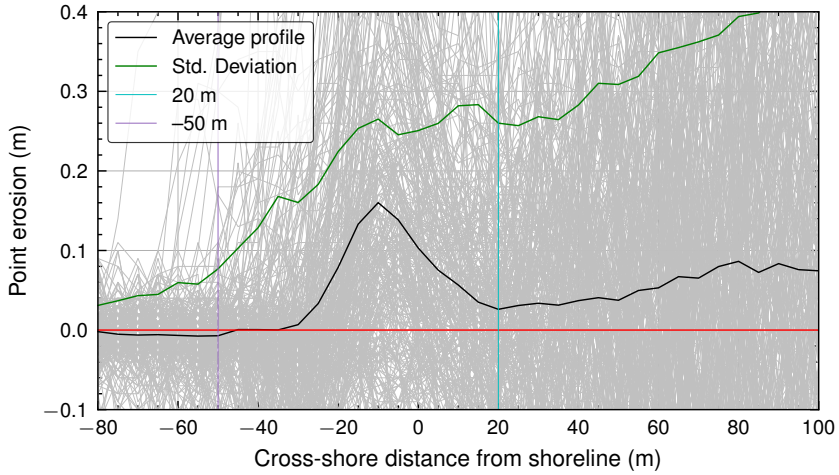

Figure 3.6: Seaward beach zone limit definition based on the closure depth (20.0 m from the shoreline position). Average point-erosion rate along the peir is considered here.

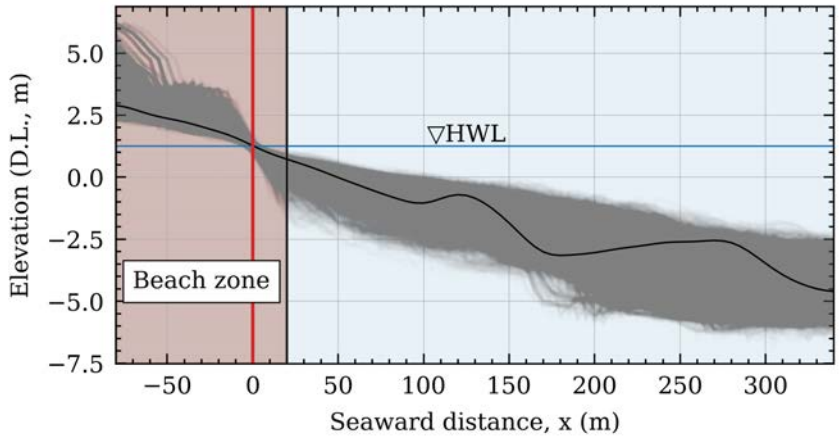

Figure 3.7: Cross-sectional profilig based on the shoreline based moving cross-shore profiling. Beach zone is highlighted in red. Mean beach profile in black is shown on the beach profile envelope in gray.

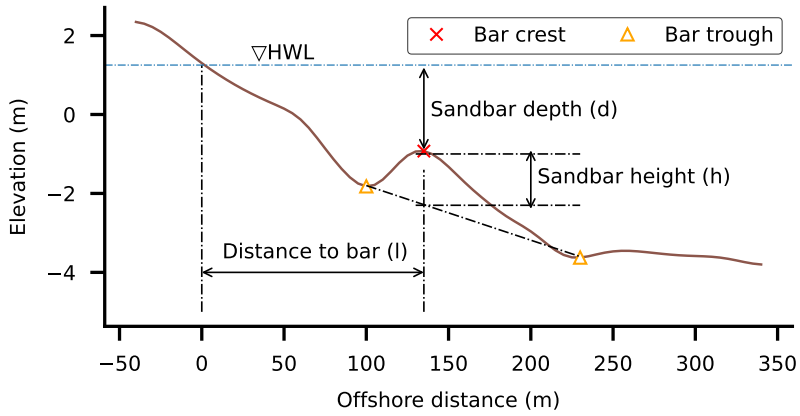

Figure 3.8: Quantifying sandbar features as morphometric indicators for beach susceptibility and resilience quantification approach.

3.3 Storm Identification

Typhoons in autumn, strong monsoons in winter, and low atmospheric pressure throughout the year produce strong wave conditions at Hasaki (Katoh, 1997). Storm classifications are generally site-specific where the peaks over a wave threshold approach are common. However, generalized storm thresholds can also be beneficial when considering the applicability of methods across different locations.

3.3.1 Global threshold approach

In most storm identification definitions, a minimum duration of six hours is considered to include only storm events of a significant duration (Ciavola and Coco, 2017). Generally, a meteorological in-dependent criterion (I) (the period between individual storm events) is employed to distinguish two storm events. Considering the wave and morphology characteristics at Hasaki, the wave threshold for storm identification in specific objective 1 follows the approach proposed by Basco and Mahmoudpour (2012). Arithmetic mean (H_{S-mean}) and standard deviation (H_{S-std}) of hourly H_S measurements for 31 years (1987-2017) are used to calculate the wave threshold to separate storm events (Equation 3.1). In addition, the minimum duration, and meteorological independent criteria (I) of a storm event are set to 6 h and 24 h, respectively (Figure 3.9).

$$\text{Wave threshold} = H_{S-mean} + 2 \times H_{S-std} \tag{3.1}$$

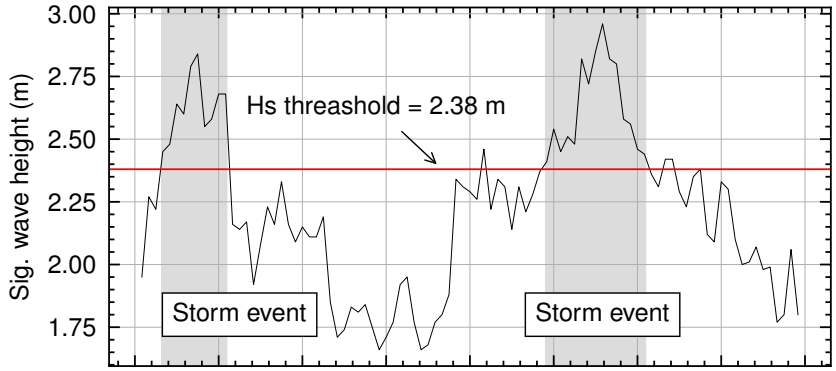

Figure 3.9: Storm event identification based on hourly significant wave height (24 h) and duration: two storm events are shown here.

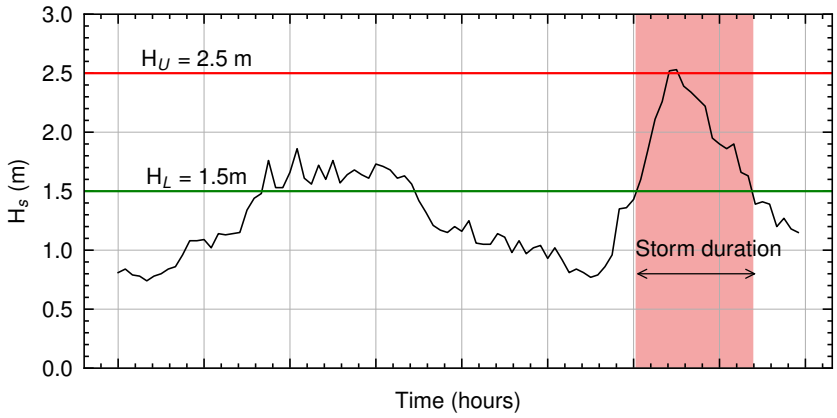

Figure 3.10: Storm event identification based on a two-threshold (Upper limit: H_U, Lower limit: H_L) significant wave height approach.

3.3.2 Site-specific threshold approach

A two-threshold approach was employed to identify storms based on significant wave height (H_S). A minimum storm duration (D_{min}) of 6 h was applied to ensure the inclusion of only significant storm events. An upper threshold of 2.5 m (H_U) was utilized to identify storms, representing the minimum requirement for Hs. Subsequently, a lower threshold of 1.5 m (H_L) was employed to identify the effective duration of the storm (Figure 3.10). These two thresholds were derived considering the long-term characteristics of the offshore wave climate at Hasaki (Kuriyama et al., 2012).

3.4 Regression models

Prior to the quantification of BVI, two regression models, MLR (in specific objective 1 & 2) and ANN (in specific objective 2), were trained to predict shoreline erosion, and based on the predictions, beach vulnerability is indexed. To train and test the two regression models, the data were randomly split using Sklearn's data splitting library (Pedregosa et al., 2011) in specific objective 2. The training data was further divided into 80 % for training and 20 % for validation, only for the ANN model, while 5 % of the initial data was reserved for testing purposes. Regression model performances were evaluated using the coefficient of determination (R^2 Score) metric, which measures the proportion of variance in the target variable that is explained by the model (Equation 3.2).

$$R^2 \text{ Score} = 1 - \frac{\sum (y_i - f_i)^2}{\sum (y_i - \bar{y})^2} \tag{3.2}$$

Where, y_i, f_i, and $\bar{y}$ denote observed data, predicted data, and the mean of the observed data set, respectively.

3.4.1 Multiple linear regression

Multiple linear regression (MLR) is a statistical technique commonly used to analyze quantitative data that models the relationship between multiple independent variables and a dependent variable. The goal of MLR is to find the best-fitting linear equation that represents the relationship between the variables, based on the available data. Initial shoreline position [m], storm power [m^2 h], and maximum surge [m] were selected as inputs for both the MLR to predict dSL [m] considering its higher correlation with dSL. Whereas for the specific objective 2, when larger storm data were tested, foreshore slope was also selected.

3.4.2 Artificial Neural Network

Artificial Neural Network (ANN) is a powerful machine learning model used in regression as well as for classification objectives. It consists of neurons and hidden layers which connect the input variables with the output (Figure 3.11). These neurons are adjusted to learn from the data using a large number of parameters, and they are updated through a process called feed-forward back-propagation. Also, hyper-parameters are used to set the Neural Net architecture where they are set

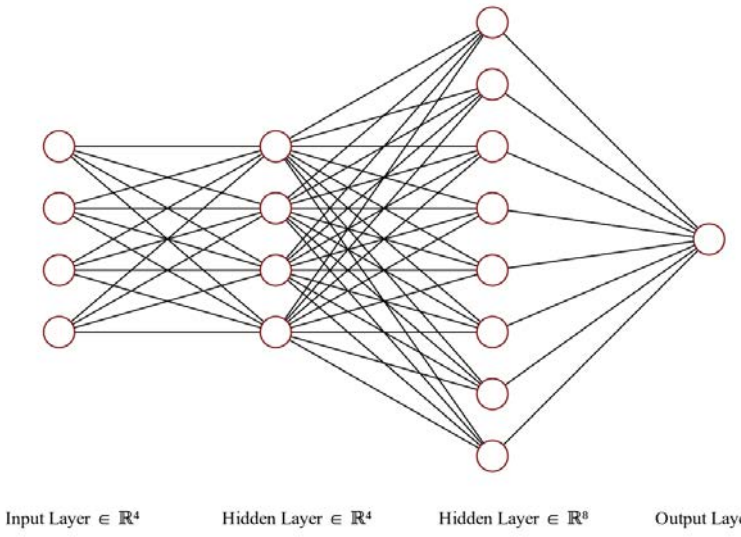

Figure 3.11: Example architecture of an artificial neural network setup with 4 input variables (indicators), two hidden layer designs with a neuron setup of (4×8).

prior to the training of the model and remain constant during the training and testing.

The accuracy of ANNs highly depends on the number of neurons and the complexity of the layers. Figure 3.12 shows the model performance variation in training and testing for different numbers of neurons and hidden layers in the ANN architecture. Once the model has been trained, it can be used to predict outputs from unseen input variables (testing). Tuning the ANN model can be a challenging task due to the need to optimize multiple hyper-parameters and select the best network architectures. The model had to be run a considerable number of times to achieve good training and testing performance before tuning the hyper-parameters. The best-performing initial ANN model was with two hidden layers, each containing 256 and 64 neurons, respectively when tested for predicting dSL. This model employs a dropout rate of 0.4 to mitigate over-fitting, a common issue in deep learning models. A learning rate of 0.01 was chosen as a starting point for optimizing the model's parameters. The batch size of 32 suggests that the model is trained on 32 samples at a time before updating the model's parameters. The model was tested for 1000 epochs, but the early stopping at 400 epochs is used to avoid over-fitting and increase the efficiency of the model. The model uses the normal distribution as the initializer for the kernels and the activation function ReLU (Schmidt-Hieber, 2020)

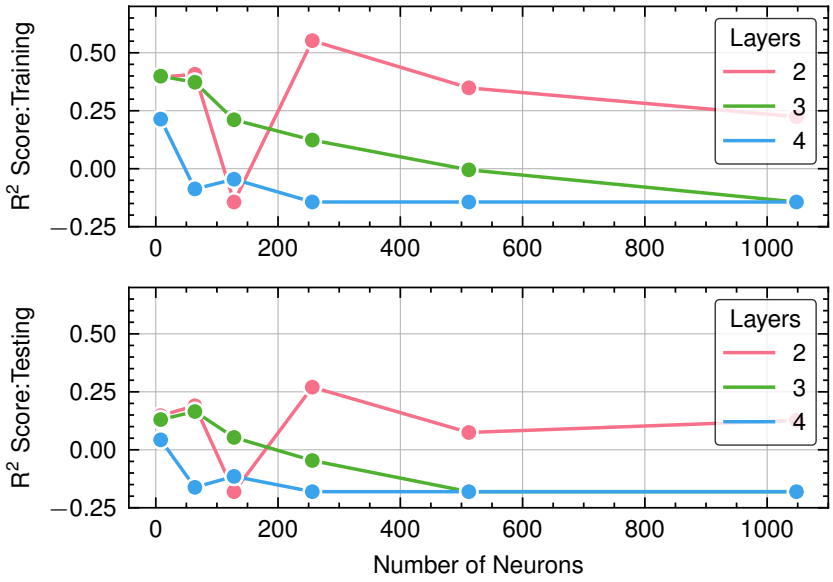

Figure 3.12: Initial Model setup: performance of ANN with training and testing data sets for shoreline change prediction in different model architectures. R^2 score is measured between prediction and observed dSL.

in the hidden layers. The activation function in the output layer is linear, which is appropriate for regression and other similar tasks (Ramsundar and Zadeh, 2018).

3.4.3 XGBoost

The eXtreme Gradient Boosting (XGBoost) algorithm was employed to correlate shoreline erosion will selected morphometric features in the specific objective 3 to quantify the feature importance in beach erosion. XGBoost is a highly scalable and efficient machine-learning algorithm used for regression and classification tasks. Based on the gradient boosting framework, the algorithm iteratively adds weak learners to an ensemble model and optimizes a loss function based on residual errors. In this dissertation, the XGBoost model and its weights in combination with SHAP feature importance are used to understand the impact of each morphometric feature on the erosion prediction. Notably, XGBoost is designed to handle missing data and outliers effectively and includes regularization parameters to prevent overfitting and improve model generalization. The use of XGBoost and SHAP feature importance allows for a comprehensive and interpretable analysis of the morphometric features that contribute most to beach erosion prediction.

The XGBoost model was trained with three hyperparameters, namely *n_estimat-*

ors, *max_depth*, and *learning_rate*. The *n_estimators* parameter defines the number of decision trees that are to be used in the model, which in this study was set to 1000. Increasing this parameter can result in better performance but at the expense of longer training times (Chen and Guestrin, 2016). The *max_depth* parameter, set to 10 in this study, specifies the maximum depth of each decision tree. This parameter affects the complexity of each decision tree and controls the level of overfitting in the model. A higher value of *max_depth* can lead to more complex trees, but also increase the risk of overfitting (Chen and Guestrin, 2016). Finally, the *learning_rate* parameter sets the step size at each iteration of the boosting process, which was set to 0.1 in this study. This parameter impacts the rate of convergence and the size of the update at each step. The XGBoost model is designed to effectively learn the complex relationships between the input features and the output target, providing accurate predictions of volumetric erosion (Chen and Guestrin, 2016).

3.5 SHAP explanation method

SHAP (SHapley Additive exPlanations) is a widely recognized technique that leverages cooperative game theory's concept of Shapley values to elucidate the predictions made by intricate machine learning models (Lundberg and Lee, 2017). The methodology quantifies the contribution of each feature in a prediction by determining the marginal contributions of every feature to the model output, ascertained by contrasting the forecast of the complete feature set with the predictions when each feature is removed. The marginal contributions are aggregated using a weighted sum to derive the Shapley value for each feature. The weighting scheme takes into account the number of conceivable feature combinations that include or exclude the evaluated feature. By calculating Shapley values for each feature across multiple predictions, SHAP can provide a global or local explanation for individual predictions. Figure 3.13 illustrates the local interpretability of SHAP explanation method, especially the black block behaviour of novel deep learning approaches can be explained by these.

The main equation used to calculate SHAP (SHapley Additive exPlanations) values is the Shapley value equation (Equation 3.3), which is used to determine the marginal contribution of each feature to the model output.

$$\Phi_i = \frac{1}{M!} \sum_{R} E[f(x)|x_{S_i^R \cup i}] - E[f(x)|x_{S_i^R}] \tag{3.3}$$

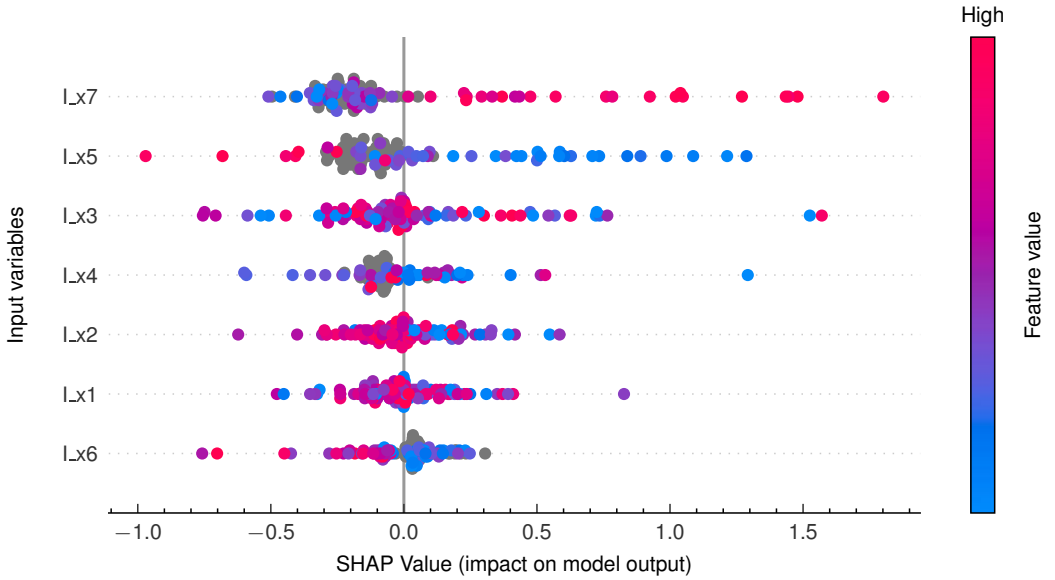

Figure 3.13: An example of the local interpretability of SHAP explanation method. Color bar shows the feature value. Positive SHAP values denote positive contributions to the output.

Where, Φ_i represents the Shapley value for feature i, $E[f(x)|x_{S_i^R \cup i}]$ represents the expected model output, for instance, R when feature i is included, $E[f(x)|x_{S_i^R}]$ represents the expected model output, for instance, R when feature i is not included, and M is the total number of possible combinations of features (coalitions).

3.6 Beach Vulnerability Application

This sub-chapter centers on the methods applied to the development of applications for beach vulnerability assessment, specifically the calculation of the Beach Vulnerability Index (BVI). The analysis begins with fitting regression models to an 8-year data set to quantify the BVI (specific objective 1). Subsequently, a larger storm data set spanning 24 years was utilized to showcase the application of a neural network-based approach for BVI quantification (specific objective 2). The aim was to gain a comprehensive understanding of beach vulnerability and its response to storm events.

3.6.1 Preliminary Approach

In this Preliminary Approach, a smaller data set of storms was utilized to quantify BVI. The data set was divided into separate groups based on chronological periods, with the training group covering 1993-1997 and the testing group covering 1997-2000. Beach erosion measurements, specifically shoreline change (dSL) and volume change (dV), were analyzed during the model training period to assess beach vulnerability to storm-induced erosion along the Hasaki coast. Based on the ranges of dSL and dV values, five vulnerability classes (1 to 5) were defined to indicate the level of vulnerability for beach erosion. A Vulnerability Index (VI) was assigned to each class, with VI_{dSL} representing shoreline change vulnerability and VI_{dV} representing volume change vulnerability. The final BVI was then calculated as the simple arithmetic mean of VI_{dSL} and VI_{dV} using Equation 3.4.

$$\mathrm{BVI} = \frac{VI_{dSL} + VI_{dV}}{2} \tag{3.4}$$

Later the predicted beach erosion measurements from the regression model and observed beach erosion measurements (from SE_{TS-1} to SE_{TS-10}) were used to calculate and compare the BVI values in the testing phase of the present study. During the preliminary stage, it was highlighted having two separate sub-Vulnerability Indices of VI_{dSL} and VI_{dV} would be helpful, as it indicates probable erosion values of dSL and dV.

3.6.2 Improved Approach

Based on the initial findings, a better understanding of data fitting was obtained, leading to the development of an improved Beach Vulnerability Index (BVI) application using the complete storm data set from 1987 to 2010. However, during the analysis of the complete data set, a strong correlation ($r^2 = 0.88$) was observed between volumetric erosion (dV) and shoreline change (dSL) of beach profile changes at HORS. As a result, only dSL was used to estimate beach vulnerability. The vulnerability ranges were defined based on the distribution of dSL values in the complete storm data set, and five vulnerability classes were proposed (Table 3.2). This was based on a frequency analysis shown in Figure 3.14. A BVI value of 1 indicates a shoreline shift seaward, indicating no erosion. Class ranges of 2, 3, 4, and 5 were defined based on the distribution of dSL values, where higher values indicate the need for precautionary measures. The BVI estimations from the ANN and MLR models are denoted as BVI_{ANN} and BVI_{MLR}, respectively, while the observed

shoreline-change-based BVI calculation is represented as BVI_{obs}. The performance of each model was compared with BVI_{obs}.

Table 3.2: Vulnerability class ranges for beach vulnerability index (BVI) quantification. Shoreline accretion is denoted as BVI of 1.

Shoreline erosion measurement ranges (dSL)	BVI
>8.0 m	5
4.0 m to 8.0 m	4
2.0 m to 4.0 m	3
0.0 m to 2.0 m	2
Shoreline accretion	1

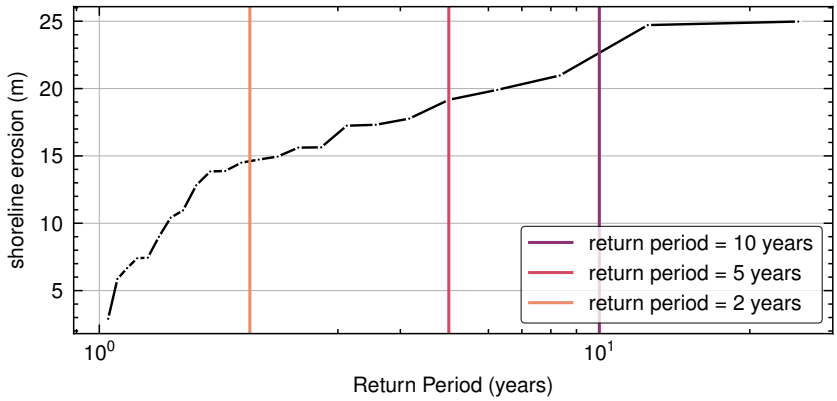

Figure 3.14: Return Period Analysis of Shoreline Changes at Hasaki Beach.

3.7 Comprehensive analysis on beach vulnerability

The comprehensive analysis on beach vulnerability delved into a detailed exploration of the factors influencing beach vulnerability and sought to enhance the current understanding of coastal process. This analysis took into account various elements such as storm characteristics, beach morphometrics, and temporal variations to evaluate the susceptibility and resilience of beaches to erosion. By conducting an in-depth examination, this chapter aims to provide valuable insights into beach vulnerability, particularly regarding its susceptibility and resilience-related characteristics.

The Hasaki beach was characterized by two distinct morphometric zones based on frequent wave breaking point: the inner zone spanning from 20.0 m to 170.0 m,

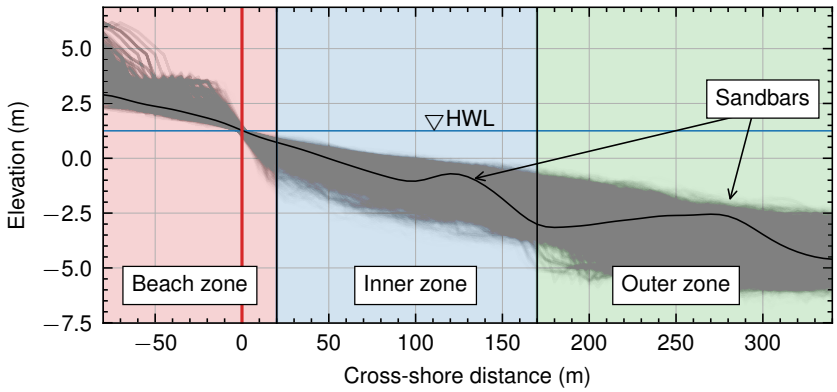

Figure 3.15: Profile definition based on shoreline position. The beach zone, the inner sandbar zone, and the outer sandbar zone are colored red, blue, and green, respectively.

and the outer zone ranging from 170.0 m to 340.0 m. Figure 3.15 illustrates the definition of these zones, with a highlighted profile displaying double sandbar formations within the profile envelope. The beach profiles were categorized into four groups based on the presence and location of sandbar formations: unbarred profiles, inner zone sandbar profiles, outer zone sandbar profiles, and double sandbar profiles (Figure 3.16). Statistical approaches were employed to quantify the internal characteristics of susceptibility and resilience for each profile type in relation to storm-induced erosion. The aim was to identify the specific characteristics that render each profile type vulnerable to erosion. Sandbar formations also indicate different stages of long-term sandbar migration, and the profile patterning was expected to aid in understanding such complexities. In a recent study, Janušaitė et al. (2021) examined the realignment of nearshore sandbars and its impact on nearshore and sub-aerial beach changes. They emphasized the significance of sandbar relocation, cross-shore position, shoreline dynamics, and sand volume changes in beach erosion. While the present dissertation primarily focuses on storm-related timescales, the findings of Janušaitė et al. (2021) regarding long-term morphological changes remain applicable and relevant.

Daily cross-shore survey data were used to identify sandbar formations. A Gaussian 1d filter from the Python library SciPy was used to obtain smooth profiling (Virtanen et al., 2020). Then, another signal processing toolbox based on Python was used to identify the bar crests and troughs (Virtanen et al., 2020). Based on the sandbar characteristics at Hasaki, minimum sandbar height threshold values of 0.2 m and 0.4 m were used to filter the inner zone and outer zone formations, respectively.

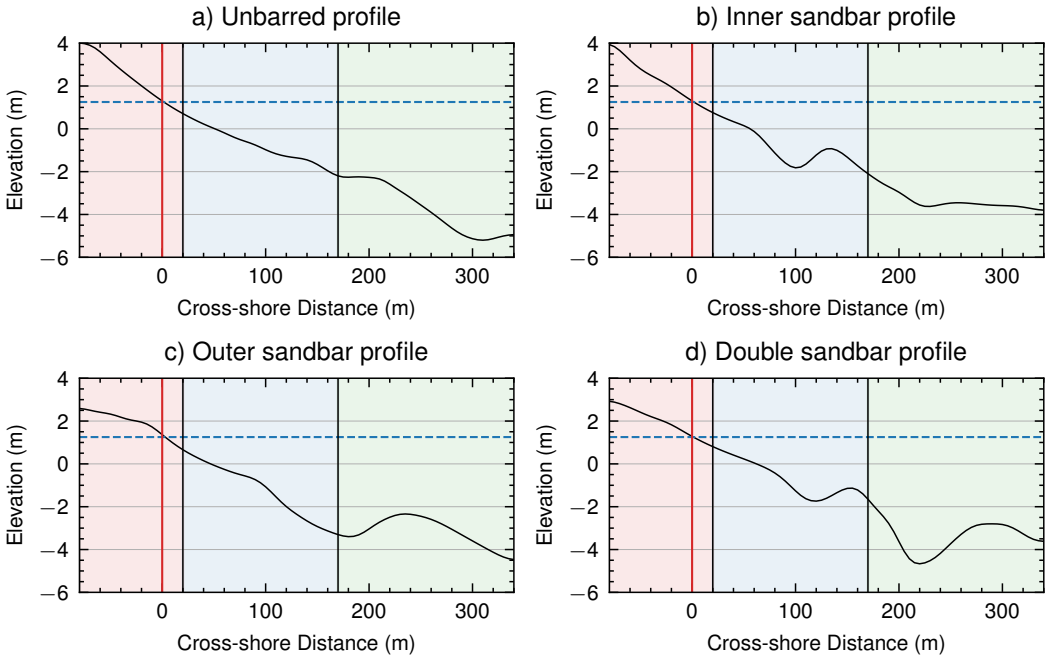

Figure 3.16: Main beach profile patterns: a) unbarred profiles, b) inner zone sandbar, c) outer zone sandbar, and d) multiple sandbar formations.

The distance to the sandbar crest was calculated from the shoreline position. Sandbar depth was defined as the water depth from the HWL (1.252 m) to bar crest. Bar height was calculated as the vertical distance between the crest and the line joining the adjoining troughs (Figure 3.8). Also, the sandbar slopes in the seaward and the landward faces were calculated and later used in the feature selection for the comprehensive analysis.

3.7.1 Beach susceptibility

Through SHAP value analysis, key morphometric indicators that influence beach erosion during storm conditions for each of the four profile types were identified. These indicators were then used to develop a susceptible metric, Beach Erosion Susceptibility Number (BESN), with each indicator weighted according to its contribution to the predictions of XGBoost model. To ensure generalizability, a weight function was introduced for each morphometric indicator that mainly depends on the value of the indicator. By incorporating these methods, it was expected to gain a better understanding of the impact of morphometric indicators on beach erosion and provide a more accurate and comprehensive tool for coastal engineering man-

agement to quantify beach susceptibility. Table 3.3 shows descriptions for all the indicators selected for this comprehensive analysis.

Table 3.3: Morphometric variables (indicators) used in this analysis to quantify the beach profile susceptibility.

Notation	indicator	Description
A	Shoreline position [m]	Shoreline of the previous day's beach profile
B	Inner zone sediment volume [$m^3\ m^{-1}$]	Volumetric sediment deposition in the inner zone
C	Outer zone sediment volume [$m^3\ m^{-1}$]	Volumetric sediment deposition in the outer zone
D	Beach slope	Tangential beach slope (vertical height/100 m)
E	Inner sandbar height [m]	Sandbar formations in the inner zone (20 m to 170 m) are characterized based on Figure 3.15
F	Inner sandbar distance [m]	
G	Inner sandbar water depth [m]	
H	Inner sandbar landward slope	
I	Inner sandbar landward slope	
J	Outer sandbar height [m]	Sandbar formations in the outer zone (170 m to 340 m) are characterized based on Figure 3.15
K	Outer sandbar distance [m]	
L	Outer sandbar water depth [m]	
M	Outer sandbar landward slope	
N	Outer sandbar landward slope	

After identifying the key indicators using XGBoost and SHAP explanation methods, the selected indicators are utilized to quantify the susceptibility characteristic of the beach profile by considering their magnitude and significance in relation to beach erosion. Each morphometric indicator is denoted as I. The steps involved in generating the BESN are outlined below.

Step 1: Indicator Normalization

Normalization was applied to each indicator to ensure the generalizability of the BESN across different sites and disregard the original value ranges. This was particularly important as the value ranges of the indicators can vary significantly. For example, the shoreline indicator might range from −36.9 m to 45.7 m, while the inner sandbar height indicator might range from 0.2 m to 2.3 m. To achieve normalization, the indicator values were transformed using Equation 3.5.

$$I_{\text{norm}} = \frac{I - I_{\text{min}}}{I_{\text{max}} - I_{\text{min}}} \tag{3.5}$$

Step 2: Weights for BESN

Weights were assigned to each normalized indicator to account for their varying contributions to beach erosion and, consequently, beach susceptibility. The weights (w_i) were determined based on the SHAP values, which quantify the impact of each indicator on beach susceptibility. Equation 3.6 was used to ensure that the weights add up to one and maintain their relative proportions.

$$\bar{w}_i = \frac{w_i}{\sum_i w_i} \tag{3.6}$$

Step 3: Linear functions for weights

A linear function was introduced to capture the relationships between SHAP values and indicator weights more accurately. This was necessary due to the observed variation in SHAP values for different indicator values, which also affected the corresponding weights. We could better account for the complex relationships between indicators and beach susceptibility by calculating coefficients c_f and m for each selected indicator within each profile pattern, leveraging the local interpretability of SHAP values (Equation 3.7).

$$\bar{w}_i = c_f I_i + m \tag{3.7}$$

Step 4: Discretization of BESN generations

In the final step of the BESN generation process, the continuous BESN data obtained by multiplying the corresponding I_i values with Equation 3.7 were discretized into five separate data bins using NumPy (Equation 3.8)(Harris et al., 2020). This dis-

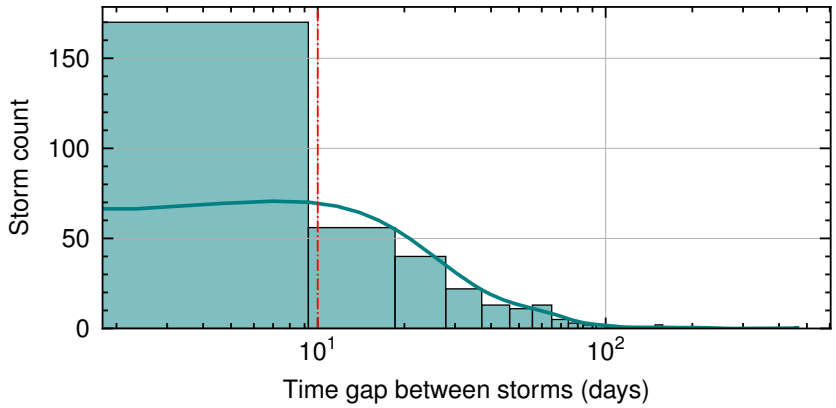

Figure 3.17: Distribution of time gap between two storm events. Based on this a 10-day period was decided for the beach recovery analysis.

cretization enabled us to categorize the beach profiles effectively according to their susceptibility to erosion. Higher BESN values indicated a greater vulnerability to erosion, while lower values suggested a lower susceptibility.

$$\text{BESN} = \text{discretize}\left(\sum (c_f I_i + m) I_i\right) \tag{3.8}$$

3.7.2 Beach resilience

The Beach Resilience Number (BRN) was proposed to quantify the recovery potential of different beach profile patterns. The ratio between the shoreline recovery after an n-day period and the shoreline erosion during the storm event was defined as the BRN in this study (Equation 3.9). Moreover, the post-storm duration to quantify short-term recovery was defined based on the study area characteristics of recovery. While Eichentopf et al. (2020) proposed using an 18-day period to identify the presence of sequencing storm events, a 10-day period was selected for this study, considering the observed recovery and the need for sufficient data for the analysis. Figure3.17 shows the distribution of the time gap to the next storm event for all the selected cases in this study. Figure 3.18 illustrates the two-step criteria for the storm event selection for the BRN analysis.

$$BRN = \frac{\text{BR}}{dSL} \tag{3.9}$$

Where BR denotes the 10-day beach recovery, and dSL represents the shoreline erosion during the storm event.

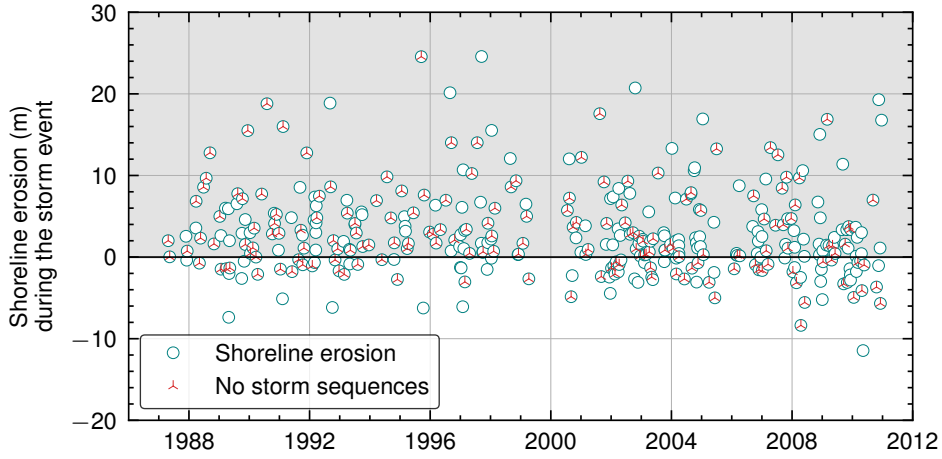

Figure 3.18: Storm event selection for the BRN analysis considering the absence of storms and positive shoreline erosion during the storm events.

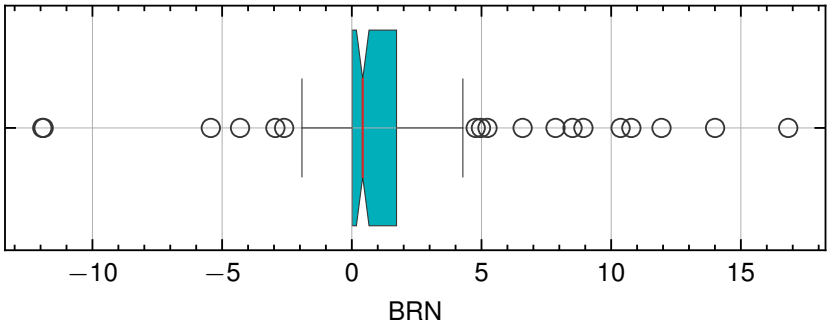

Figure 3.19: Outlier identification of the BRN distribution based on the first and third quantiles and interquartile ranges.

To begin, storm events with a sequenced occurrence during the 10-day post-storm period and those associated with shoreline accretion during the storm were excluded. Subsequently, the Beach Resilience Number (BRN) was calculated for the selected events. As BRN represents beach recovery relative to shoreline erosion, considering larger outliers would not yield meaningful insights. Thus, identification of outliers was based on the inter-quartile range of the BRN distributions. Outliers in the BRN calculation were then eliminated. Figure 3.19 shows the outlier identification approach employed in this study. A BRN value of 1 indicates complete recovery of the shoreline from the erosion attributed to the respective storm event (Equation 3.9). Conversely, a negative BRN indicates negative recovery, implying further erosion instances.

Given the limited number of storm datasets, particularly following the filtering process, applying XGBoost models to fit data for a regression model while incorporating influential morphological features and BRN could potentially raise concerns regarding the reliability of analysis results. However, four distinct XGBoost models were developed to evaluate beach resilience. Subsequently, the SHAP explanation method was employed to quantify the significance of each morphometric indicator.

Chapter 4

Beach vulnerability Index Application

In this chapter, the results of the developments in the Beach Vulnerability Index (BVI) are presented and discussed. Initially, a preliminary approach was employed with the smaller data set by applying the MLR model. Subsequently, the complete data set was utilized to enhance vulnerability prediction through the implementation of ANN.

- **Preliminary approach to quantify the beach vulnerability using linear regression models.**
- **Improved approach to quantify the beach vulnerability adding neural networks to the preliminary study.**

4.1 Preliminary approach to quantifying beach vulnerability

The reliminary approach tried to extend the research work by Malek et al. (2020) related to quantifying probable erosion in Hasaki beach. They have discussed the behavior of Hasaki beach morphology under storm conditions using a storm data set from 1993 to 1997. Hence, the preliminary approach also commenced with the same time period as a foundational point for exploring the development of BVI. It is important to note that this sub-chapter serves as an introductory exploration, laying the groundwork for the subsequent analysis with a larger data set, which will provide more comprehensive insights into beach vulnerability assessment.

4.1.1 Storm event identification

Over the 8-year study period, a total of 48 storm events were identified. The first 38 storm events, occurring between 1993 and 1997, were selected to train regression models for the purpose of predicting beach erosion. Among these events, the longest duration was 169 h with a maximum surge of 0.34 m, while another event experienced a maximum surge of 1.13 m. Additionally, the highest recorded energy flux reached 2.4×10^{11} kN s^{-1}.

Figure 4.1 shows scatter plots and individual linear regression lines of dSL and dV against each input variable. Colored triangular markers within the figure emphasize the four most severe storm events (shown in blue, orange, green, and purple) from the training data set. Despite two of these events having similar energy fluxes, the third event demonstrated substantial differences in dSL and dV. This divergence could be attributed to clear differences in initial shoreline positions, resulting in significant variations in beach erosion quantities.

During the testing period spanning from 1998 to 2000, a total of 10 storm events were identified. For instance, one storm event lasting 75 h (with an energy flux of 1.06×10^{10} kN s^{-1}) induced a volumetric alteration of 17.22 m^3 m^{-1} in the beach zone, along with a shoreline shift of 6.39 m. In contrast, another storm, lasting 25 h (with an energy flux of 3.45×10^9 kN s^{-1}), led to a more substantial beach zone erosion of 26.40 m^3 m^{-1} and a shoreline retreat of 15.5 m, signifying the most significant impact on the beach. Consequently, it became evident that beyond hydrodynamic factors, other contributing elements, such as morphological features, necessitate testing to establish a more precise framework for beach vulnerability assessment.

4.1.2 Multiple linear regression model

38 storm events in the training set were employed to create regression models for beach erosion predictions. Based on the distributions of dSL and dV with input parameters (E_f, SL_i, and S_{max}), a linear relationship is understood to be the best fit for regression models (Figure 4.1). Equation 4.1 and Equation 4.2 show the generated regression models to predict dSL and dV, respectively.

$$\mathrm{dSL} = 5.7 \times 10^{-10}(E_f) + 0.17(SL_i) + 10.8(S_{max}) - 2.1 \tag{4.1}$$

$$\mathrm{dV} = 13.3 \times 10^{-10}(E_f) + 0.19(SL_i) + 25.8(S_{max}) - 7.8 \tag{4.2}$$

Even though only four storm events had surpassed the energy flux of 1.0 ×

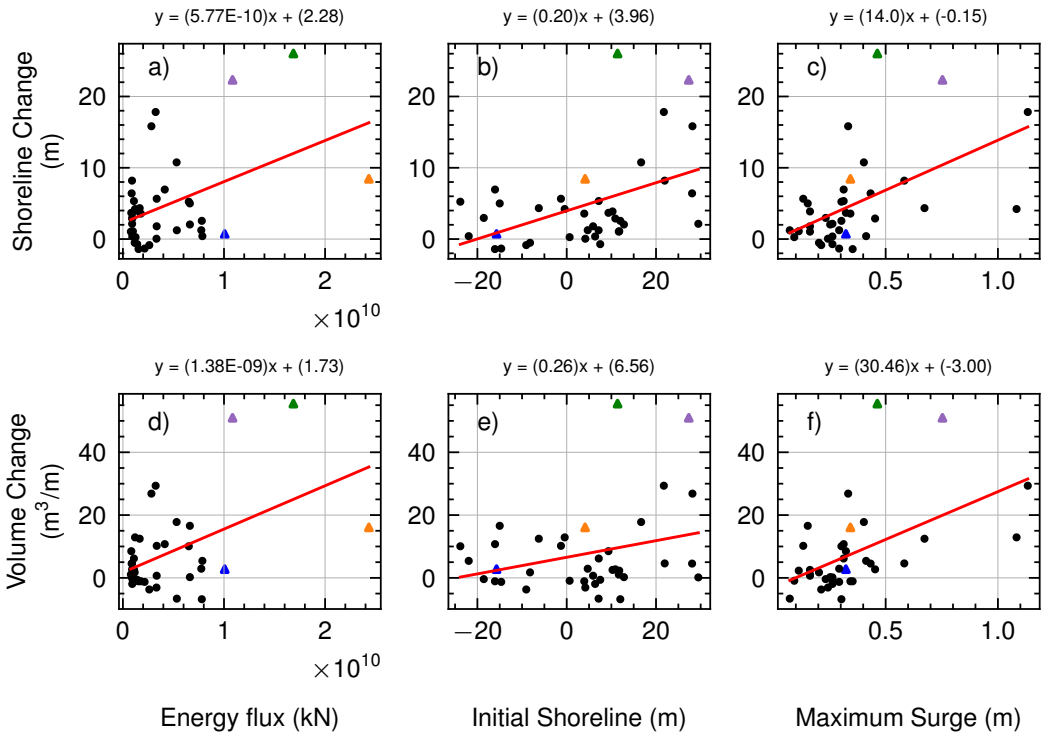

Figure 4.1: Scatter plots: shoreline change variation with: (a) energy flux, (b) initial shoreline, and (c) maximum surge and volume change variation with: (d) energy flux, (e) initial shoreline, and (f) maximum surge.

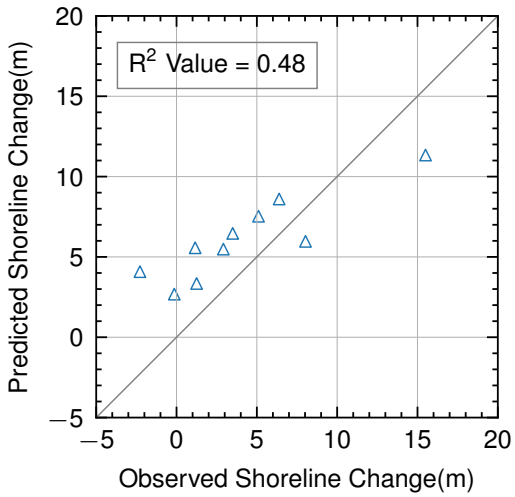

Figure 4.2: Validation of shoreline change (m) prediction of the linear regression model (Equation 4.1).

10^{10} kN s^{-1} (Figure 4.1 (a)), their inclusion in the regression model was vital as they incorporate extreme storm conditions to the model. Furthermore, R_2 scores (R_2) for each regression model on the training data set were 0.58 (Equation 4.1) and 0.52 (Equation 4.2) which showed a tolerable fit. Then the 10 storm events in the testing set were used to test the performance of the above two linear regression models. Figure 4.2 and Figure 4.3 show the scatter plot of observed and predicted values of dSL and dV, respectively. Model predictions showed that Equation 4.1 tends towards over predictions (positive error) of dSL while Equation 4.2 holds a much broader distribution of dV predictions which explains the relatively lower R_2 value compared to Equation 4.1. However, Root Mean Square Error (RMSE) values of dSL and dV predictions were 3.46 m and 6.56 m^3 m^{-1}, respectively. Whereas the Scatter Index (SI) values (Equation 4.3) indicated tolerable estimations (for dSL and dV, SI were 0.83 and 0.90, respectively).

$$SI = \frac{RMSE}{\text{mean of observed data}} \tag{4.3}$$

Despite the limited use of linear regression models in coastal morphological assessments, especially under strong wave conditions, the preliminary results demonstrated reliable accuracies. However, it is important to test recent advancements in advanced regression models such as ML for more precise beach change predictions. The simplicity of linear regression models, along with an acceptable degree of accuracy, provides a distinct advantage compared to the mostly black-box appli-

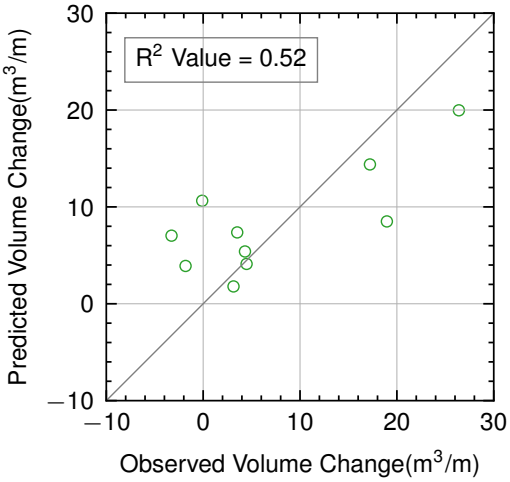

Figure 4.3: Validation of volumetric change ($m^3\,m^{-1}$) prediction of the linear regression model (Equation 4.2).

cations of ML and Deep Learning (DL) algorithms. Linear regression models allow for easier implementation and interpretation, as well as the ability to identify and visualize inconsistencies and anomalies in the data. Additionally, individual data sets can be checked for the presence of anomalies. However, linear regression models are sensitive to outliers and prone to noise and overfitting, which is a significant drawback.

During this stage of the study, a total of 48 storm events were analyzed, allowing for the assessment of morphological and hydrodynamical conditions for each event. This explicit understanding of missing data, anomalies, and storm event characteristics greatly influenced the setup of the regression model. While the statistical indices indicated a promising performance of linear regression in predicting beach change, it was further observed that many of the data points were concentrated near the origin [0,0] (Figure 4.1).

4.1.3 BVI calculations

The 10 selected storm events from the testing period were utilized to establish and validate the preliminary Beach Vulnerability Index (BVI) approach. Firstly, two classes of Vulnerability Indices (VI), denoted as VIdSL and VIdV, were defined based on the historical distribution of changes in shoreline position (dSL) and volumetric changes (dV), respectively. The lowest VI value of 1 was assigned when the shoreline shifted seaward and beach volume experienced accretion, indicating no

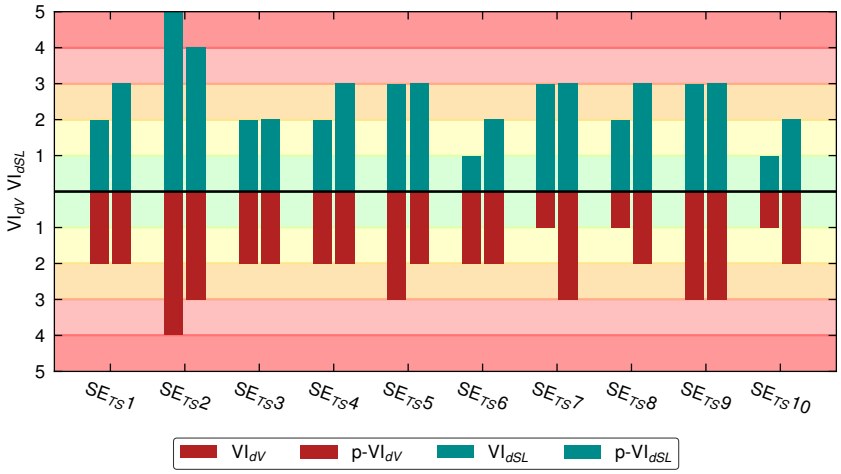

Figure 4.4: Components of BVIs during the testing period of 10 storm events. p-VI$_{dSL}$ and p-VI$_{dV}$ denote the predicted VI$_{dSL}$ and VI$_{dV}$ values.

erosion. Subsequently, following coastal vulnerability frameworks (Koroglu et al., 2019; Gornitz et al., 1991), VIdSL and VIdV class ranges of 2, 3, 4, and 5 were defined by categorizing dV and dSL values into four distinct classes. The subsequent calculation of the BVI was conducted for both observed and predicted measurements of beach erosion.

Figure 4.4 shows the distribution of observed and predicted BVI of storm events in the testing group. This graphical presentation further disintegrates BVI to VI$_{dSL}$ and VI$_{dV}$ to identify the dominant erosion factor (either dSL or dV). For example, SE$_{TS7}$ has a VI$_{dSL}$ of 3 and a VI$_{dV}$ of 1 which indicates a significant change to the shoreline, yet the volume change is negligible. In that event, the eroded volume remained within the beach zone limits, hence a negligible volumetric change and a significant shoreline change were observed. The majority of model predictions were slightly over-estimated. The model accurately predicted both components of BVI during SE$_{TS3}$ and SE$_{TS9}$. Only the BVI predictions of SE$_{TS27}$ and SE$_{TS5}$ were under-predicted and the prediction of VI$_{dV}$ (p-VI$_{dV}$) in SE$_{TS7}$ was also substandard. Nevertheless, five of the p-VI$_{dV}$ and four of p-VI$_{dSL}$ were accurate. Also, the relatively lower R^2 value of regression Equation 4.1 (for dSL) during the testing stage (0.48) compared with what was achieved during the training stage (0.58) might suggest an over-trained condition of the dSL model.

It is important to note that the interpretation of vulnerability is predominantly specific to the site in question. Therefore, the defined vulnerability class ranges should be applied cautiously and tailored to different locations and time frames as

needed.

4.2 Improved approach to quantifying beach vulnerability

This method parallels the approach outlined in the first specific objective, initially utilizing Multiple Linear Regression (MLR) in its analysis. However, to further refine the accuracy of capturing shoreline change and its subsequent integration into BVI calculations, a novel ANN regression model was employed. Moreover, considering the robust linear relationship observed between the variables dSL and dV, the investigation was confined to dSL. The assignment of BVI vulnerability classes for each dSL estimation was determined based on the criteria detailed in Table 3.2. The linear relationship between dV and dSL is shown in Figure 4.5, while Figure 4.6 provides a depiction of storm duration in relation to the initial shoreline variation for each storm event.

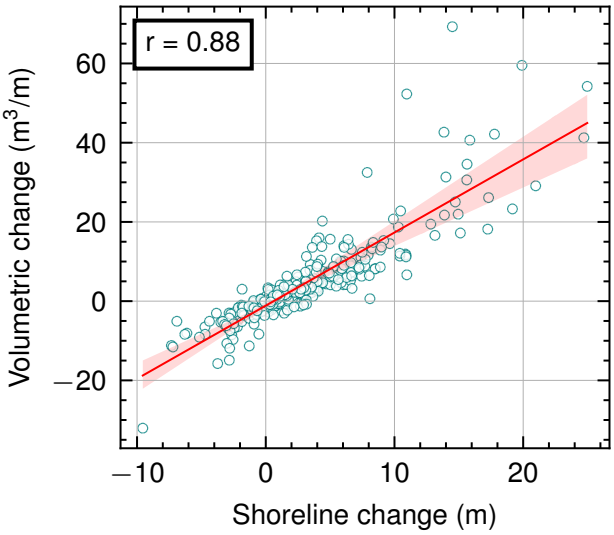

Figure 4.5: Correlation between the shoreline change [m] and volume change in the beach zone [$m^3\ m^{-1}$].

4.2.1 Storm event identification

During the 24-year study period, a total of 347 storm events were identified. To train and test the ANN and MLR models, the Sklearn library Pedregosa et al. (2011) randomly split these events into 329 storms for training and 18 storms for testing.

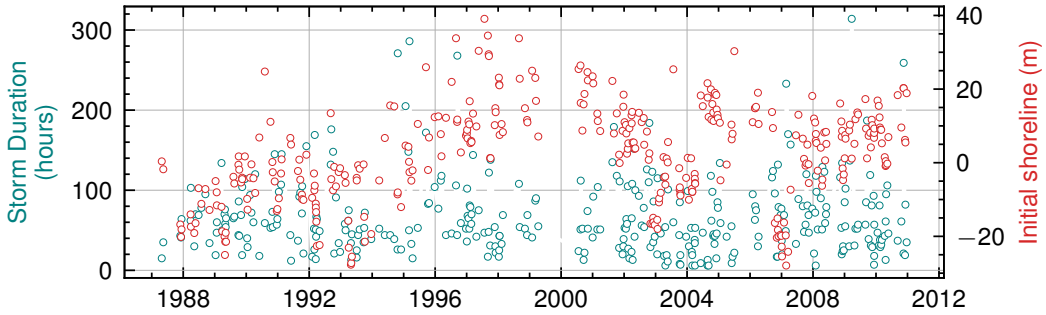

Figure 4.6: Distribution of storm duration and initial shoreline position: complete data set (1987-2010) - 347 storm events.

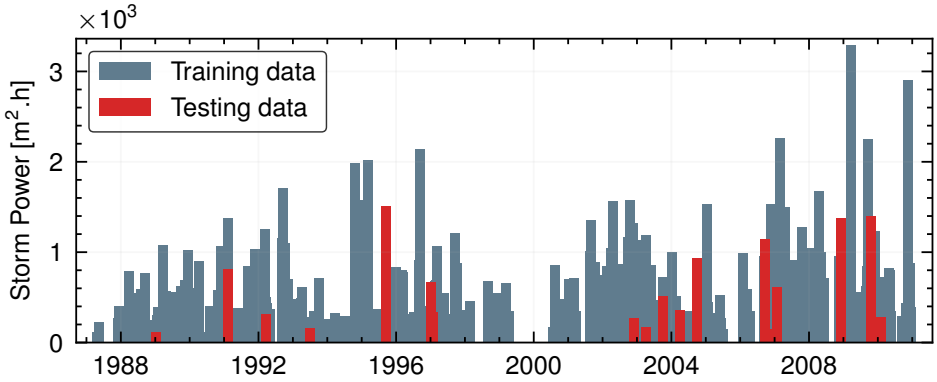

Figure 4.7: Storm event selection for training and testing of regression models: ANN and MLR.

The distribution of storm power for each storm is shown in Figure 4.7, with a suitable characteristic distribution achieved for both training and testing data sets. The longest storm event lasted for 314 h, while a separate storm event had a maximum surge of 1.5 m. The maximum initial beach slope was 0.0653 and the maximum storm power was 3296.25 m^2 h.

4.2.2 Multiple Linear Regression model

Figure 4.8 shows the distribution of the MLR prediction with the observed dSL. The R^2 score for the testing data was 0.35, indicating that the model can explain only 35% of the variance in the target variable. The R^2 Score for the training data is 0.26, suggesting that the model fails to exhibit satisfactory performance even when evaluated on the data used for its training. MLR tends to under-predict most of the dSL, especially the severe shoreline changes (Figure 4.8-(b)). This questions the

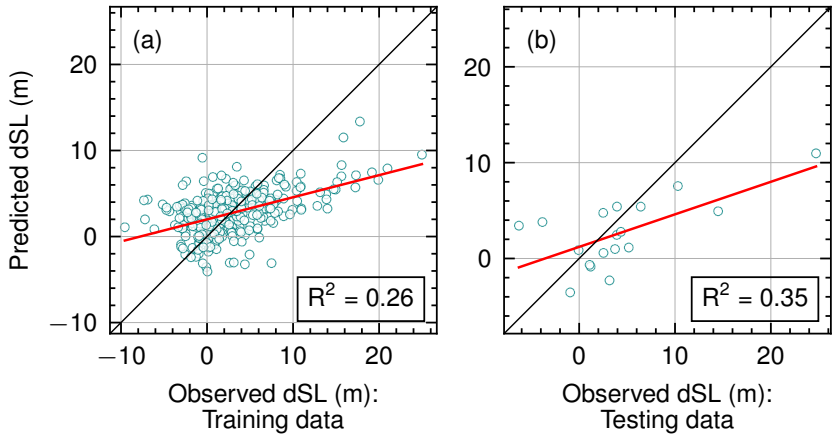

Figure 4.8: Multiple Linear Regression (MLR) model performance: (a) training data set (329 storms) and (b) testing data set (18 storms).

prediction capabilities of MLR especially for extreme erosion conditions.

4.2.3 Artificial Neural Networks

Figure 4.9 shows the distribution of the ANN prediction with the actual observation of dSL. The performance of the described ANN model was evaluated using the R^2 score metric. The R^2 Score for the testing data was 0.62, indicating that the model can explain 62% of the variance in the target variable. An R^2 Score of 0.68 was achieved for training data. The training and testing performances of a model need careful attention to balance the generalization with good prediction capability.

4.2.4 Beach Vulnerability Index calculations

The violin plots in Figure 4.10 compare BVI_{ANN} and BVI_{MLR} with BVI_{obs}. The second specific objective also revolves around assessing the BVI prediction accuracy of the two regression models. As anticipated, ANN demonstrated superior performance compared to MLR. There is a noticeable deviation in the distribution of BVI_{MLR} from BVI_{obs} for classes 1, 2, and 3. However, for class 4 of BVI_{obs}, which corresponds to dSL values in the range of 4.0 m to 8.0 m, BVI_{MLR} exhibited relatively accurate results. On the contrary, for class 5 of BVI_{obs}, representing the highest vulnerability category, BVI_{MLR} displayed significant underestimation, while BVI_{ANN} showed promising outcomes.

The Kernal Density Estimate (KDE) plots were also used to compare the BVI_{ANN} and BVI_{MLR} (Figure 4.11). Darker areas of the KDE plotS in Figure 4.11 show higher

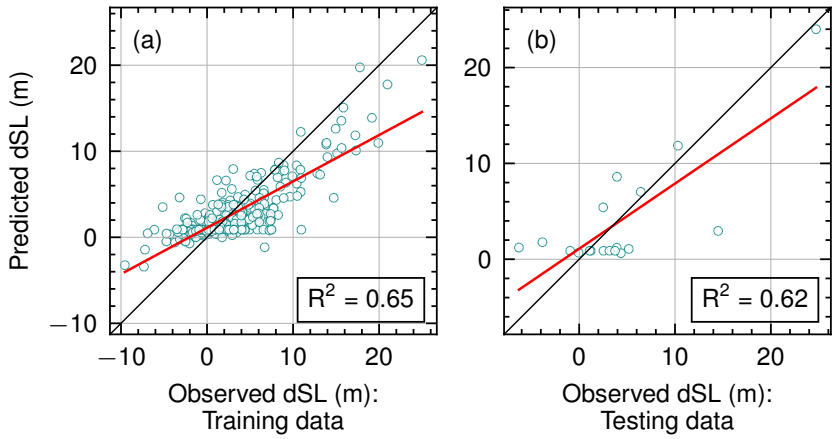

Figure 4.9: Artificial Neural network (BVI_{MLR}) model performance: (a) training data set (329 storms) and (b) testing data set (18 storms).

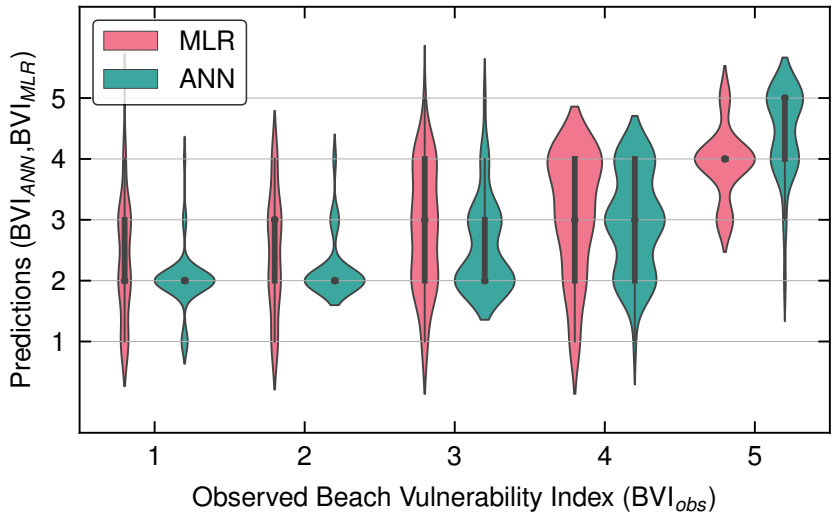

Figure 4.10: Violin plots showing the distribution of BVI predictions (BVI_{ANN} and BVI_{MLR}) of each model with respect to observed BVI. The bar in the violin plots shows the first quantile, median, and third quantile of distribution. The width of the violins indicates the number of observations in each bin (1 to 5).

frequency distributions of BVI_{MLR} and BVI_{ANN}. The Mean Absolute Errors (MAE) for each of the five BVI classes (from 1 to 5) were calculated and found that the ANN model performed better than MLR. BVI_{ANN}: 1.00, 0.20, 0.69, 1.05, 0.57 and BVI_{MLR}: 1.33, 0.83, 0.78, 0.90, 1.07 for which showed the better prediction capabilities of BVI_{MLR}, especially for BVIs 2, 3, and 5. The vertically concentrated distribution in Figure 4.11-(e) emphasizes the poor predictions of MLR when severe erosion-driven vulnerabilities were present.

4.3 Summary of the findings

The preliminary approach to quantifying beach vulnerability employed linear regression models to predict dSL and dV based on storm characteristics of energy flux, maximum surge, and initial shoreline as the morphological characteristic. These models exhibited a satisfactory fit on the training data set. When tested on a separate dataset of 10 storm events, they slightly over-predicted dSL. The preliminary outcomes showcased reliable accuracies of the linear regression models in forecasting beach change, while acknowledging their limitations such as sensitivity to outliers and overfitting. The graphical representation of BVI components aided in identifying the dominant erosion factor for each storm event. While most model predictions slightly overestimated BVI, the overall performance was deemed acceptable, despite some instances of under-predictions and substandard results. Additionally, the regression model's performance during testing exhibited a lower R^2 value compared to the training stage, suggesting potential over-training.

In the improved approach, which utilized the complete storm data set, the focus narrowed down to dSL, and a novel ANN model was tested. The performance of the ANN model was assessed using the R^2 score metric, achieving a score of 0.62 for the testing data. This score indicates its enhanced ability to explain the variance in the target variable compared to linear regression models. Particularly, the ANN model outperformed the MLR model for higher vulnerability classes. Further validation was confirmed through MAE calculations, substantiating the superior prediction capabilities of the ANN model.

While the preliminary approach demonstrated reliable accuracies of linear regression models with short-term storm data, their performance was less favorable with a larger dataset, emphasizing the importance of a better sample size of beach responses to storms. The improved approach, incorporating ANN models, exhibited enhanced prediction capabilities and surpassed the linear regression models.

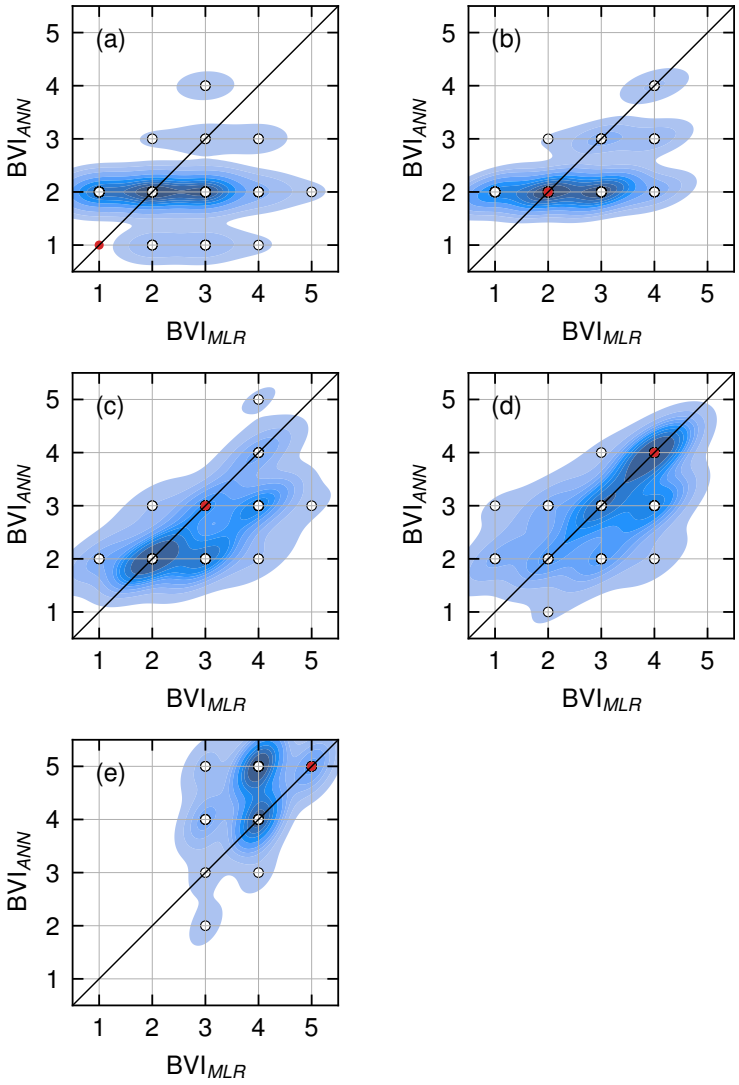

Figure 4.11: Density plots showing the distribution of BVI predictions (BVI_{ANN} and BVI_{MLR}) of ANN and MLR models for the extreme BVI_{obs}. (a) to (e) are for BVI_{obs} values of 1 to 5, respectively.

Nonetheless, it is essential to strike a balance between the model's generalization and its prediction capability. The BVI methodology presented in this chapter finds applicability in sandy beaches with ecological and economic values. The findings contribute to comprehending the quantification of beach vulnerability and underscore the potential of machine learning algorithms in erosion prediction.

Chapter 5

Comprehensive analysis on beach vulnerability

In this chapter, the results of quantifying beach susceptibility using SHAP value explanations and XGBoost regression approaches, along with the analysis of beach resilience, are presented and discussed. The same storm data set used in the second specific objective was employed for this analysis. Fourteen beach morphometric variables were utilized to quantify the vulnerability components of susceptibility and resilience. A summary of the statistical data for these 14 morphometric variables corresponding to each pre-storm beach profile is presented in Table 5.1.

5.1 Beach susceptibility

Statistical tests were conducted on 14 morphometric variables, encompassing shoreline position, sediment volume in each zone, beach slope, and sandbar characteristics. These tests aimed to investigate the correlation between these variables and beach erosion, thereby determining beach susceptibility. By analyzing the SHAP feature importance values, specific morphometric variables were identified as key factors for each profile type. To provide a quantitative assessment of the susceptibility of each profile type to beach erosion, a metric called the Beach Erosion Susceptibility Number (BESN) was developed.

5.1.1 Key morphometric indicators on beach vulnerability

The classification of the four beach profile patterns was established according to the presence and location of sandbar formations. These patterns are referred to as

Table 5.1: Variable description and statistics summary of all the 14 morphometric variables.

ID	Morphometric Variable	Mean	Min	Max	St. d
A	Shoreline [m]	2.66	-27.93	39.09	12.97
B	Inner zone volume [$m^3\ m^{-1}$]	382.90	71.47	489.83	76.01
C	Outer zone volume [$m^3\ m^{-1}$]	436.13	187.77	611.63	83.32
D	Beach slope	0.0336	0.172	0.0653	0.0107
E	Inner zone sandbar Height ([m]	0.90	0.25	2.32	0.48
F	Inner zone sandbar distance [m]	132.15	55.00	170.00	27.59
G	Inner zone sandbar depth [m]	2.31	1.04	4.10	0.65
H	Inner zone sandbar slope landward	0.0105	0.0003	0.0396	0.0083
I	Inner zone sandbar slope seaward	0.0312	0.0116	0.0605	0.0092
J	Outer zone sandbar height [m]	1.32	0.50	2.67	0.51
K	Outer zone sandbar distance [m]	245.65	175.00	335.00	48.86
L	Outer zone sandbar depth [m]	3.63	2.23	6.54	0.75
M	Outer zone sandbar slope landward	0.0177	0.0016	0.0483	0.0091
N	Outer zone sandbar slope seaward	0.0215	0.0001	0.0474	0.0113

Unbarred profiles, Inner zone sandbar profiles, Outer zone sandbar profiles, and Double sandbar profiles. The distribution of profiles within each pattern is presented in Table 5.2.

Table 5.2: Number of beach profiles in each of four group.

Profile pattern	Number of profiles
Unbarred profiles	40
Inner sandbar profiles	92
Outer sandbar profiles	130
Double sandbar profiles	85

To create quantitative indicators of susceptibility for each profile type, distinct XGBoost regression models were trained employing the entire data set of storm events for each profile pattern, as detailed in Table 5.2. The models were evaluated in terms of their capacity to precisely fit the training data set, and all four models exhibited 100% accuracy, signifying a flawless fit. These outcomes indicate that the formulated models align perfectly with the training data, thus validating their use in generating SHAP values.

SHAP values were extracted for each storm case in each profile pattern (as local interpretations), resulting in a set of values quantifying the contribution of each

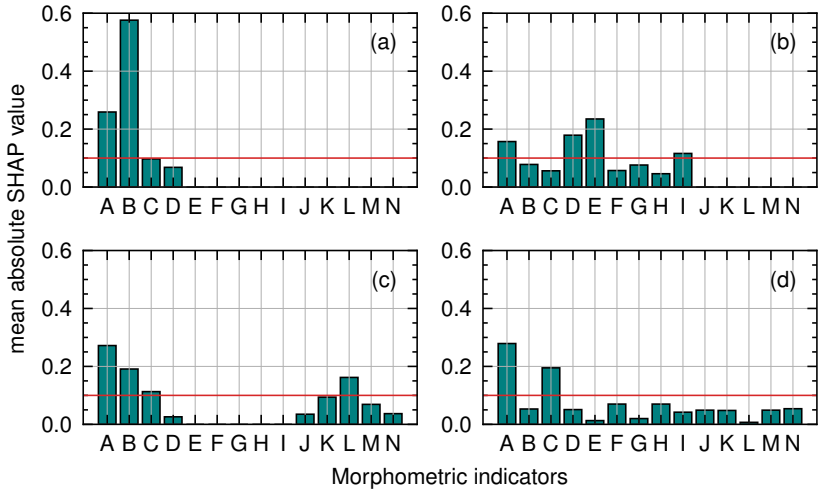

Figure 5.1: Indicator selection based on the SHAP values: Bar plots of mean absolute SHAP values for each morphometric indicator within each profile pattern. Table 5.1 presents terminologies of each ID.

morphometric in each event. Mean absolute values for each morphometric were calculated in each profile pattern to identify key morphometrics (w_i) in Equation3.6). To determine the relative contribution of each morphometric within the profile pattern, ($\bar{w}_i$) was calculated as described in Equation3.7. These SHAP values ($\bar{w}_i$), referred to as weights in the BESN generation, were normalized by dividing their sum. Further, a threshold of 0.1 was applied to identify the most significant morphometrics in each profile pattern.

Figure 5.1 shows the indicator selection for each profile pattern using the mean absolute SHAP values of each indicator. This analysis led to the identification of 7 significant morphometric variables that play a crucial role in influencing shoreline erosion. These variables were subsequently chosen for the development of BESN. The distribution of each of these selected morphometric indicators is shown in Figure 5.2. Furthermore, Figure 5.3 provides a graphical representation of the local interpretations of SHAP values for each morphometric indicator within each profile pattern. In this depiction, a positive value (+) indicates a contribution to beach erosion, while a negative value signifies the opposite effect.

5.1.2 Linear weight functions for each profile pattern

The relationships between the SHAP values and morphometric indicators are illustrated in Figure 5.4 through Figure 5.7. Utilizing these relationships, linear func-

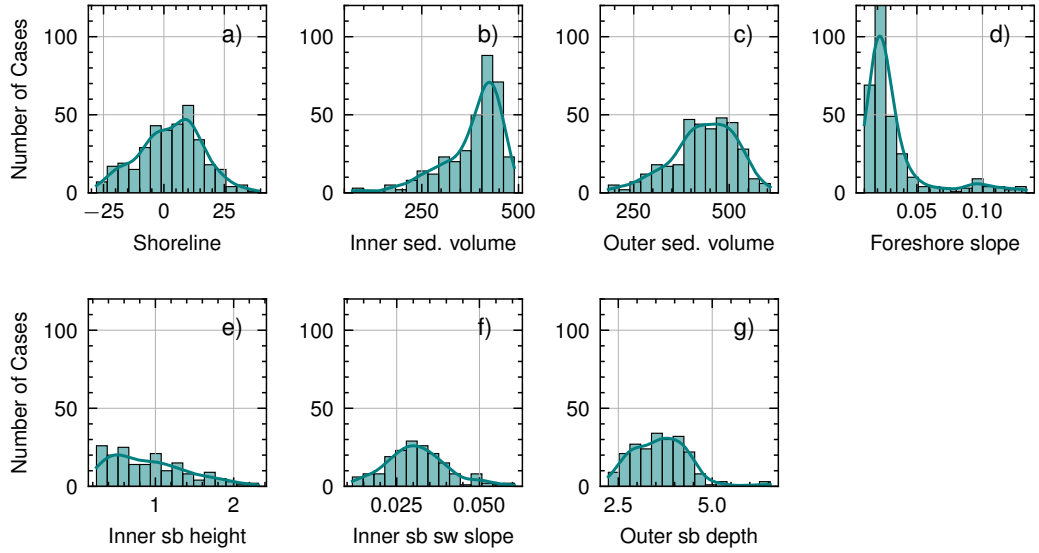

Figure 5.2: Histograms of the selected 7 morphometric indicators for the BESN quantification.

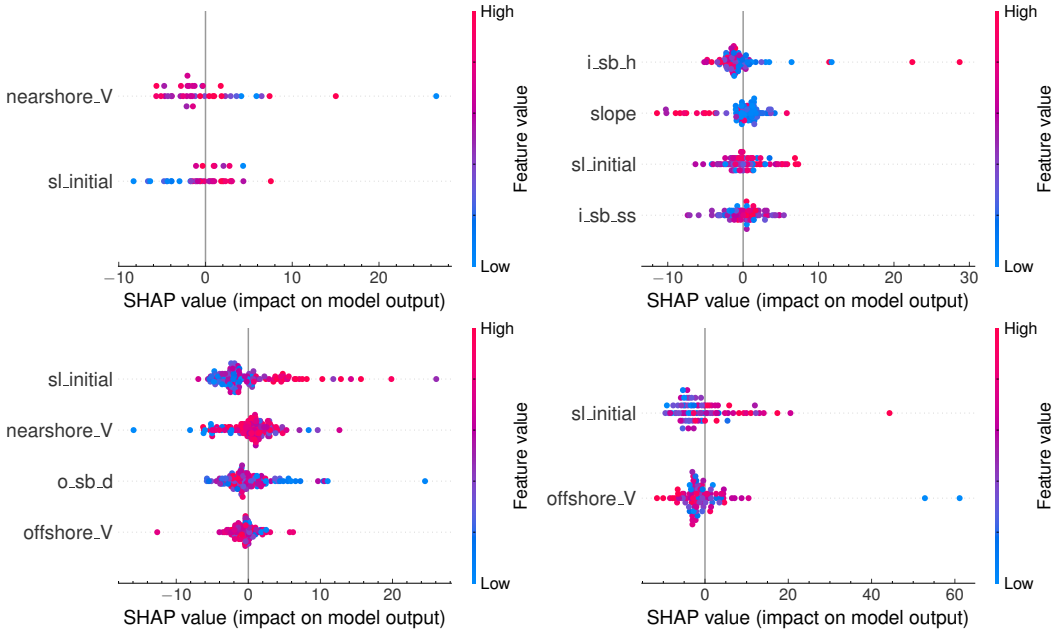

Figure 5.3: Distribution of the SHAP values for significant indicators of each of the profile pattern.

tions for the weights were formulated using Equation 3.7. The resultant weight functions are detailed in Table 5.3. Subsequently, BESN values were computed by applying the weight functions to the normalized indicators as described in Equation 3.8.

Table 5.3: Gradients (m) and coefficients (c_f) of weight functions for each morphometric indicator for different profile patterns.

Profile type	$\bar{w}_i$	**Morphometric values**						
		A	B	C	D	E	I	L
Unbarred	m	9.97	−21 04	–	–	–	–	–
	c_f	−4 67	17.08	–	–	–	–	–
Inner sandbar	m	4.77	–	–	−7 89	2.48	1.70	–
	c_f	−1 90	–	–	1.91	−1 15	−0 52	–
Outer sandbar	m	14.65	4.71	−2 89	–	–	–	−6 47
	c_f	−6 93	−3 13	1.40	–	–	–	1.99
Double sandbar	m	19.51	–	−31 28	–	–	–	–
	c_f	−8 85	–	20.88	–	–	–	–

Unbarred profiles

Figure 5.4 shows the distribution of SHAP values for each indicator in the presence of unbarred profiles. As shown in Figure5.4a and Figure5.4b, the initial shoreline (A) and inner-zone sediment volume (B) are the most influential indicators contributing to erosion susceptibility. Therefore, these indicators are identified as significant contributors to beach susceptibility. Figure5.4c clearly demonstrates the positive and negative influences of shoreline position on beach susceptibility. Although the linearity between SHAP values and inner-zone sediment volume is unclear, Figure5.4d shows relatively larger SHAP values, indicating the significant influence of inner-zone sediment volume on beach susceptibility.

The inner-zone sediment volume is the primary indicator influencing beach erosion, and it exhibits a negative correlation. However, Figure 5.4d reveals that the SHAP values demonstrate a positive correlation when the inner-zone sediment volumes exceed 0.9. Interestingly, we also observed that the relationship between erosion susceptibility and inner-zone sediment volume depends on the initial condition of the beach profile. Specifically, already eroded inner-zone profiles were more prone to erosion than uneroded profiles with the same sediment volume. This

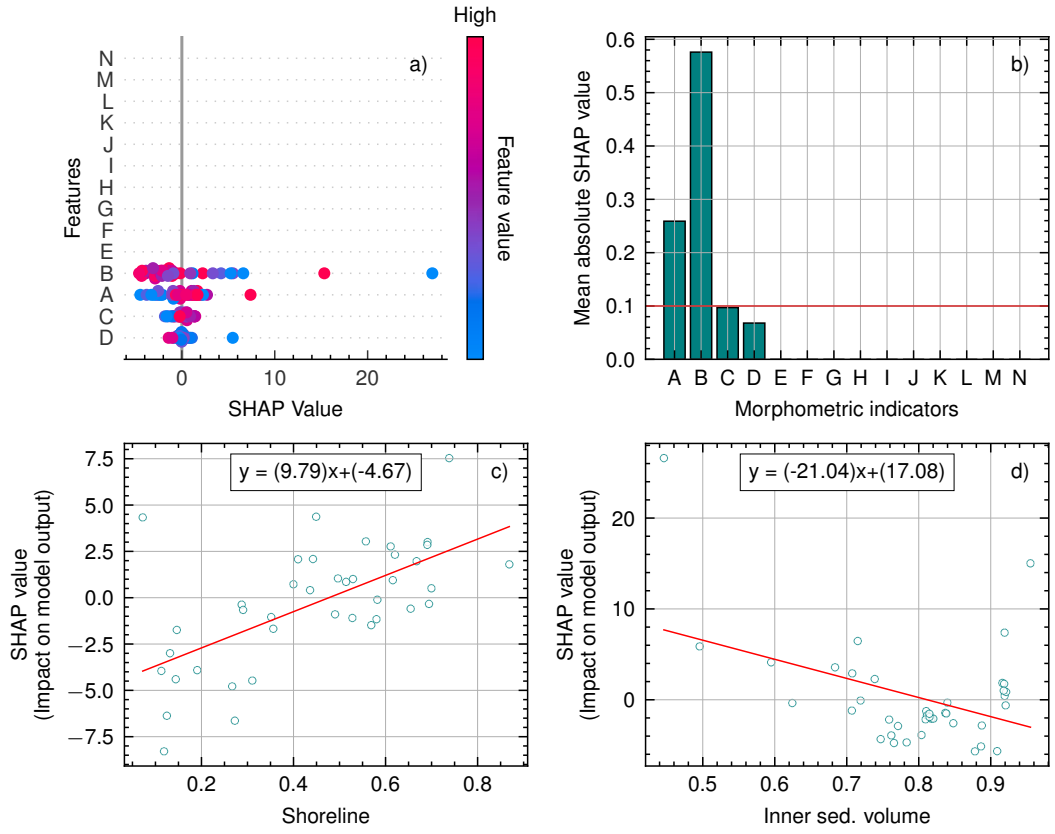

Figure 5.4: SHAP value variation with each morphometric for unbarred profile patterns: a) SHAP summary plot, b) bar plot of mean absolute SHAP values, c) correlation between SHAP values and normalized initial shoreline, d) correlation between SHAP values and normalized inner zone sediment volumes.

highlighted the importance of considering the initial condition of the beach profile in erosion vulnerability assessments. However, the slope of the beach profile was found to have no significant impact on erosion susceptibility, implying that other factors may be more effective in erosion mitigation efforts for unbarred profiles. Additionally, the impact of outer-zone sediment volume on erosion susceptibility was negligible.

Inner sandbar profiles

Figure 5.5 shows an overview of the distribution of SHAP values for each indicator in inner sandbar profiles. Figure5.5a and Figure5.5b reveal that the initial shoreline (A), foreshore slope (D), inner sandbar height (E), and inner-sandbar seaward slope (I) are the most influential indicators contributing to erosion susceptibility. However, the impact of indicators A and I on erosion susceptibility is unclear, as indicated by the scattered data points observed in Figure5.5c and Figure5.5f. Conversely, indicator D exhibits higher SHAP values, suggesting its significance in influencing the erosion susceptibility of beach profiles. Additionally, while the linearity between SHAP values and inner sandbar height is not clearly shown, Figure5.5e consistently demonstrates negative SHAP values.

In the presence of an inner sandbar, the formation of bars reduces beach erosion and, subsequently, beach susceptibility. This observation aligns with the hypothesis that inner sandbar formation has a beneficial impact on reducing beach erosion. However, when milder seaward slopes are present, the influence of the indicator becomes less clear, as indicated by the scattered positive and negative SHAP values in Figure5.5f. This finding is supported by Bujan et al. (2019), who showed that gentle slopes encourage beach erosion, resulting in highly susceptible and fragile beach profiles. Notably, the majority of SHAP values for indicator E display a consistent negative pattern, suggesting its contribution to reducing beach susceptibility. Moreover, the higher outer-zone sediment volumes are not necessarily significant, as their contribution is negligible, as shown in Figure 5.5b. Furthermore, the location and depth of the inner sandbar have no significant influence on beach susceptibility.

Outer sandbar profiles

Figure 5.6 shows an overview of the distribution of SHAP values for each indicator in outer sandbar profiles. Figure5.6a and Figure5.6b reveal that the initial shoreline (A), inner-zone sediment volume (B), outer-zone sediment volume (C),

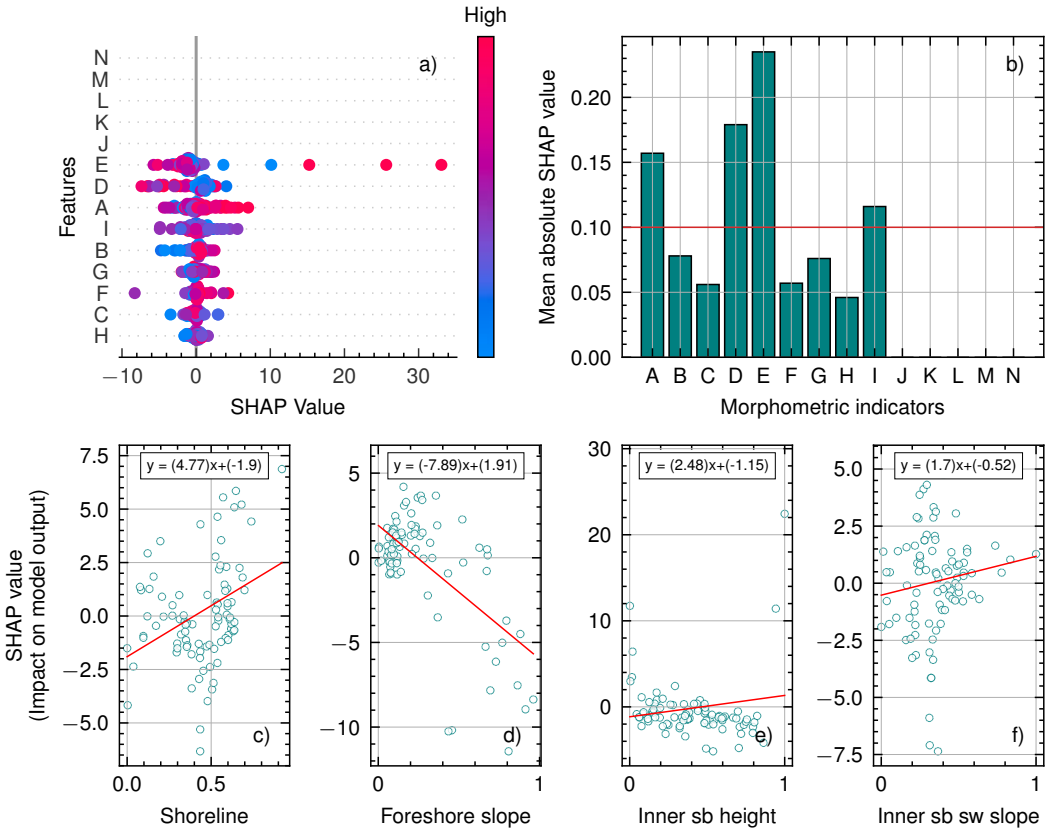

Figure 5.5: Variation of SHAP values with each morphometric for inner sandbar profile patterns: a) SHAP summary plot; b) bar plot of mean absolute SHAP values; c) correlation between SHAP values and initial shoreline; d) correlation between SHAP values and foreshore slope; e) correlation between SHAP values and inner sandbar height; f) correlation between SHAP values and inner sandbar seaward slope.

and outer sandbar depth (L) are the most influential indicators contributing to erosion susceptibility in outer sandbar profiles. The initial shoreline position shows a good linear fit, indicating its importance in quantifying beach susceptibility for this profile pattern. Sandbar depth has the most significant influence on erosion susceptibility among the other outer sandbar characteristics, as evidenced by its significant mean SHAP value. Although both indicators B and C have an impact, the impact of B, inner-zone sediment volume, is significantly greater.

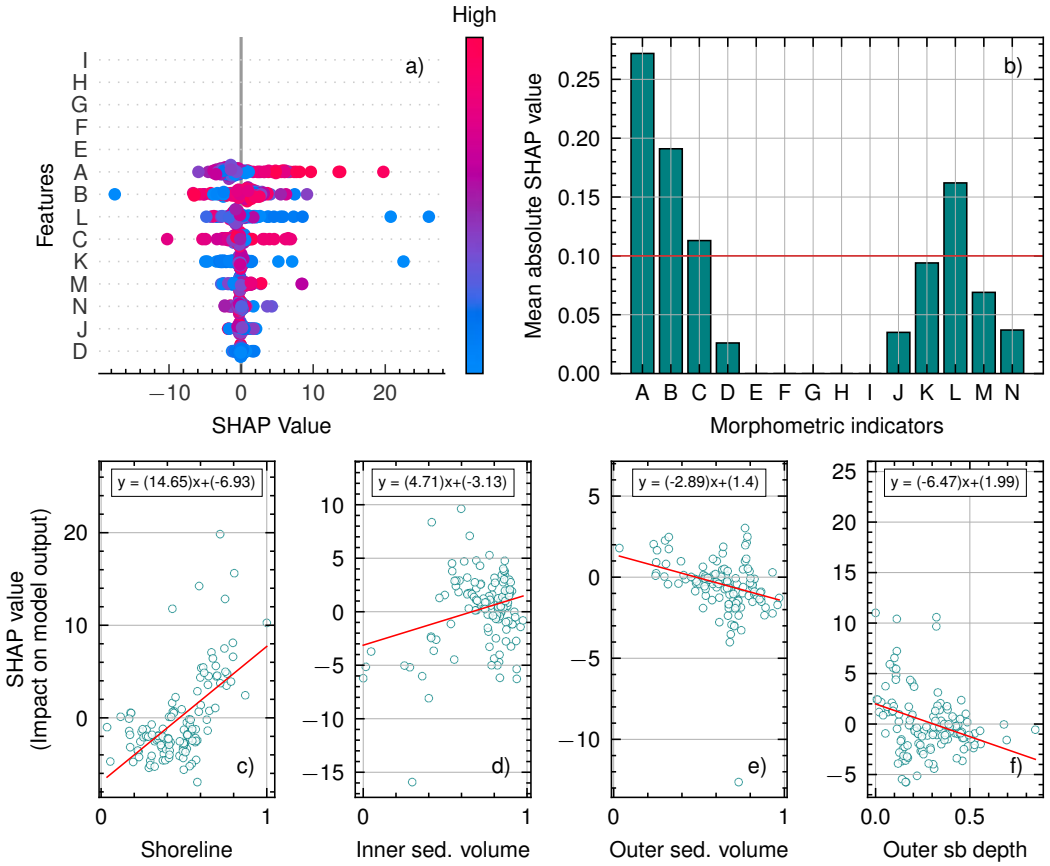

Figure 5.6: Variation of SHAP values with each morphometric for outer sandbar profile patterns: a) SHAP summary plot; b) bar plot of mean absolute SHAP values; c) correlation between SHAP values and normalized initial shoreline; d) correlation between SHAP values and normalized inner zone sediment volumes; e) correlation between SHAP values and normalized outer zone sediment volumes; f) correlation between SHAP values and normalized outer sandbar depth.

Figure5.6c illustrates that eroded beaches, i.e., landward shorelines, result in low susceptibility beach profiles, whereas higher seaward shorelines increase sus-

ceptibility. The staggered higher indicator values of B indicate its importance in quantifying susceptibility, as reflected by the higher SHAP values in Figure5.6d. Although indicator C is less influential, it is a good fit for a linear function used in BESN calculations. A satisfactory linear fit is crucial for a better BESN quantification. Additionally, indicator L demonstrates a good linear fit to the data in Figure5.6f. However, lower outer sandbar depths help to reduce erosion susceptibility. This is primarily because lower water depths cause wave breaks before reaching the beach, resulting in lower wave energy reaching the beach and reduced erosion susceptibility.

Double sandbar profiles

Figure 5.7 shows an overview of the distribution of SHAP values for each indicator in double sandbar profiles. Figure5.7a and Figure5.7b reveal that the initial shoreline (A) and outer-zone sediment volume (C) are the most influential indicators contributing to erosion susceptibility in double sandbar profiles. These selected indicators exhibit a good linear fit, indicating their importance in quantifying beach susceptibility for this profile pattern. Both indicators A and C demonstrate the influence on erosion susceptibility, as they exhibit relatively higher mean absolute SHAP values than the other 12 indicators.

Although 14 morphometric indicators were tested, using the same threshold of 0.1 for significant indicator selection may not be appropriate. However, the selected indicators and the other 12 indicators clearly showed mean SHAP value differences (Figure5.7b), indicating their relative importance. Specifically, advanced shoreline positions, i.e., seaward shorelines, were associated with increased susceptibility to erosion, as indicated by the finer distribution of SHAP values in Figure5.7c. This behavior was consistent with the findings observed in other profile patterns. However, the impact of outer-zone sediment volume (C) was predominantly negative, indicating its significance in reducing the susceptibility of the beach to storm-induced erosion, as shown in Figure5.7d.

The formation of double sandbar profiles is generally considered the final phase of long-term sandbar migration in winter profiles (Vidal-Ruiz and Ruiz de Alegría-Arzaburu, 2019). However, understanding the comprehensive physical mechanisms related to all 14 morphometric indicators in the context of sediment exchange is complex. Nevertheless, this study highlights the importance of carefully considering the effects of shoreline position and outer-zone sediment volume when designing coastal protection measures for double sandbar profiles.

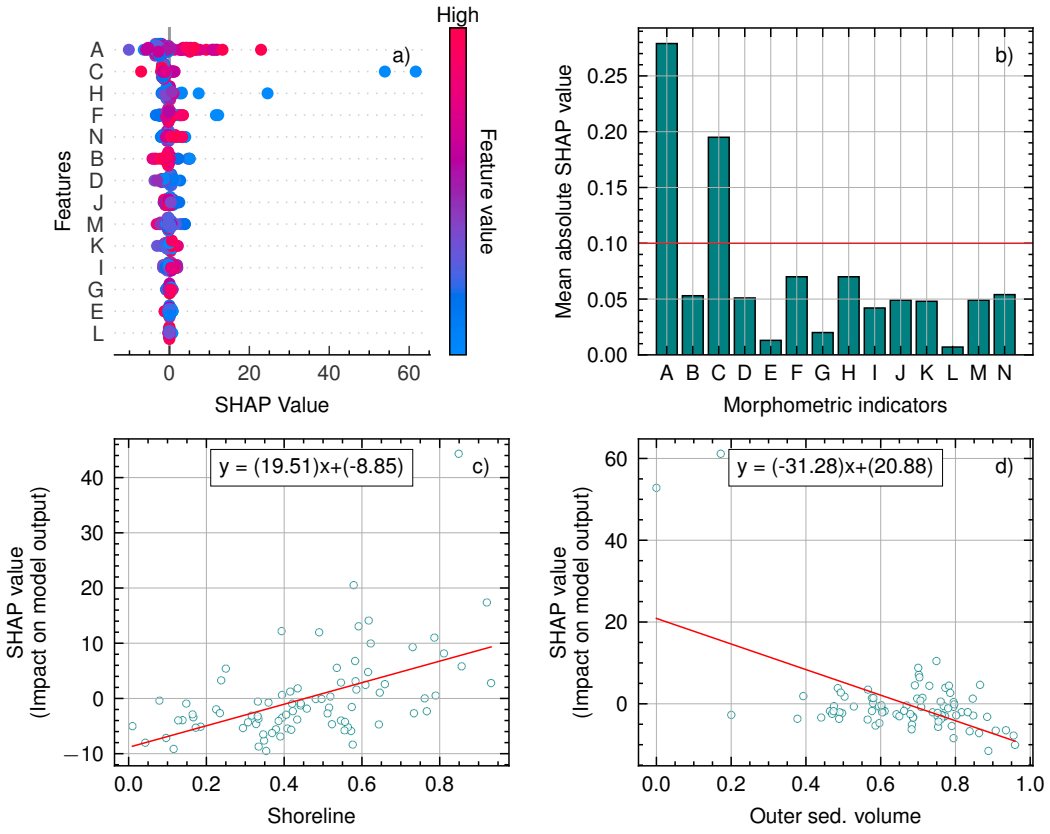

Figure 5.7: SHAP value variation with each morphometric for double sandbar profile patterns: a) SHAP summary plot; b) bar plot of mean absolute SHAP values; c) correlation between SHAP values and Initial shoreline; d) correlation between SHAP values and outer zone sediment volume.

5.1.3 Performance of Beach Erosion Susceptibility Number

Actual measurements of beach erosion are compared to the corresponding BESN values to determine the accuracy of BESN predictions. Higher BESN values indicate a higher susceptibility of beach profiles to erosion, implying a higher probability of significant erosion. However, it is important to note that beach erosion is also influenced by wave energy conditions during a storm event. The storm power (P) is calculated using the maximum significant wave height ($H_{\text{S-max}}$) recorded during the storm duration (D) in hours to quantify the wave energy condition. The storm power (P) can be calculated using the following equation:

$$\text{Storm Power} = H_{\text{s-max}}^2 \times D \tag{5.1}$$

The 347 observed erosion events were divided into three categories based on their storm power values: mild, average, and severe storm conditions. The thresholds of 500 m^2 h and 1000 m^2 h were used to classify the erosion events into these categories, as shown in Figure 5.8. This categorization enabled for a comprehensive evaluation of BESN performance under different storm power conditions, providing insights into its effectiveness in capturing the susceptibility of beach profiles to erosion.

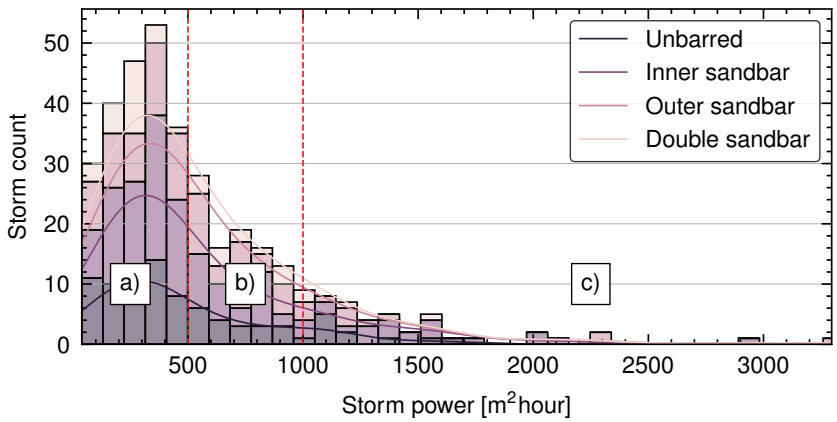

Figure 5.8: Storm power histogram was used to divide the complete data set into three groups for BESN validation based on storm power [m^2 h]: a) mild storm conditions, b) average storm conditions, and c) severe storm conditions. The red vertical dotted lines indicate the boundaries separating the groups.

It was assumed that grouping erosion events based on similar storm conditions would result in a consistent impact on erosion by wave conditions. The perfor-

Table 5.4: Performance of the BESN for different profile types and storm conditions. The Pearson correlation coefficient (r) values between BESN and observed beach erosion are utilized as a measure of the performance of BESN.

Profile type	**Pearson r values**		
	Mild storms	Average storms	Severe storms
Unbarred	0.53	0.75	0.05
Inner sandbar	0.22	0.40	0.42
Outer sandbar	0.54	0.40	0.46
Double sandbar	0.31	0.26	0.40

mance of BESN for three different storm conditions is illustrated in Figure5.9. Table 5.4 summarizes the statistical performance of BESN for each profile pattern and storm condition based on the Pearson correlation coefficient (r). Moderate correlations were observed for inner, double, and outer sandbar profiles during severe storm conditions. However, unbarred profiles showed minimal correlation. Both unbarred and outer sandbar profile patterns displayed significant correlations under mild storm conditions, which encompassed many storm cases. In the case of average storm conditions, unbarred profiles exhibited a strong correlation coefficient of 0.75. Inner and outer sandbar profiles also demonstrated good performance, while the correlation for double sandbar profiles was relatively weaker. Although some BESN predictions did not fully satisfy expectations, most cases indicated a positive relationship between BESN values and observed erosion.

5.1.4 Applicability of the BESN

The BESN was introduced to quantify the beach susceptibility, also referred to as fragility or sensitivity in other studies, of different beach profile patterns. The BESN was designed to act as an indicator of a beach profile's susceptibility to erosion. Our observations at Hasaki indicated that morphological characteristics such as sandbar formations also influence beach susceptibility. Previous studies have overlooked the importance of considering beach vulnerability in their research. Although long-term changes in beach morphology, such as sandbar migration, are often seasonal, our focus in the development of BESN was on a storm-wise susceptibility quantification approach rather than long-term changes.

The Pearson correlation coefficient (r) was initially used to assess the relation-

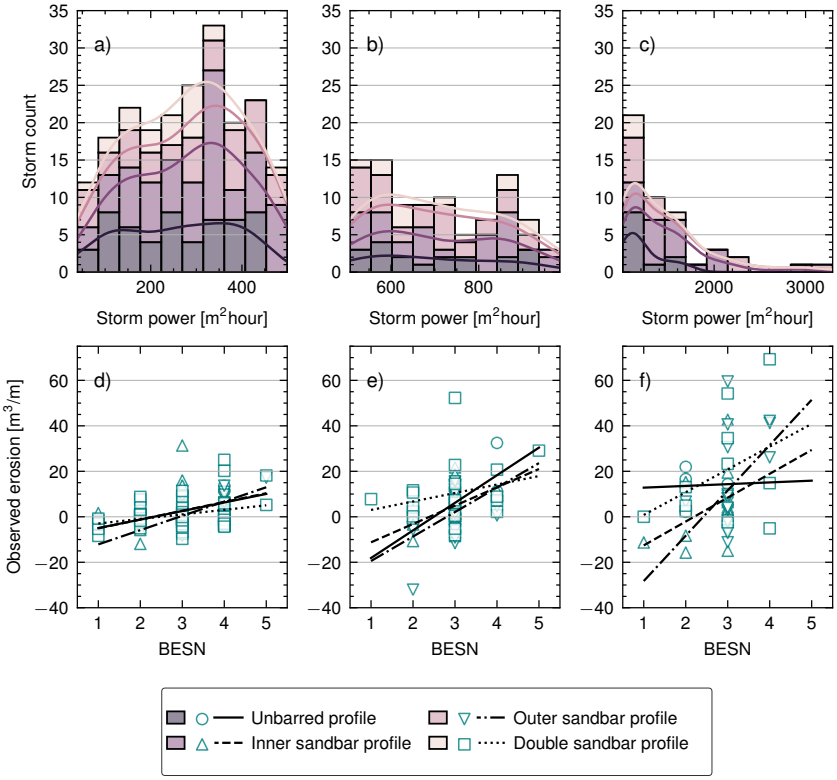

Figure 5.9: BESN Validation for different storm conditions: Storms are categorized into three groups based on storm power thresholds of 500 m^2 h and 1000 m^2 h. Panels (a-c) display the distribution of storms across the storm power groups, with different profile patterns represented by different colors. Panels (d-f) illustrate the correlation between eroded volume and BESN, where distinct markers and lines depict each of the four profile patterns.

ship between the selected 14 morphometric indicators and beach susceptibility. However, it was acknowledged that relying solely on Pearson r has limitations because it provides only a single value to represent the relationship between an indicator and beach erosion. This approach did not consider the specific contribution of each indicator, which can vary in importance. The SHAP explanation method was employed to address this limitation, which offers both local and global interpretability for the models. The SHAP values provided insights into the contribution of each indicator on a local level, allowing for a more comprehensive understanding of their significance in predicting beach erosion. When combined with theoretical knowledge, the SHAP findings helped to validate the findings and ensure the robustness of the approach.

Although the seasonality factor was not explicitly considered in this study, it is recognized that seasonal variations, particularly during winter, play a crucial role in severe erosion events and the formation of sandbars with mild slopes in the outer zone. The presence of sandbars and milder slopes could impact beach profile susceptibility. Although three groups were defined based on different wave conditions in this study, it is recommended to further validate the approach through numerical simulations under consistent wave conditions in future work. This would provide a more comprehensive validation of the proposed methodology and enhance the accuracy of beach profile susceptibility quantification.

The importance of maintaining natural sediment balance in a coastal system, particularly in the face of human disturbances, has led to the popularity of relatively low-cost beach nourishment efforts. To optimize these efforts, a holistic approach is required to assess the susceptibility of a beach profile to erosion. In this regard, the proposed BESN effectively identifies the most susceptible areas and aid to conduct nourishment accordingly. Long-term analysis of beach susceptibility also enables coastal stakeholders to make informed decisions regarding the need for shore protection action. Although many previous studies on beach nourishment have focused on dunes, sandbar formations have been relatively understudied due to a lack of data. Our study provides valuable insights into the impact of sandbars on beach susceptibility, which can guide future research in this area and help justify the omission of certain indicators. Furthermore, BESN can also be used to determine the optimal timing for soft protection measures such as nourishment. Artificial nourishment has been shown to have minimal negative impact compared to other shore protection options. The use of BESN to identify vulnerable locations along a coastline allows for the effective execution of necessary shore protection

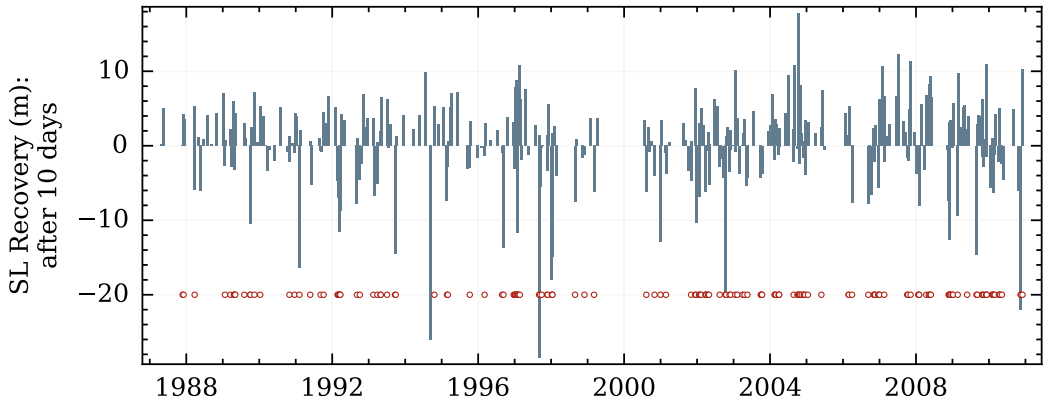

Figure 5.10: Beach response after 10 days of the end of the storm. Red colour markers denote the cases where a sequencing storm is present in the post-storm 10-day period. Negative recovery indicates continued erosion.

actions.

5.2 Beach recovery potential

Figure 5.10 illustrates the distribution of beach recovery (m) for all of the identified storm events during the study period. Out of the 347 storm events identified, 176 cases did not have any sequencing storms during the 10-day post-storm period. Additionally, some storm cases exhibited shoreline accretion during the storm event. After filtering the data, 125 cases were obtained, and then BRN values were calculated and outliers were removed, resulting in 104 storm cases for the beach resilience analysis. Initially, the impact of hydrodynamic conditions on the recovery process was examined, considering the relationship between BRN and mean hydrodynamic indicators of wave and surge heights.

In a manner similar to the BESN approach, the profiles were divided into four groups. However, upon separation, a clear distinct impact of the profile pattern was not evident (Figure 5.11). One contributing factor to this outcome might be the absence of storm sequencing in the analysis, leading to a higher number of positive BRNs, indicative of beach recovery. Furthermore, 28 cases exhibited BRN values higher than 1, signifying that in those instances, the shoreline had recovered beyond the erosion extent during the storm event.

Equation 5.2 explains the relationship between wave steepness, sediment grain size, and bottom slope related to cross-shore sediment movement. However, this

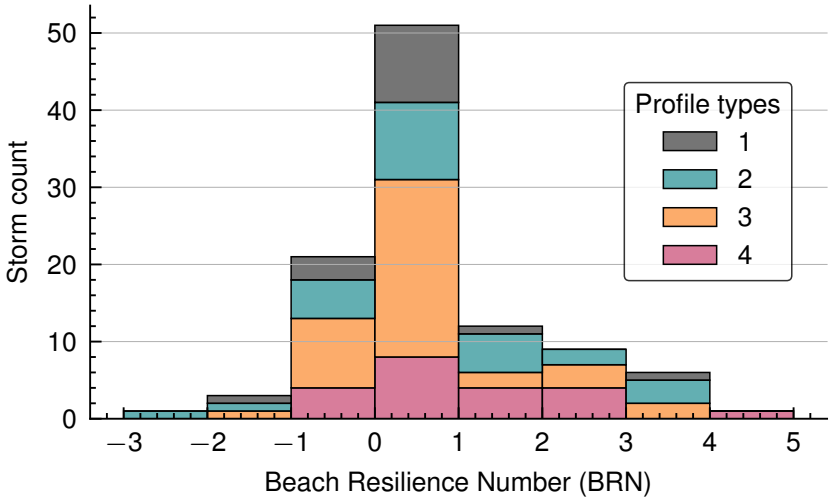

Figure 5.11: Histogram of Beach Recovery Number with different profile types, utilizing a total of 104 storm data sets.

study did not incorporate sediment size information into the analysis. Nevertheless, the clear relationship between beach slope and sediment size implies that the use of slope would already account for sediment characteristics to some extent.

$$\frac{H_0}{L_0} = C_s \left(\tan\beta\right)^{-0.27} \left(\frac{d}{L_0}\right)^{0.67} \tag{5.2}$$

5.2.1 Post-storm hydrodynamic condition on beach recovery

Figure 5.12 shows the distribution of BRN with the mean significant wave height (H_S) during the 10-day post-storm period. The mean wave height during the study period was 1.19 m, and there were 32 cases where the mean H_S exceeded this threshold. Interestingly, even with relatively higher mean H_S, positive BRNs were still observed. However, when the mean H_S during the post-storm period exceeded 1.6 m, negative BRNs were more prevalent. Additionally, it was observed that most of the positive BRN cases occurred under milder wave conditions, suggesting that the wave conditions were similar in these cases.

Figure 5.13 shows the distribution of BRN with the mean surge height during the 10-day post-storm period. The surge calculations were derived as the difference between water level observations (η) and tidal predictions. It was observed that smaller surge values has less impact on the recovery process and were not sig-

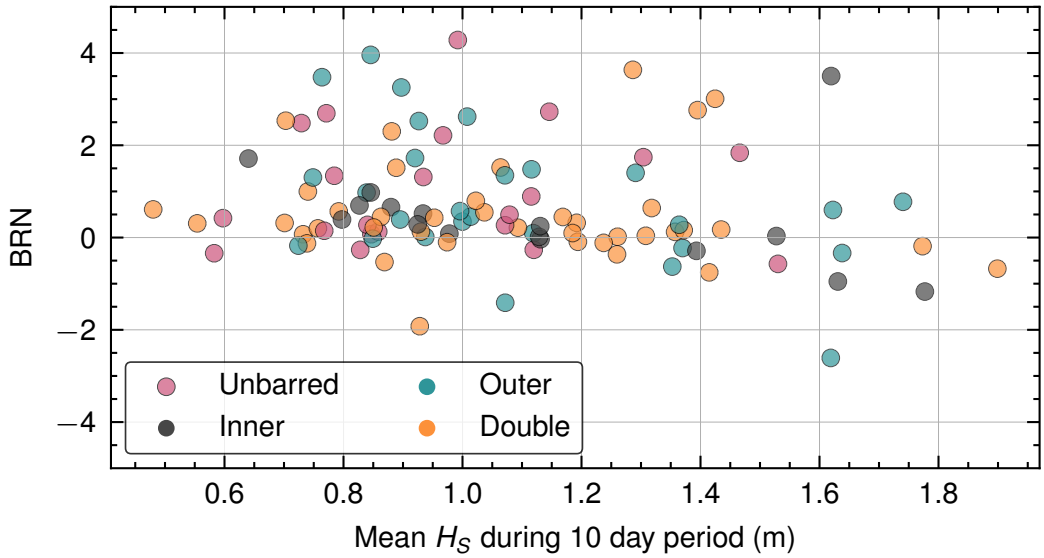

Figure 5.12: Variation of BRN with mean significant wave height during the 10-day post-storm period.

nificant contributors. Based on the statistical analysis, the impact of surge on the recovery process was found to be not significant.

5.2.2 Key morphometric indicators on beach resilience

Initially, without the separation of profile patterns, a single XGBoost model was trained using all 104 cases. The mean SHAP values for all 14 indicators are depicted in Figure 5.14. Subsequently, an assessment of significant morphometric indicators was conducted. The influence of each indicator on Beach Recovery Number (BRN) is presented in Table 5.5 based on this initial analysis. However, a subsequent statistical analysis driven by machine learning (ML) was carried out to determine the importance of features for beach resilience, taking into account each of the four profile patterns. The findings of this analysis are presented in the following sections.

Unbarred profiles

Figure 5.15 shows the distribution of SHAP values for each morphometric indicator in unbarred profiles. Outer zone sediment volume, shoreline position, and foreshore slope were found to exert significant control over short-term recovery. In the case of unbarred profiles, the outer zone is abundant in sediment depositions, consequently contributing to the recovery during the milder post-storm period.

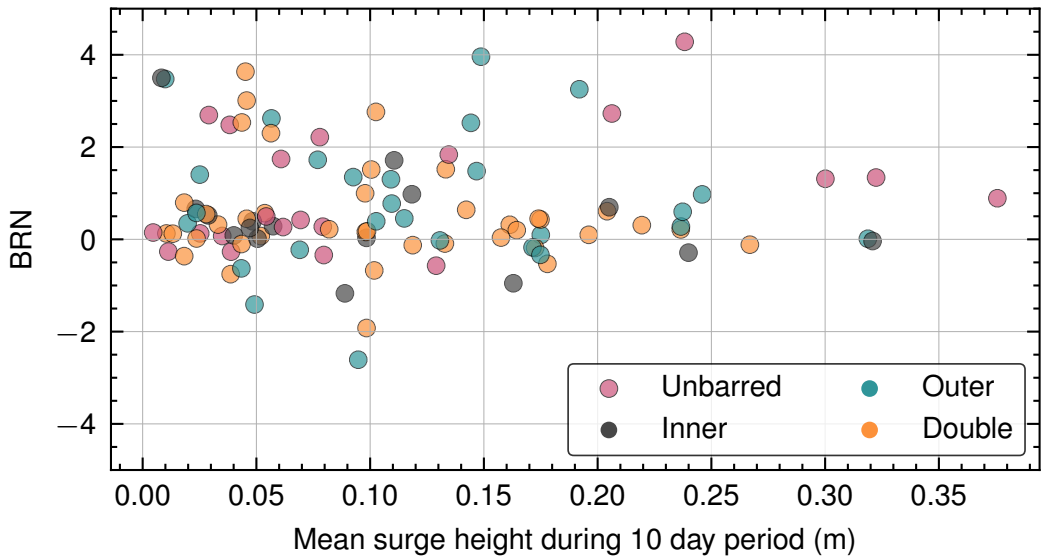

Figure 5.13: Variation of BRN with mean surge height during the 10-day post-storm period.

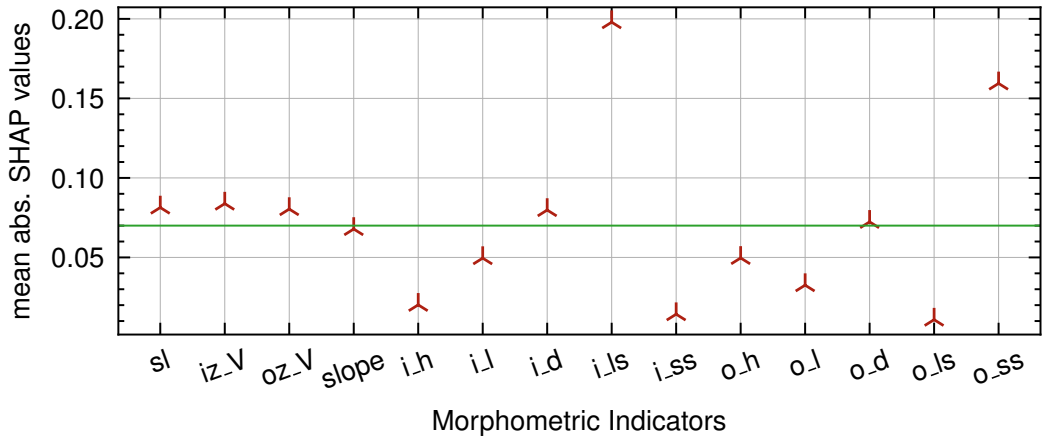

Figure 5.14: Mean SHAP values for all 14 indicators.

Table 5.5: Mean SHAP values for significant morphometric indicators. All the 104 storm cases were used for this analysis.

Morphometric indicator	mean SHAP value
Shoreline position	0.081
Inner zone sed. vol	0.084
Outer zone sed. vol	0.080
Inner sandbar depth	0.080
Inner sandbar landward slope	0.200
Outer sandbar depth	0.072
Outer sandbar seaward slope	0.169

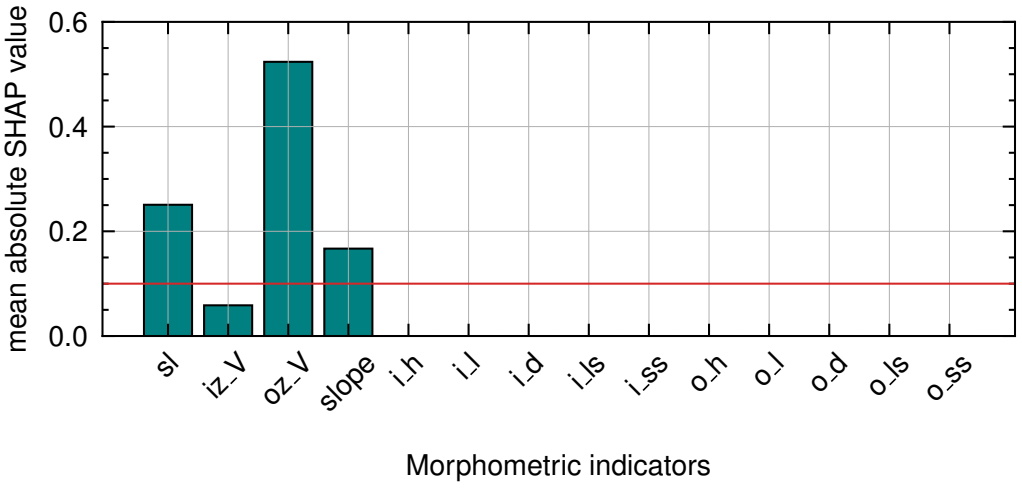

Figure 5.15: Bar plot of mean absolute SHAP values for unbarred profiles. 16 profiles were used to fit the data to a XGBoost model.

Inner sandbar profiles

Figure 5.16 shows the distribution of SHAP values for each morphometric indicator in inner sandbar profiles. The results indicated that inner sandbar height, inner sandbar landward slope, foreshore slope, and shoreline position influence short-term recovery, as evident from their normalized SHAP values for BRN. Similar to beach susceptibility, inner sandbar height also facilitates the recovery process. Additionally, the landward slope of the inner sandbar contributes to recovery by acting as a berm formation. The SHAP values revealed that lower slopes, which indicates a presence of berm formation, result in rapid recovery.

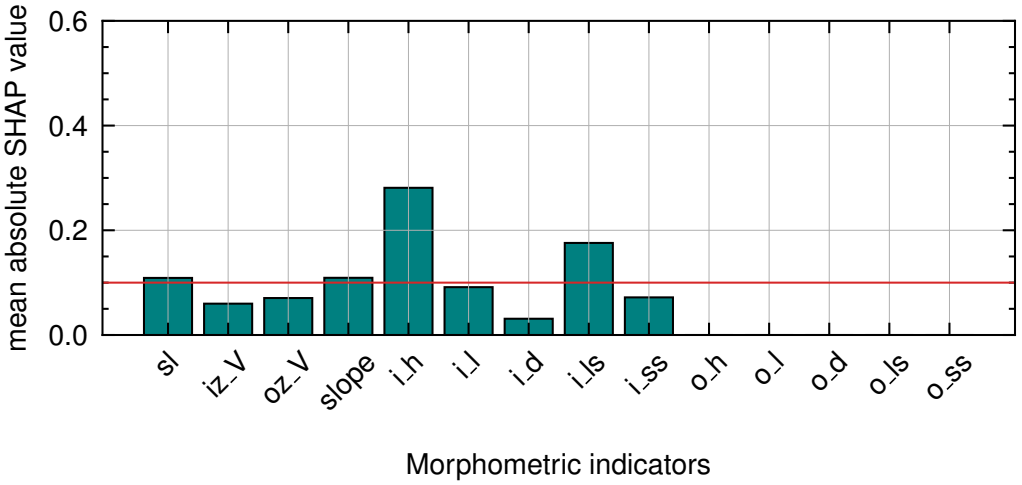

Figure 5.16: Bar plot of mean absolute SHAP values for inner sandbar profiles. 27 profiles were used to fit the data to a XGBoost model.

Outer sandbar profiles

Figure 5.17 shows the distribution of SHAP values for each morphometric indicator in outer sandbar profiles. Short-term recovery in these profiles is influenced by the seaward slope of the outer sandbar, outer zone sediment volume, shoreline position, and outer sandbar height, as evidenced by their respective normalized SHAP values. Particularly noteworthy was the significant impact of the seaward slope on the recovery process. Higher sandbar slopes indicated more unstable bar formations, leading to sediment being prone to move to the foreshore during the post-storm period. Although water depth played a role in beach susceptibility, its influence was not clearly visible in this context.

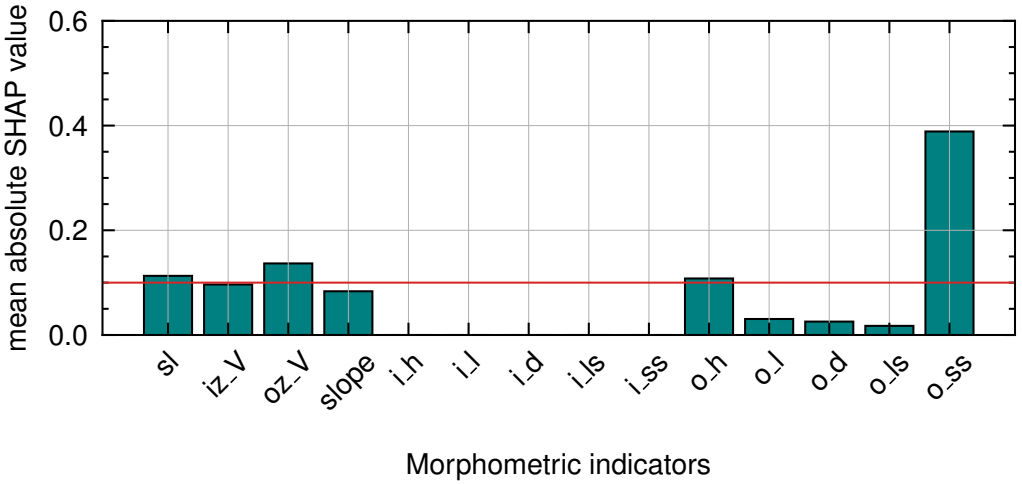

Figure 5.17: Bar plot of mean absolute SHAP values for outer sandbar profiles. 40 profiles were used to fit the data to a XGBoost model.

Double sandbar profiles

Figure 5.18 shows the distribution of SHAP values for each morphometric indicator in double sandbar profiles. Among the indicators tested, outer sandbar depth stands out as the only significant factor controlling short-term recovery. However, it is worth noting that out of the 14 indicators trialed and considering the normalized SHAP values obtained by dividing the sum of the SHAP value of each indicator, the contributions of other morphometric values appeared relatively insignificant. Nevertheless, the impact of shoreline position and inner sandbar water depth seemed somewhat significant, as they approached the threshold value of 0.1. The role of outer sandbar depth in recovery is relatively straightforward. Lower depths suggest a more abundant supply of sediment available for transportation to the foreshore zone, thereby facilitating sediment transportation during the recovery process.

5.3 Summary of the comprehensive analysis

The proposed Beach Erosion Susceptibility Number (BESN) could be noted as a valuable tool for identifying vulnerable areas along coastlines and measuring their temporal fragility. It utilized the SHAP feature importance from the XGBoost model to assess beach susceptibility and further examines the correlation between morphometric indicators and shoreline erosion (i.e., susceptibility). The effectiveness

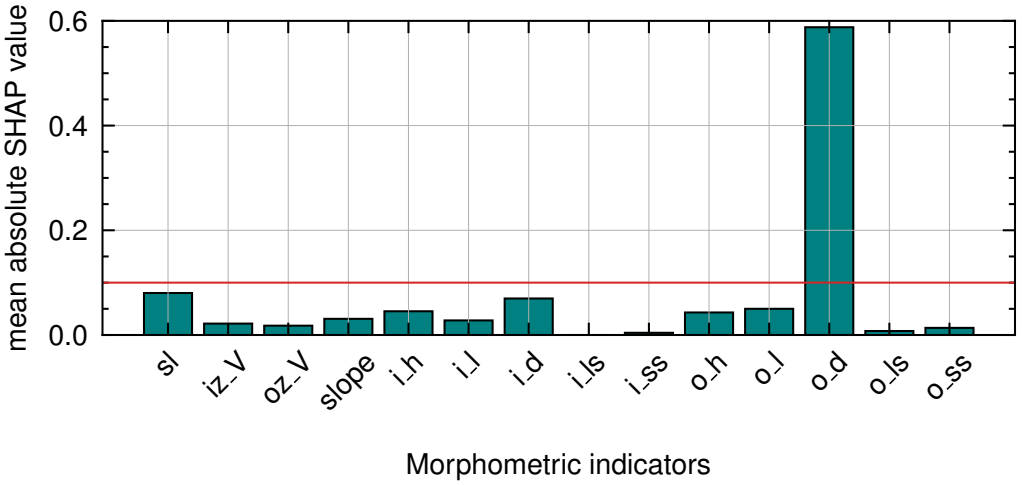

Figure 5.18: Bar plot of mean absolute SHAP values for double sandbar profiles. 21 profiles were used to fit the data to a XGBoost model.

of BESN was validated under various storm conditions, showcasing its potential in identifying weak locations. The use of SHAP analysis might be questionable, especially with environmental data sets. However, it provided valuable insights into the relative importance of different features in determining beach susceptibility.

Next, BRN investigated the recovery potential of beaches after storm events. The methodology employed included MLR model training and input variable selection based on their coefficients. The distribution of BRN revealed that full recovery is not common, highlighting the challenges in beach restoration. The role of factors such as foreshore slope and sediment transport in the recovery process was also examined, emphasizing their significance. The analysis considered the influence of climate variations and sedimentary stock preservation, shedding light on the complex nature of beach resilience. By identifying these factors that contribute to successful recovery, this dissertation aimed to enhance the current understanding of beach dynamics and improve future mitigation strategies.

In addition to assessing beach susceptibility and recovery potential, the study delved into the analysis of storm events during the study period. It identified cases of significant shoreline erosion and further explored the factors influencing beach recovery and further erosion cases. The statistical significance of input variables was discussed, emphasizing the importance of the foreshore slope and the impact of mild waves during the post-storm period on the recovery process. The study further revealed that even with similar wave conditions, it could lead to different

erosion outcomes, indicating the influence of beach characteristics on the recovery process. Therefore, long-term resilience studies and a comprehensive understanding of coastal erosion systems are essential for effective coastal management, highlighting the need for further research and the implementation of ecosystem-based approaches to mitigate the impacts of coastal storms.

Chapter 6

Conclusion

6.1 Concluding remarks

In recent years, beach vulnerability assessment has gained significant attention in the field of coastal research and management. This dissertation aimed to enhance the accuracy of beach vulnerability assessments through the utilization of various novel methodologies and techniques. Three specific objectives were addressed, each contributing to a deeper understanding of beach vulnerability and its associated factors.

The first objective focused on evaluating the performance of a linear regression model in predicting beach erosion measures. The results demonstrated that the model provided reasonable predictions, allowing for the development of a satisfactory Beach Vulnerability Index (BVI) during the testing period. While the findings were limited to the site-specific characteristics of Hasaki, this study serves as a foundation for further research in diverse coastal conditions. Future investigations should consider the application of alternative regression models and assess their performance.

Building upon the initial findings, the second objective incorporated a machine learning algorithm, specifically Artificial Neural Networks (ANN), into the BVI methodology. This integration aimed to enhance the accuracy of beach vulnerability predictions, particularly in cases of severe erosion. The study confirmed the applicability of ANN in BVI assessments and highlighted the importance of key vulnerability indicators such as shoreline position, foreshore slope, and sandbar depth. Additionally, the research identified the need to explore other morphometric characteristics and their impact on beach susceptibility. The findings suggest the potential for more sophisticated predictive models and informed coastal man-

agement decisions.

The third objective investigated the relationship between morphometric variables and beach erosion, considering the shape of the beach profile and shoreline position. The study revealed that the impact of these variables on beach susceptibility is highly dependent on the specific profile type. Key factors such as sediment deposition, sandbar formations, and beach slopes were found to influence the beach vulnerability to storm-induced erosion. However, further research is necessary to comprehensively investigate these factors and their contribution to beach susceptibility and recovery potential. The study acknowledged the limitations of the research, including the need for numerical simulations and validation of the proposed BESN under controlled hydrodynamic conditions (further discussed in Chapter 6.2.

In conclusion, this study has made contributions to the field of Coastal Engineering & Management by proposing novel approaches to quantify beach vulnerability. It has demonstrated the effectiveness of linear regression models and machine learning algorithms, such as ANN & XGBoost, in predicting beach erosion and enhancing vulnerability assessments. The findings underscore the importance of key vulnerability indicators and the need for a comprehensive understanding of morphometric variables. Further analysis results of beach resilience highlight the key morphometrics that controls the short-term recovery of beach morphology. Focusing on integrating susceptibility and recovery potential into a final beach vulnerability index is recommended, ultimately leading to a real-time vulnerability calculation approach. Additionally, the applicability of the proposed methodologies should be tested in different coastal locations with diverse data sets to ensure their generalizability.

6.2 Limitations and recommendations

Beach Vulnerability Index

The development of the BVI in this dissertation, relying on readily available morphological and storm characteristics, does possess certain limitations that warrant consideration for future research work. Firstly, the generalizability of the linear regression model used for predicting beach erosion measures and developing the BVI is limited to the site-specific characteristics of Hasaki. Caution should be exercised when applying the index-based vulnerability approach in diverse coastal

settings, as the findings may not directly apply. Future research should assess the performance of other regression models to determine their effectiveness in beach vulnerability prediction.

Although ANN showed effectiveness in predicting beach erosion, especially in severe cases, limitations were identified when using MLR for fitting long-term data with large variations. MLR performed well with small data sets but requires refinement for larger data sets. Further studies should explore strategies to improve the performance of MLR and consider the application of other machine learning algorithms to enhance beach vulnerability assessments. It is important to acknowledge that the findings are specific to the data set and site conditions, and their applicability to other coastal locations may vary. By addressing these limitations, future research can enhance beach vulnerability assessment methodologies.

Comprehensive analysis on beach vulnerability

The comprehensive analysis of beach susceptibility and resilience using the BESN and BRN also brings about certain limitations. The validation of BESN was affected by the significant influence of different storm conditions, highlighting the limitation of the validating phase. Conducting numerical simulations with controlled storm characteristics and generating synthetic data sets could address this limitation and validate the BESN, particularly focusing on different beach profile settings and sandbar formations. Additionally, the use of linear functions for the weights of BESN generation is a limitation that was not addressed in this study to maintain simplicity. Future research could explore the application of more complex functions to improve the accuracy of BESN generation.

Furthermore, the study acknowledges the challenge of clear descriptions of utilization of machine learning techniques such as XGBoost and SHAP explanation methods. While these techniques have demonstrated noteworthy predictive capabilities in other contexts, their application in the current research could benefit from more extensive explanation and exploration. Moreover, the restricted data set comprising 104 cases, which was used to establish the statistically analyzed beach resilience, imposes a limitation. To mitigate this limitations, numerical simulations involving various profile configurations could be employed. Additionally, investigating recovery over different time-frames could provide valuable insights into the short-term beach responses to storm events.

During the present dissertation work, the methodology was not tested on differ-

ent sandy beaches. However, based on the general characteristics of Hasaki Beach as a representative sandy beach, it is reasonable to expect that the methodology can be directly applied or slightly modified for other similar beaches.The trained model for predicting beach vulnerability could be particularly valuable in low-resource areas, especially in developing countries, with the support of relevant government agencies. By utilizing the BESN and BRN, temporal changes in beach profiles can be identified, enabling informed actions to sustain beach zones and mitigate erosion impacts.

By acknowledging these limitations, future research can focus on addressing these challenges and expanding the knowledge base in beach vulnerability assessment.

Bibliography

Abuodha, P. A. and Woodroffe, C. D. (2006). Assessing vulnerability of coasts to climate change: A review of approaches and their application to the Australian coast.

Adeli, H. (2001). Neural Networks in Civil Engineering: 1989-2000. *Computer-Aided Civil and Infrastructure Engineering*, 16(2):126–142. _eprint: https://onlinelibrary.wiley.com/doi/pdf/10.1111/0885-9507.00219.

Alexandrakis, G. and Kampanis, N. A. (2013). Estimation of the climatic change impact on beach tourism: the case of a mass tourist destination. In *Proceedings of the International Conference on Tourism (ICOT 2013)*, pages 19–32, Limassol, Cyprus.

Alexandrakis, G. and Poulos, S. ☒. (2014). An holistic approach to beach erosion vulnerability assessment. *Scientific Reports*, 4(1):6078. Number: 1 Publisher: Nature Publishing Group.

Balica, S. F., Wright, N. G., and van der Meulen, F. (2012). A flood vulnerability index for coastal cities and its use in assessing climate change impacts. *Natural Hazards*, 64(1):73–105.

Banno, M., Nakamura, S., Kosako, T., Nakagawa, Y., Yanagishima, S.-i., and Kuriyama, Y. (2020). Long-Term Observations of Beach Variability at Hasaki, Japan. *Journal of Marine Science and Engineering*, 8(11):871. Number: 11 Publisher: Multidisciplinary Digital Publishing Institute.

Barnard, P. L., Short, A. D., Harley, M. D., Splinter, K. D., Vitousek, S., Turner, I. L., Allan, J., Banno, M., Bryan, K. R., Doria, A., Hansen, J. E., Kato, S., Kuriyama, Y., Randall-Goodwin, E., Ruggiero, P., Walker, I. J., and Heathfield, D. K. (2015). Coastal vulnerability across the Pacific dominated by El Niño/Southern Oscilla-

tion. *Nature Geoscience*, 8(10):801–807. Number: 10 Publisher: Nature Publishing Group.

Basco, D. R. and Mahmoudpour, N. (2012). THE MODIFIED COASTAL STORM IMPULSE (COSI) PARAMETER AND QUANTIFICATION OF FRAGILITY CURVES FOR COASTAL DESIGN. *Coastal Engineering Proceedings*, (33):66–66. Number: 33.

Bianco, F. and García-Ayllón, S. (2021). Coastal resilience potential as an indicator of social and morphological vulnerability to beach management. *Estuarine, Coastal and Shelf Science*, 253:107290.

Bird, E. and Lewis, N. (2015). Causes of Beach Erosion. In Bird, E. and Lewis, N., editors, *Beach Renourishment*, SpringerBriefs in Earth Sciences, pages 7–28. Springer International Publishing, Cham.

Bridges, T. S., Burks-Copes, K. A., Bates, M. E., Collier, Z. A., Fischenich, J. C., Piercy, C. D., Russo, E. J., Shafer, D. J., Suedel, B. C., Gailani, J. Z., and others (2015). *Use of natural and nature-based features (NNBF) for coastal resilience*. US Army Engineer Research and Development Center, Environmental Laboratory ….

Bujan, N., Cox, R., and Masselink, G. (2019). From fine sand to boulders: Examining the relationship between beach-face slope and sediment size. *Marine Geology*, 417:106012.

Callaghan, D. P., Nielsen, P., Short, A., and Ranasinghe, R. (2008). Statistical simulation of wave climate and extreme beach erosion. *Coastal Engineering*, 55(5):375–390.

Chen, T. and Guestrin, C. (2016). XGBoost: A Scalable Tree Boosting System. In *Proceedings of the 22nd ACM SIGKDD International Conference on Knowledge Discovery and Data Mining*, KDD '16, pages 785–794, New York, NY, USA. Association for Computing Machinery.

Ciavola, P. and Coco, G. (2017). *Coastal Storms: Processes and Impacts*. John Wiley & Sons. Google-Books-ID: ETuKDgAAQBAJ.

Clark, J. R. (2018). *Coastal zone management handbook*. CRC press.

Corbella, S. and Stretch, D. D. (2012). Shoreline recovery from storms on the east coast of Southern Africa. *Natural Hazards and Earth System Sciences*, 12(1):11–22. Publisher: Copernicus GmbH.

de Andrade, T. S., Sousa, P. H. G. d. O., and Siegle, E. (2019). Vulnerability to beach erosion based on a coastal processes approach. *Applied Geography*, 102:12–19.

Defeo, O., McLachlan, A., Schoeman, D. S., Schlacher, T. A., Dugan, J., Jones, A., Lastra, M., and Scapini, F. (2009). Threats to sandy beach ecosystems: A review. *Estuarine, Coastal and Shelf Science*, 81(1):1–12.

Eichentopf, S., Alsina, J. M., Christou, M., Kuriyama, Y., and Karunarathna, H. (2020). Storm sequencing and beach profile variability at Hasaki, Japan. *Marine Geology*, 424:106153.

Field, C. B., Stocker, T. F., Barros, V. R., Qin, D., Ebi, K. L., and Midgley, P. M. (2011). IPCC Special Report on Managing the Risks of Extreme Events and Disasters to Advance Climate Change Adaptation. 2011:NH12A–02. Conference Name: AGU Fall Meeting Abstracts ADS Bibcode: 2011AGUFMNH12A..02F.

Gornitz, V., White, T. W., and Cushman, R. M. (1991). Vulnerability of the US to future sea level rise. Technical Report CONF-910780-1, Oak Ridge National Lab., TN (USA).

Gornitz, V. M., Daniels, R. C., White, T. W., and Birdwell, K. R. (1994). The Development of a Coastal Risk Assessment Database: Vulnerability to Sea-Level Rise in the U.S. Southeast. *Journal of Coastal Research*, pages 327–338. Publisher: Coastal Education & Research Foundation, Inc.

Harley, M. (2017). Coastal Storm Definition. In *Coastal Storms*, pages 1–21. John Wiley & Sons, Ltd. Section: 1 _eprint: https://onlinelibrary.wiley.com/doi/pdf/10.1002/9781118937099.ch1.

Harris, C. R., Millman, K. J., Walt, S. J. v. d., Gommers, R., Virtanen, P., Cournapeau, D., Wieser, E., Taylor, J., Berg, S., Smith, N. J., Kern, R., Picus, M., Hoyer, S., Kerkwijk, M. H. v., Brett, M., Haldane, A., Río, J. F. d., Wiebe, M., Peterson, P., Gérard-Marchant, P., Sheppard, K., Reddy, T., Weckesser, W., Abbasi, H., Gohlke, C., and Oliphant, T. E. (2020). Array programming with NumPy. *Nature*, 585(7825):357–362. Publisher: Springer Science and Business Media LLC.

Hegde, A. V. and Reju, V. R. (2007). Development of Coastal Vulnerability Index for Mangalore Coast, India. *Journal of Coastal Research*, 23(5):1106–1111. Publisher: Coastal Education and Research Foundation.

Hieu, P. D., Phan, V. N., Nguyen, V. T., Nguyen, T. V., and Tanaka, H. (2020). Numerical study of nearshore hydrodynamics and morphology changes behind offshore breakwaters under actions of waves using a sediment transport model coupled with the SWASH model. *Coastal Engineering Journal*, 62(4):553–565. Publisher: Taylor & Francis _eprint: https://doi.org/10.1080/21664250.2020.1828016.

Hillyer, T. M. (1996). *Shoreline Protection and Beach Erosion Control Study: Final Report : an Analysis of the U.S. Army Corps of Engineers Shore Protection Program*. The Institute. Google-Books-ID: LiQYAQAAIAAJ.

Horikawa, K. (1988). *Nearshore dynamics and coastal processes*. University of Tokyo Press.

Janušaitė, R., Jukna, L., Jarmalavičius, D., Pupienis, D., and Žilinskas, G. (2021). A Novel GIS-Based Approach for Automated Detection of Nearshore Sandbar Morphological Characteristics in Optical Satellite Imagery. *Remote Sensing*, 13(11):2233. Number: 11 Publisher: Multidisciplinary Digital Publishing Institute.

Kantamaneni, K., Du, X., Aher, S., and Singh, R. M. (2017). Building Blocks: A Quantitative Approach for Evaluating Coastal Vulnerability. *Water*, 9(12):905. Number: 12 Publisher: Multidisciplinary Digital Publishing Institute.

Kantamaneni, K., Phillips, M., Thomas, T., and Jenkins, R. (2018). Assessing coastal vulnerability: Development of a combined physical and economic index. *Ocean & Coastal Management*, 158:164–175.

Karunarathna, H., Horrillo-Caraballo, J., Kuriyama, Y., Mase, H., Ranasinghe, R., and Reeve, D. E. (2016). Linkages between sediment composition, wave climate and beach profile variability at multiple timescales. *Marine Geology*, 381:194–208.

Katoh, K. (1997). Hazaki oceanographical research station (HORS). *Marine Technology Society. Marine Technology Society Journal*, 31(4):49. Publisher: Marine Technology Society.

Kim, T. and Lee, W.-D. (2022). Review on Applications of Machine Learning in Coastal and Ocean Engineering. *Journal of Ocean Engineering and Technology*, 36(3):194–210. Publisher: Ocean Engineering and Technology.

Kim, T.-K., Lim, C., and Lee, J.-L. (2021). Vulnerability Analysis of Episodic Beach Erosion by Applying Storm Wave Scenarios to a Shoreline Response Model. *Frontiers in Marine Science*, 8.

Koroglu, A., Ranasinghe, R., Jiménez, J. A., and Dastgheib, A. (2019). Comparison of Coastal Vulnerability Index applications for Barcelona Province. *Ocean & Coastal Management*, 178:104799.

Kuriyama, Y., Banno, M., and Suzuki, T. (2012). Linkages among interannual variations of shoreline, wave and climate at Hasaki, Japan. *Geophysical Research Letters*, 39(6). _eprint: https://onlinelibrary.wiley.com/doi/pdf/10.1029/2011GL050704.

Lundberg, S. M. and Lee, S.-I. (2017). A Unified Approach to Interpreting Model Predictions. In Guyon, I., Luxburg, U. V., Bengio, S., Wallach, H., Fergus, R., Vishwanathan, S., and Garnett, R., editors, *Advances in Neural Information Processing Systems*, volume 30. Curran Associates, Inc.

Malek, M. A., Suzuki, T., Higa, H., and Nakamura, Y. (2020). Analyze the Coastal Storm Impulse (cosi) Parameter and Beach Erosion at Hasaki Coast, Japan. *土木学会論文集 b3（海洋開発）*, 76(2):I_1061–I_1066.

Martzikos, N. T., Prinos, P. E., Memos, C. D., and Tsoukala, V. K. (2021). Statistical analysis of Mediterranean coastal storms. *Oceanologia*, 63(1):133–148.

Mendoza, E. T., Torres-Freyermuth, A., Ojeda, E., Medellín, G., Rioja-Nieto, R., Salles, P., and Turki, I. (2022). Seasonal changes in beach resilience along an urbanized barrier island. *Frontiers in Marine Science*, 9.

Pedregosa, F., Varoquaux, G., Gramfort, A., Michel, V., Thirion, B., Grisel, O., Blondel, M., Prettenhofer, P., Weiss, R., Dubourg, V., Vanderplas, J., Passos, A., and Cournapeau, D. (2011). Scikit-learn: Machine Learning in Python. *MACHINE LEARNING IN PYTHON*.

Peponi, A., Morgado, P., and Trindade, J. (2019). Combining Artificial Neural Networks and GIS Fundamentals for Coastal Erosion Prediction Modeling. *Sustain-*

ability, 11(4):975. Number: 4 Publisher: Multidisciplinary Digital Publishing Institute.

Perch-Nielsen, S. L. (2010). The vulnerability of beach tourism to climate change–an index approach. *Climatic Change*, 100(3):579–606.

Portillo Juan, N. and Negro Valdecantos, V. (2022). Review of the application of Artificial Neural Networks in ocean engineering. *Ocean Engineering*, 259:111947.

Ramsundar, B. and Zadeh, R. B. (2018). *TensorFlow for deep learning: from linear regression to reinforcement learning*. " O'Reilly Media, Inc.".

Ruessink, B. G., Blenkinsopp, C., Brinkkemper, J. A., Castelle, B., Dubarbier, B., Grasso, F., Puleo, J. A., and Lanckriet, T. (2016). Sandbar and beach-face evolution on a prototype coarse sandy barrier. *Coastal Engineering*, 113:19–32.

Ruggiero, P., Kaminsky, G. M., Gelfenbaum, G., and Voigt, B. (2005). Seasonal to interannual morphodynamics along a high-energy dissipative littoral cell. *Journal of Coastal Research*, 21(3):553–578.

Sambah, A. B. and Miura, F. (2014). Integration of Spatial Analysis for Tsunami Inundation and Impact Assessment. *Journal of Geographic Information System*, 2014. Publisher: Scientific Research Publishing.

Schmidt-Hieber, J. (2020). Nonparametric regression using deep neural networks with ReLU activation function. *The Annals of Statistics*, 48(4):1875–1897. Publisher: Institute of Mathematical Statistics.

Shaw, J., Taylor, R. B., Solomon, S., Christian, H. A., and Forbes, D. L. (1998). Potential Impacts of Global Sea-Level Rise on Canadian Coasts. *Canadian Geographies / Géographies canadiennes*, 42(4):365–379. _eprint: https://onlinelibrary.wiley.com/doi/pdf/10.1111/j.1541-0064.1998.tb01352.x.

Small, C. and Naumann, T. (2001). The global distribution of human population and recent volcanism. *Global Environmental Change Part B: Environmental Hazards*, 3(3):93–109. Publisher: Taylor & Francis _eprint: https://doi.org/10.3763/ehaz.2001.0309.

Suzuki, T. and Kuriyama, Y. (2012). FIELD OBSERVATIONS OF SHORELINE CHANGE BY FREQUENCY-BANDED WAVE ENERGY FLUX AND FORESHORE SHAPE. *Coastal Engineering Proceedings*, (33):10–10. Number: 33.

Thilakarathne, S., Suzuki, T., Mäll, M., Higa, H., and Malek, M. A. (2022). A Simple Approach to Predict the Beach Vulnerability to Storm-induced Erosion in Hasaki Coast, Japan. *Journal of Japan Society of Civil Engineers b2(Coastal Engineering)*, 78(2):985–990.

Turner, I. L., Harley, M. D., Short, A. D., Simmons, J. A., Bracs, M. A., Phillips, M. S., and Splinter, K. D. (2016). A multi-decade dataset of monthly beach profile surveys and inshore wave forcing at Narrabeen, Australia. *Scientific Data*, 3(1):160024. Number: 1 Publisher: Nature Publishing Group.

Vidal-Ruiz, J. A. and Ruiz de Alegría-Arzaburu, A. (2019). Variability of sandbar morphometrics over three seasonal cycles on a single-barred beach. *Geomorphology*, 333:61–72.

Virtanen, P., Gommers, R., Oliphant, T. E., Haberland, M., Reddy, T., Cournapeau, D., Burovski, E., Peterson, P., Weckesser, W., Bright, J., van der Walt, S. J., Brett, M., Wilson, J., Millman, K. J., Mayorov, N., Nelson, A. R. J., Jones, E., Kern, R., Larson, E., Carey, C. J., Polat, ⊠., Feng, Y., Moore, E. W., VanderPlas, J., Laxalde, D., Perktold, J., Cimrman, R., Henriksen, I., Quintero, E. A., Harris, C. R., Archibald, A. M., Ribeiro, A. H., Pedregosa, F., and van Mulbregt, P. (2020). SciPy 1.0: fundamental algorithms for scientific computing in Python. *Nature Methods*, 17(3):261–272. Number: 3 Publisher: Nature Publishing Group.

Wei, Z. (2021). Forecasting wind waves in the US Atlantic Coast using an artificial neural network model: Towards an AI-based storm forecast system. *Ocean Engineering*, 237:109646.

Appendix

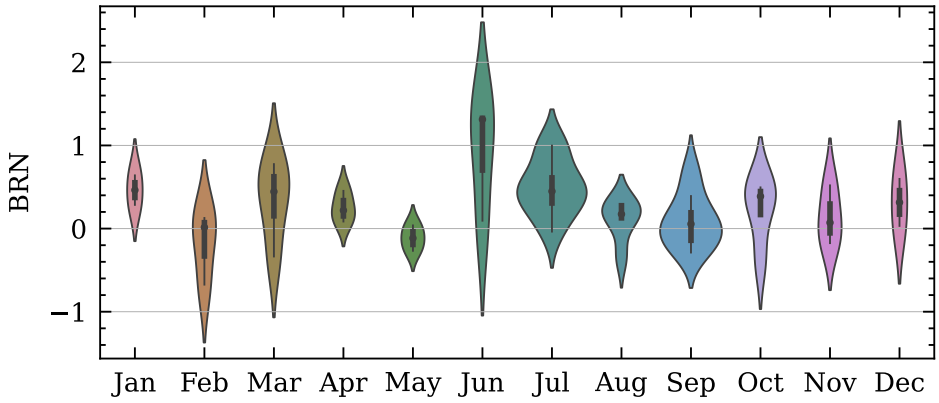

Figure A.1: Monthly distribution of Beach Resilience Number (BRN). Both of the recovered profiles as well as further eroded cases are considered here.

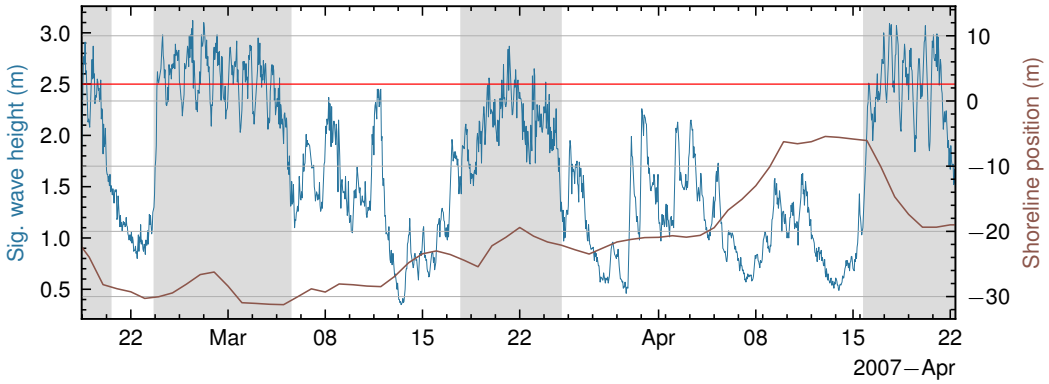

Figure A.2: Storm sequencing at Hasaki. The time gap between storms are used to separate the sequencing storms.

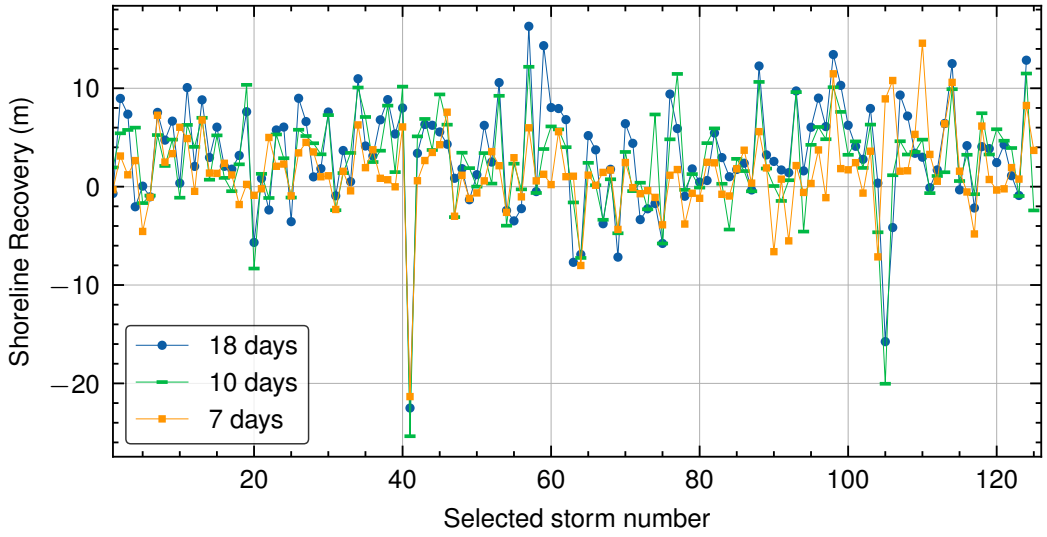

Figure A.3: Post-storm duration selection based on the different time gaps of sequencing storms at Hasaki.

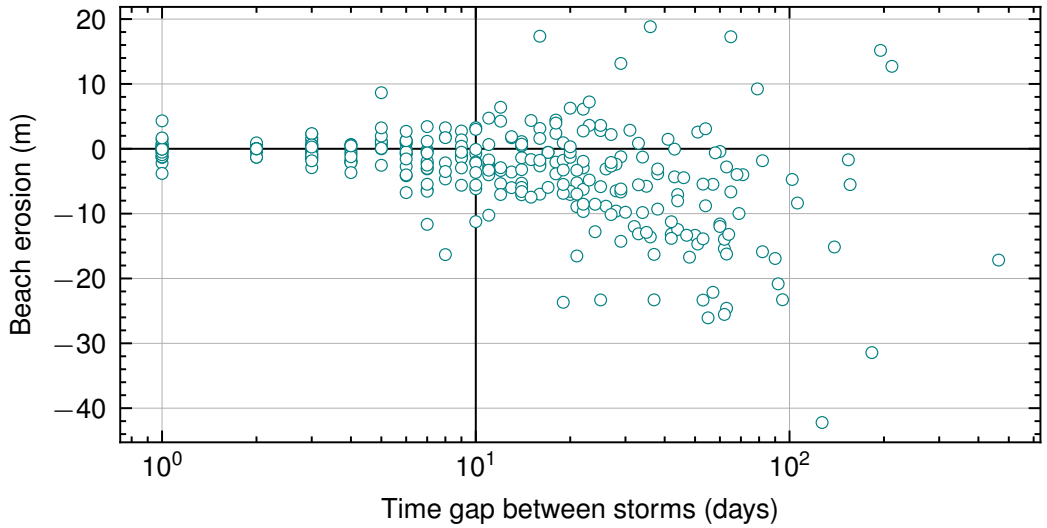

Figure A.4: Comparison of the time gap between two storm events and beach erosion during the time. A negative erosion denotes beach recovery.

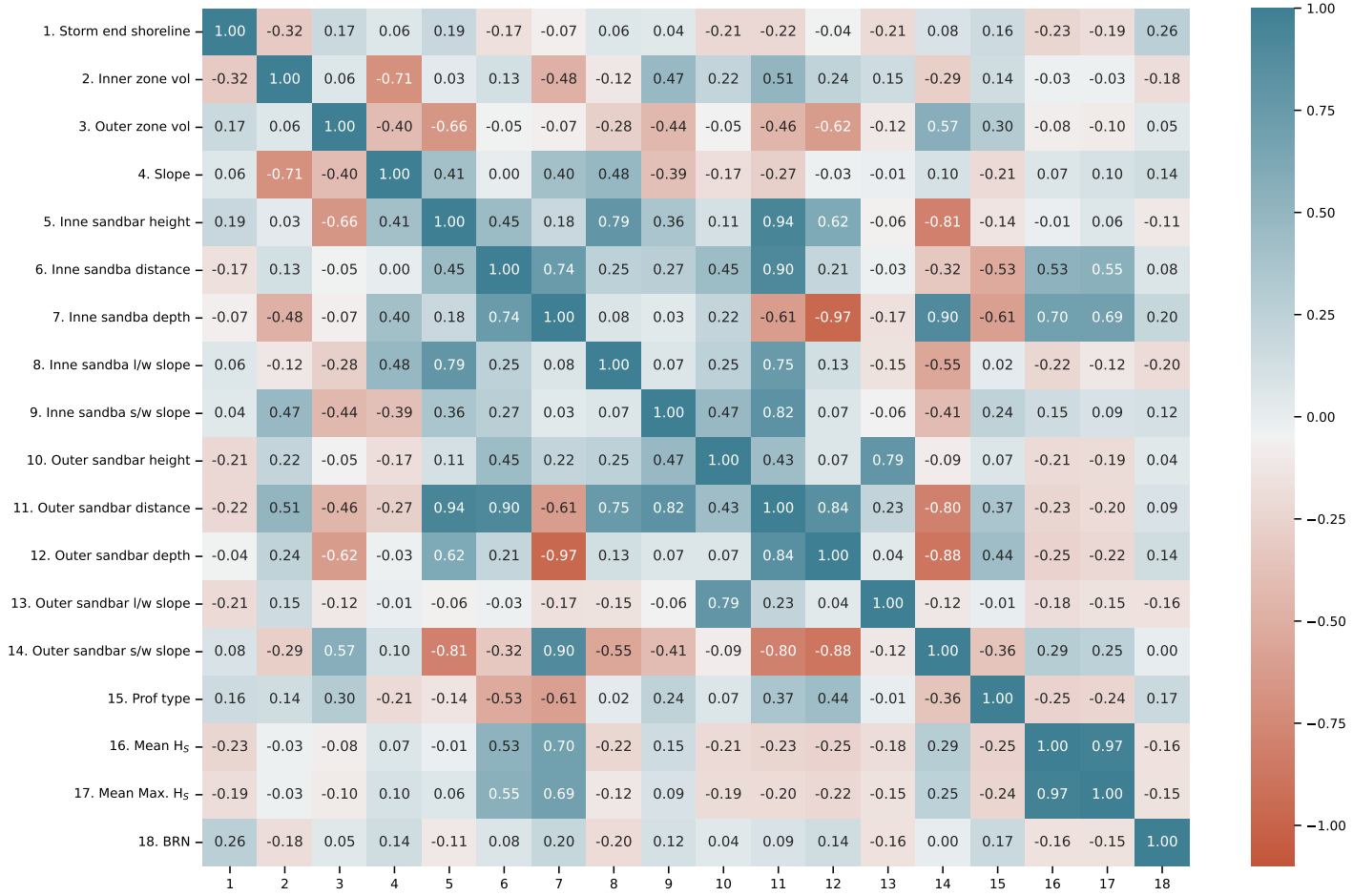

Figure A.5: Correlation matrix of extended input features and BRN.

List of research achievements

Peer reviewed articles

Thilakarathne, S., Suzuki, T., Mäll, M., Hiaga H. and Md Malek A., A Simple Approach to Predict the Beach Vulnerability to Storm-induced Erosion in Hasaki Coast, Japan, Journal of Japan Society of Civil Engineers,
https://doi.org/10.2208/kaigan.78.2 I 985, (2022)

Thilakarathne, S., Suzuki, T. and Mäll, M., Applying Artificial Neural Networks for Storm-induced Beach Erosion Vulnerability Prediction, Journal of Japan Society of Civil Engineers, (2023).

Thilakarathne, S., Suzuki, T. and Mäll, M., Machine learning-driven approach to quantify the beach susceptibility to storm-induced erosion, Coastal Engineering Journal (under review).

Conference presentations

Thilakarathne, S., Suzuki, T., Mäll, M., Hiaga H. and Md Malek A., A Simple Approach to Predict the Beach Vulnerability to Storm-induced Erosion in Hasaki Coast, Japan. Coastal Engineering Conference. Yokohama, Japan, November 8-11, 2022.

Thilakarathne, S., Suzuki, T. and Mäll, M., Applying Artificial Neural Networks for Storm-induced Beach Erosion Vulnerability Prediction. 48^{th}Ocean Development Symposium 2023. Hokkaido, Japan, June 28-30, 2023.